

POLITECNICO DI MILANO
Scuola di Ingegneria Industriale e dell'Informazione



Design of a Mechanical Filter for Sensors on the Railway

Supervisor: Prof. Emanuele Zappa

Master degree thesis of:
Name Surname ID: Wang Bing 892350

Academic year 2019/2020

Acknowledgements

I am using this opportunity to thank the organization and the people of the Politecnico di Milano who have been interested in this thesis project. Thank professor Emanuele Zappa for the guidance and advice; thank Simone Paganoni for helping of test in laboratory and providing test data; thank Politecnico for library resources available.

Abstract

In order to measure the vibration of the rail way, accelerometers are used. The accelerometer shall be used well below its fundamental resonance frequency, so every sensor has its measuring range, and the vibration and noise of rail usually have a wide range. To avoid measuring error, it is necessary to use mechanical filter to cut high frequency components. This paper contains four chapters: in the first chapter, the importance of reducing high frequency signals is introduced; in the second chapter, a review of commercial mechanical filters and relevant researches is made; in the third chapter, a suitable model of mechanical filter is created through ABAQUS simulation; in the final chapter, this model is produced and goes through laboratory tests. By comparing the results of the simulation and the laboratory test, evaluations and analysis about the mechanical filter is made.

Table of contents

| | |
|--|----|
| Acknowledgements | 2 |
| Abstract | 3 |
| Table of contents | 4 |
| Figure index | 6 |
| Table index | 10 |
| CHAPTER 1 INTRODUCTION | 11 |
| CHAPTER 2 STATE OF THE ART | 12 |
| 2.1 Ways to reduce vibration and noise | 12 |
| 2.2 Use of mechanical filters | 13 |
| 2.3 Basic knowledge of mechanical filters | 14 |
| 2.4 Mounting of accelerometers | 16 |
| 2.5 Mechanical filters on the market | 17 |
| 2.5.1 Electrical filter | 17 |
| 2.5.2 Mechanical filter | 18 |
| 2.5.3 Sensors with built-in filter | 20 |
| 2.6 Relevant researches | 22 |
| 2.6.1 Example of design | 22 |
| 2.6.2 Procedures of design | 23 |
| 2.6.3 Researches on materials | 24 |
| 2.7 Conclusion | 24 |
| CHAPTER 3 TESTS AND SIMULATIONS | 26 |
| 3.1 Basic procedure of simulation | 26 |
| 3.2 Factors affecting the natural frequency | 33 |
| 3.2.1 Configuration | 33 |
| 3.2.2 Results | 34 |
| 3.2.3 Conclusion | 38 |
| 3.3 Polynomial reduced model | 39 |

| | | |
|-------------------------|--|----|
| 3.3.1 | Configuration of real tests | 39 |
| 3.3.2 | Configuration of simulation | 39 |
| 3.3.3 | Comparison of different cases | 40 |
| 3.4 | Creating of suitable model | 47 |
| 3.4.1 | Common settings | 47 |
| 3.4.2 | Basic model | 47 |
| 3.4.3 | Model with steel shell | 50 |
| 3.4.4 | Model without base interaction | 54 |
| 3.4.5 | Improved model | 57 |
| 3.4.6 | Improved model with larger size | 61 |
| 3.5 | Dynamic analysis | 64 |
| 3.5.1 | Collision risk assessment | 64 |
| 3.5.2 | Rough FRF estimation | 66 |
| 3.5.3 | Dynamic analysis using real data | 68 |
| CHAPTER 4 | REAL MODEL SIMULATION AND TEST | 73 |
| 4.1 | Real model | 73 |
| 4.2 | Geometry parameter | 74 |
| 4.3 | Simulation of real model | 79 |
| 4.3.1 | Natural frequency | 79 |
| 4.3.2 | FRF simulation using real data | 80 |
| 4.4 | Test of real model and comparison | 81 |
| 4.5 | Simulation using different parameters | 83 |
| 4.6 | Conclusions | 87 |
| References | | 88 |

Figure index

| | |
|--|----|
| Figure 2.2.1:mechanical filter [6] | 13 |
| Figure 2.2.2:effect of mechanical filter [6] | 13 |
| Figure 2.3.1:glued accelerometer as a 1-dof system [7] | 14 |
| Figure 2.3.2:system with moving base | 14 |
| Figure 2.3.3:transfer function..... | 14 |
| Figure 2.5.1: RLC CIRCUIT [14] | 17 |
| Figure 2.5.2: 2-POLE GENERIC LOW-PASS ACTIVE FILTER [14] | 17 |
| Figure 2.5.3: Model 35771 Programmable filter | 18 |
| Figure 2.5.4: Exploded View of Improved SNL Mechanical | 19 |
| Figure 2.5.5:built in mechanical filter [3]..... | 20 |
| Figure 2.5.6:PCB damped sensor [19] | 21 |
| Figure 2.6.1:design of clamped mechanical filter [20] | 22 |
| Figure 2.6.2:improvement of the mechanical filter [20]..... | 22 |
| Figure 2.6.3:simplified structure [20] | 23 |
| Figure 2.6.4:combine of viscoelastic and piezoelectric materials [23]..... | 24 |
| Figure 3.1.1:create parts..... | 26 |
| Figure 3.1.2:create instances | 27 |
| Figure 3.1.3:edit materials | 27 |
| Figure 3.1.4:create sections..... | 28 |
| Figure 3.1.5:create boundary conditions | 28 |
| Figure 3.1.6:create steps | 29 |
| Figure 3.1.7:step configuration (1) | 29 |
| Figure 3.1.8:step configuration (2) | 30 |
| Figure 3.1.9:create outputs | 30 |
| Figure 3.1.10:create seeds and mesh | 31 |
| Figure 3.1.11:submit job and run | 31 |
| Figure 3.1.12:check results..... | 32 |
| Figure 3.2.1:material property..... | 33 |
| Figure 3.2.2:coordinate..... | 33 |
| Figure 3.2.3:natural frequency(mode1,2,3)..... | 34 |
| Figure 3.2.4:natural frequency(mode4,5,6) | 34 |
| Figure 3.2.5: natural frequency(mode1,2,3) | 35 |
| Figure 3.2.6: natural frequency(mode4,5,6) | 35 |
| Figure 3.2.7:natural frequency(mode1,2,3) | 36 |
| Figure 3.2.8: natural frequency(mode4,5,6) | 36 |
| Figure 3.2.9:natural frequency(mode1,2,3)..... | 37 |

| | |
|--|----|
| Figure 3.2.10:natural frequency(mode4,5,6) | 37 |
| Figure 3.3.1:real test | 39 |
| Figure 3.3.2:parameters | 40 |
| Figure 3.3.3: mode 4 of part 1 2 3 | 40 |
| Figure 3.3.4: mode 6 of part 1 2 3 | 41 |
| Figure 3.3.5: mode 5 of part 4..... | 41 |
| Figure 3.3.6: mode 6 of part 4 | 41 |
| Figure 3.3.7:part 1..... | 42 |
| Figure 3.3.8: natural frequency in simulation..... | 42 |
| Figure 3.3.9: natural frequency in test | 42 |
| Figure 3.3.10:part 2 | 43 |
| Figure 3.3.11: natural frequency in simulation..... | 43 |
| Figure 3.3.12: natural frequency in test..... | 43 |
| Figure 3.3.13:part 3..... | 44 |
| Figure 3.3.14: natural frequency in simulation | 44 |
| Figure 3.3.15: natural frequency in test..... | 44 |
| Figure 3.3.16:part 4..... | 45 |
| Figure 3.3.17: natural frequency in simulation..... | 45 |
| Figure 3.3.18: natural frequency in test..... | 45 |
| Figure 3.4.1:basic model | 47 |
| Figure 3.4.2:translation(basic model) | 48 |
| Figure 3.4.3:torsion(basic model) | 48 |
| Figure 3.4.4:bending(basic model)..... | 48 |
| Figure 3.4.5: vertical vibration (basic model)..... | 49 |
| Figure 3.4.6:natural frequency (basic model) | 49 |
| Figure 3.4.7:sketch of the model (model with steel shell) | 50 |
| Figure 3.4.8:dimension of the shell (model with steel shell) | 50 |
| Figure 3.4.9:steel shell (model with steel shell) | 50 |
| Figure 3.4.10:rubber (model with steel shell) | 51 |
| Figure 3.4.11:steel mass (model with steel shell)..... | 51 |
| Figure 3.4.12: diameter of the steel mass (model with steel shell)..... | 51 |
| Figure 3.4.13:total model (model with steel shell) | 52 |
| Figure 3.4.14:mode 1 (model with steel shell) | 52 |
| Figure 3.4.15:mode 2 (model with steel shell)..... | 52 |
| Figure 3.4.16:mode 3 (model with steel shell)..... | 53 |
| Figure 3.4.17: natural frequency (model with steel shell) | 53 |
| Figure 3.4.18:sketch of the model (model without base interaction)..... | 54 |
| Figure 3.4.19:dimension of the shell (model without base interaction)..... | 54 |
| Figure 3.4.20:diameter of steel mass (model without base interaction)..... | 54 |
| Figure 3.4.21:rubber (model without base interaction) | 55 |
| Figure 3.4.22: dimension of rubber (model without base interaction)..... | 55 |
| Figure 3.4.23:total model (model without base interaction) | 55 |
| Figure 3.4.24:mode 1 (model without base interaction) | 56 |
| Figure 3.4.25:mode 2 (model without base interaction) | 56 |
| Figure 3.4.26:mode 3 (model without base interaction)..... | 56 |
| Figure 3.4.27:natural frequency (model without base interaction) | 56 |

| | |
|--|----|
| Figure 3.4.28:sketch of the model (improved model) | 57 |
| Figure 3.4.29:dimension of the shell (improved model) | 57 |
| Figure 3.4.30:steel shell (improved model) | 57 |
| Figure 3.4.31: dimension of rubber ring (improved model)..... | 58 |
| Figure 3.4.32:rubber ring (improved model) | 58 |
| Figure 3.4.33:steel mass (improved model) | 58 |
| Figure 3.4.34: diameter of big cylinder (improved model) | 58 |
| Figure 3.4.35: diameter of small cylinder (improved model)..... | 59 |
| Figure 3.4.36:total model (improved model) | 59 |
| Figure 3.4.37:bottom view (improved model)..... | 59 |
| Figure 3.4.38:natural frequency (improved model)..... | 59 |
| Figure 3.4.39:mode 1 (improved model) | 60 |
| Figure 3.4.40: mode 2 (improved model) | 60 |
| Figure 3.4.41: mode 3 (improved model) | 60 |
| Figure 3.4.42: mode 5 (improved model)..... | 60 |
| Figure 3.4.43: dimension of shell (improved model with larger size)..... | 61 |
| Figure 3.4.44: dimension of rubber ring (improved model with larger size)..... | 61 |
| Figure 3.4.45: diameter of bigger cylinder (improved model with larger size)..... | 61 |
| Figure 3.4.46: diameter of smaller cylinder (improved model with larger size)..... | 62 |
| Figure 3.4.47:natural frequency (improved model with larger size)..... | 62 |
| Figure 3.4.48:mode 1 (improved model with larger size) | 62 |
| Figure 3.4.49: mode 2 (improved model with larger size) | 62 |
| Figure 3.4.50: mode 3 (improved model with larger size) | 63 |
| Figure 3.4.51: Figure 3.4.50: mode 5 (improved model with larger size) | 63 |
| Figure 3.5.1: time history of the noise | 64 |
| Figure 3.5.2: spectrum of the noise | 64 |
| Figure 3.5.3:motion of improved model..... | 65 |
| Figure 3.5.4: motion of improved model with larger size | 65 |
| Figure 3.5.5: acceleration on the bottom (input: noise) | 66 |
| Figure 3.5.6: acceleration on the top (input: noise) | 66 |
| Figure 3.5.7:FRF (input: noise) | 67 |
| Figure 3.5.8: natural frequency (improved model) | 67 |
| Figure 3.5.9:displacement | 68 |
| Figure 3.5.10:acceleration..... | 68 |
| Figure 3.5.11: original acceleration | 69 |
| Figure 3.5.12: spectrum of original acceleration | 69 |
| Figure 3.5.13: resampled acceleration | 70 |
| Figure 3.5.14: spectrum of resampled signal..... | 70 |
| Figure 3.5.15:base motion..... | 70 |
| Figure 3.5.16:short signal after cut | 71 |
| Figure 3.5.17: spectrum of short signal..... | 71 |
| Figure 3.5.18: acceleration on the bottom (input: real data)..... | 71 |
| Figure 3.5.19: acceleration on the top (input: real data) | 72 |
| Figure 3.5.20:FRF (input: real data) | 72 |
| Figure 4.1.1:real model shape | 73 |
| Figure 4.2.1:shell..... | 74 |

| | |
|--|----|
| Figure 4.2.2:diameter (top, mid, bottom) | 74 |
| Figure 4.2.3:rubber dimension..... | 74 |
| Figure 4.2.4:steel mass | 75 |
| Figure 4.2.5:original cylinder | 75 |
| Figure 4.2.6:cut 1 2 3 | 75 |
| Figure 4.2.7:bolt screw..... | 76 |
| Figure 4.2.8:dimension of head..... | 76 |
| Figure 4.2.9:nut | 76 |
| Figure 4.2.10:gasket..... | 77 |
| Figure 4.2.11:gasket dimension | 77 |
| Figure 4.2.12:sensor..... | 77 |
| Figure 4.2.13:final model..... | 78 |
| Figure 4.2.14:bottom view | 78 |
| Figure 4.3.1:natural frequency..... | 79 |
| Figure 4.3.2:mode 1 | 79 |
| Figure 4.3.3:acceleration on the bottom..... | 80 |
| Figure 4.3.4: acceleration on the top | 80 |
| Figure 4.3.5:FRF simulation..... | 80 |
| Figure 4.4.1:FRF from test..... | 81 |
| Figure 4.4.2:relationship between dynamic amplification factor and damping ratio | 81 |
| Figure 4.4.3:relationship between maximum amplitude and damping ratio | 82 |
| Figure 4.5.1: Neo-Hooke model..... | 83 |
| Figure 4.5.2:damping..... | 83 |
| Figure 4.5.3:viscoelasticity | 84 |
| Figure 4.5.4:natural frequency | 84 |
| Figure 4.5.5:mode 1 | 84 |
| Figure 4.5.6:acceleration on the bottom..... | 85 |
| Figure 4.5.7: acceleration on the top | 85 |
| Figure 4.5.8:FRF..... | 85 |
| Figure 4.5.9:FRF from test | 86 |

Table index

Table 1:nylon10134
Table 2:PE low density.....35
Table 3:nitrile rubber.....36
Table 4:silicone37
Table 5: Neo-Hooke model83
Table 6: viscoelastic property definition.....83

CHAPTER 1

INTRODUCTION

Vibration and noise are two major factors in the performance assessment of rail transit systems, particularly in an urban environment where elevated systems are used [1]. To measure these vibration and noise, sensors are used, such as accelerometers and displacement sensors. The accelerometer shall be used well below its fundamental resonance frequency, so every sensor has its measuring range, and the vibration and noise of rail usually have a wide range. Roughly speaking, vibrations and structure-born noise occur in the frequency range 0~100 Hz and noise 30~2000 Hz [2]. Though sensors of good quality can have wide measuring range, they are expensive.

Since most Shock Response Spectra stop at 10 kHz or 20 kHz, accelerometers with resonance in the neighborhood of 100 kHz are considered adequate for high g-shock applications, ignoring the fact that there is much energy beyond 20 kHz. The problem is further complicated by the issue of damage potential of high frequency. It is a well established fact that shock energy above 10 kHz seldom causes any damage to the test article, and it is routinely overlooked in most data analysis. These high frequency components, although posing no danger to the article, seriously affect the linear operation of any spring-mass type accelerometer [3].

Since vibrations mainly occur at 0~100 Hz, and high frequency components pose no danger but will cause measuring error, to measure only the vibration, it is better to reduce those high frequency vibration and noise. If the vibration and noise are reduced, it is also possible to use cheaper sensors to measure, which is more economical.

CHAPTER 2

STATE OF THE ART

2.1 Ways to reduce vibration and noise

There are four main groups of rail traffic noise and vibration mitigation measures [4]:

- 1.reduction at source,
- 2.reduction of propagation,
- 3.isolation of receiver,
- 4.economic measures and regulations.

The first method is to reduce the vibration and noise that train and rail makes, for example, use rail vibration dampers and damped wheels, improve the quality of the rail surface, reduce the speed of the train. These methods are effective, but it costs a lot to change the structure of the train and rail, so it is not always possible.

The second and third methods shows us a new idea: if the sensor is considered as the receiver, isolate the sensor and use some methods to reduce the propagation, the vibration and noise measured by the sensor can be reduced too. Instead of reducing at source, this method is reducing at the end of the measuring chain. In this paper, only vibration measurement is considered, so the aim is to reduce vibration. Actually, because noise is the vibration of sound, it may also affect the result of vibration measurement, but the reduction of noise is another area.

2.2 Use of mechanical filters

As mentioned before, the accelerometer shall be used well below its fundamental resonance frequency. The working frequency bands for commercial transducers range between 100 Hz for servo and seismic accelerometers, up to 100 kHz for specific shock and hi-performance accelerometers [5]. If the bandwidth of the sensor is higher than the working bandwidth, it can work properly; but if the working bandwidth exceeds the sensor bandwidth, saturation will happen, which means wrong data.

To reduce vibration on the sensor and avoid sensor saturation, a very useful mounting accessory is the Mechanical Filter, which is mounted between the accelerometer and the point of measurement in order to prevent the accelerometer from detecting high frequency vibration [6].



Figure 2.2.1: mechanical filter [6]

The filter shown in figure 2.2.1 is useful where the measuring instrumentation is not equipped with a choice of low-pass filters to prevent the erroneous measurement of high frequency vibration components which can be amplified by the accelerometer's resonance. Even when using electronic integrators or low pass filters the mechanical filter will prevent overloading the input stage of the preamplifier. It protects accelerometers and amplifiers against high level, high frequency shock transients in both the accelerometer main and transverse axis directions.

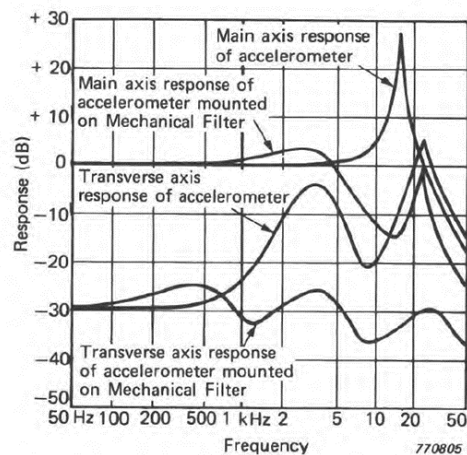


Figure 2.2.2: effect of mechanical filter [6]

2.3 Basic knowledge of mechanical filters

The simplest filter structure is a 1-dof system:

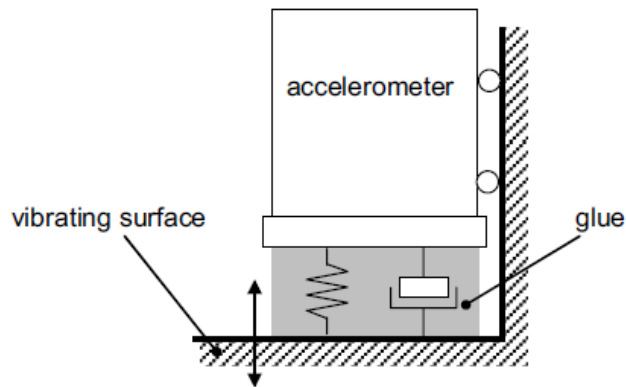


Figure 2.3.1:glued accelerometer as a 1-dof system [7]

Because the sensor is used on the rail, it can be seen as a moving base, the following sketch shows that:

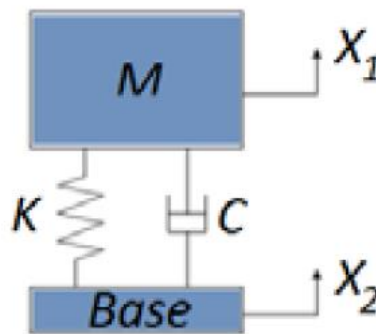


Figure 2.3.2:system with moving base

$$\frac{X_1}{X_2} = \frac{1 + j2\zeta \left(\frac{\omega}{\omega_n} \right)}{1 - \left(\frac{\omega}{\omega_n} \right)^2 + j2\zeta \left(\frac{\omega}{\omega_n} \right)}$$

Figure 2.3.3:transfer function

This formula shows the transfer function between X1 and X2. From the transfer function, it is known that the higher ω/ω_n is, the lower the ratio. ω is the working frequency, which cannot be changed, so to reduce the vibration, the nature

frequency ω_n needs to be decreased. The nature frequency equals to $\sqrt{k/m}$, which means increasing the mass of the system or decrease the stiffness. This is the basic idea of design the mechanical filter.

2.4 Mounting of accelerometers

To design and use a mechanical filter for accelerometers, it is necessary to know how to mount accelerometers. There are some standards about mechanical mounting of accelerometers [8].

An accelerometer will achieve optimal performance only if the following general procedures are followed:

a) the accelerometer shall perform as nearly as possible the same motion as the structure under test at the accelerometer attachment;

b) the motion of the structure shall be changed as little as possible by the addition of the accelerometer;

c) the ratio of the signal from the accelerometer to the motion of the accelerometer shall not be distorted by operating too near to its mounted fundamental resonance frequency.

In order to achieve these ideal conditions, it is necessary to ensure that:

a) the accelerometer and its mounting are as rigid and firm as possible (the mounting surfaces shall be as clean and flat as possible);

b) the mounting introduces minimum distorting motions of its own (for example, simple symmetrical mountings are best);

c) the mass of the accelerometer and mounting are small in comparison with that of the dynamic mass of the structure under test.

Because now the accelerometers are mounted with mechanical filters, it needs to be noticed that those requirements are not affected by filters. For example, the motion of accelerometer should not change because of filter; the mass of mechanical filter must be small in comparison with the structure so that the motion of the structure won't be changed so much (in this paper, the structure is the railway, so this is not a problem); the mechanical filter is better to be symmetric.

2.5 Mechanical filters on the market

There are already many kinds of mechanical filters available on the market, such as products of PCB, Endevco, Bruel & Kjaer. [9] [10] [11] When searching for the word “mechanical filter” on the Internet, it contains not only filters made of pure mechanical components, but also filters made of electrical components.

2.5.1 Electrical filter

As the technique develops, more and more filters are made of electrical components: they use piezoelectric ceramic transducer [12]. Piezoelectric accelerometers are the first choice for most vibration measurements since they have a wide frequency response, good sensitivity and resolution and are easy to install. There are two subdivisions of piezoelectric accelerometers which include the basic charge-mode accelerometer and the voltage mode Internal Electronic Piezoelectric (IEPE) types [13]. So, to in cooperation with piezoelectric accelerometers, it is good to use also electric filters. The working principle of those piezoelectric filters can be seen as simple RLC circuits. The output measured across the capacitor is in fact a low-pass filter [14].

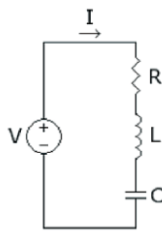


Figure 2.5.1: RLC CIRCUIT [14]

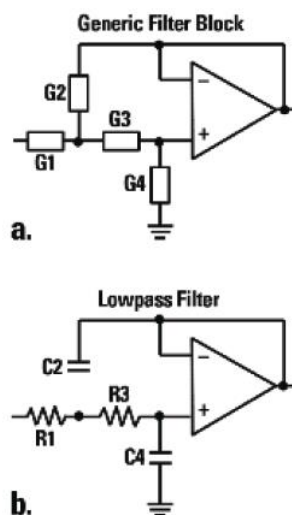


Figure 2.5.2: 2-POLE GENERIC LOW-PASS ACTIVE FILTER [14]

Model 35771 Programmable filter

Features

- Plug in filter card
- Used in 2775A/AM4
- Two pole Butterworth filtering
- Low pass, high pass or band pass
- Jumper selectable corner frequencies

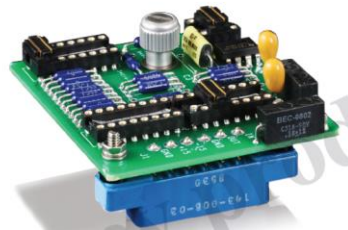


Figure 2.5.3: Model 35771 Programmable filter

The Endevco model 35771 programmable filter is a plug-in filter designed for use in the Endevco models 2775A and 2775AM4 signal conditioners. It contains an active high pass (HP) two pole Butterworth filter stage, followed by an active low pass (LP) two pole Butterworth filter stage. DIP programming jumpers select any combination of these two stages; the resulting overall response is HP, LP, or band pass (BP). The corner frequencies are also selected via programming jumpers. One HP corner frequency and one LP corner frequency may be established by customer-installed resistors. The remaining 2 HP and 7 LP corners are determined by factory-installed components.

As can be seen, these electrical filters are very flexible: the frequency band can be tuned, and even the functions can be changed.

2.5.2 Mechanical filter

Though programmable electrical filters have many advantages, but for some simple uses, only ordinary filters are needed. That is why traditional mechanical filters are still on the market.

Company Endevco has products with mechanical components. Their idea is: An obvious solution to the accelerometer resonance problem is to isolate the sensor from high frequency inputs. When an appropriate material is placed between the structural mounting surface and the transducer, a mechanical low-pass filter is formed [3]. They put the sensor in an aluminum shell, then cover the top and bottom with elastic rubber [15].

They point out four critical design parameters in a mechanical filter [3]:

- 1) First, the filter/accelerometer combination must be robust enough to withstand high level shocks. Many “isolators” designed for vibration isolation will simply disintegrate under shock.

2) The Q (amplification) of the mechanical filter must be very low in order to maintain and maximize frequency response linearity. Damping characteristic is a critical consideration in matching the accelerometer to the mechanical filter.

3) The relative displacement between the transducer and the mounting surface must not exceed the linear range of the spring/damper. When the accelerometer “bottoms out”, its high frequency isolation characteristic of the filter vanishes, and the protection to the sensor fades.

4) The transfer characteristics of the mechanical filter must be clearly defined. The result has to be repeatable and predictable.

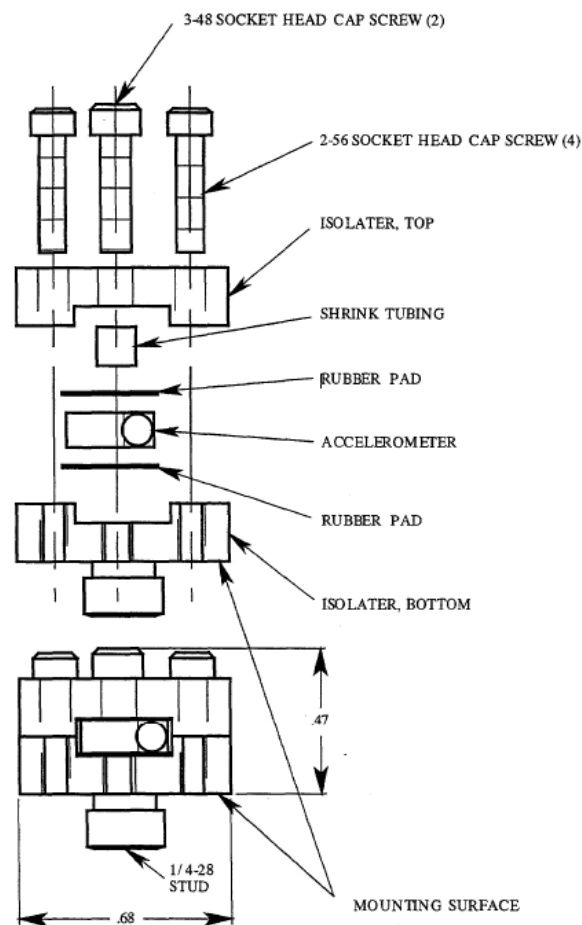


Figure 2.5.4: Exploded View of Improved SNL Mechanical Isolator [16]

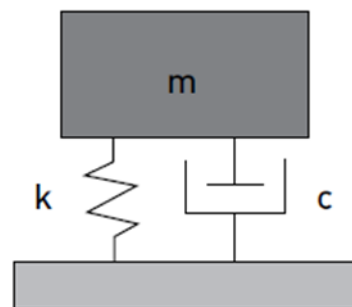
This mechanical filter shown in figure 2.5.4 is the filter designed for one piezoresistive accelerometer, the ENDEVCO 7270AM6. The material used in the mechanical isolator is polysulfide rubber which is sold as an adhesive in semi-solid form. This material was used for historical reasons because early mechanical isolator designs used a layer of polysulfide rubber between two plates. The accelerometer was then mounted on the top plate with screws in the usual manner, and the assembly was mounted on the structure with a 1/4-28 stud in the bottom plate [16].

2.5.3 Sensors with built-in filter

Nowadays, companies already have the ability to miniaturize mechanical filters and integrate them inside sensors.

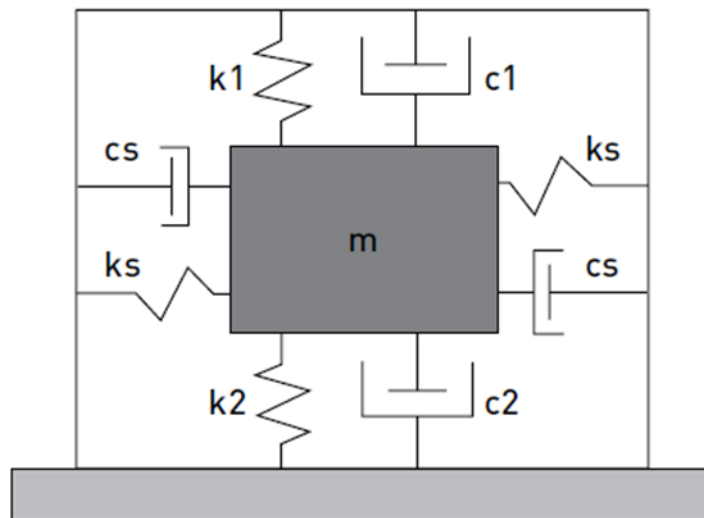
Endevco has successfully built mechanical filters inside sensor, the Endevco Model 7255A is a piezoelectric accelerometer with integral electronics and built-in mechanical filter designed specifically for near-field (close-range) pyrotechnic shock measurement [17].

Figure 4a.



External mechanical filter model

Figure 4b.



Internal mechanical filter model

Figure 2.5.5: built in mechanical filter [3]

Company PCB also has similar damped sensors. The micro-electromechanical systems (MEMS) sensor incorporates sufficient squeeze-film damping to reduce resonant amplification during violent events by orders of magnitude over conventional undamped PR MEMS designs [18]. The MEMS sensor was intentionally designed with a relatively low resonant frequency. The relatively low resonance enables displacements of the seismic element sufficient to introduce squeeze film

damping using air as the medium. Air is used since thermal effects on its performance are negligible. This is natural filtering, attenuation of frequency components above the resonance. The intent of the damping is to reduce the extremely high resonant amplification inherent in single crystal silicon [19].

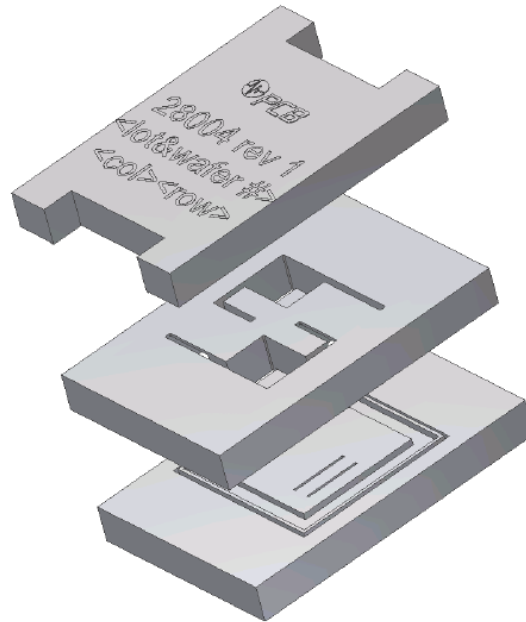


Figure 2.5.6: PCB damped sensor [19]

Figure 2.5.6 shows the spacing and the saw cuts to singulate the sensors from the stacked assembly of three wafers. The identification is seen on top of the Lid wafer, and aluminum wire-bond pads on the Core wafer are seen through an access hole in the Lid. Beneath the Core is the Base layer, which forms a stop to prevent overtravel of the inertial mass downward during positive accelerations, just as the Lid provides protection during upward motion from negative accelerations. In both the Lid and Base stop region are grooves to control the damping of the squeeze film of trapped air. Glass frit is applied in the area around the central region to hold the layers together, as well as to provide a hermetic seal [19].

2.6 Relevant researches

There are also many researches about mechanical filters.

2.6.1 Example of design

According to the idea of Endevco [15], someone in China designed one kind of clamped mechanical filter and improved his work [20]. It also puts rubber above and under the sensor. The structure can be simplified as figure 2.6.3.

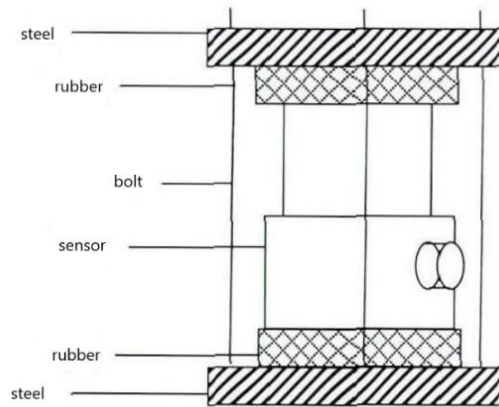


Figure 2.6.1: design of clamped mechanical filter [20]

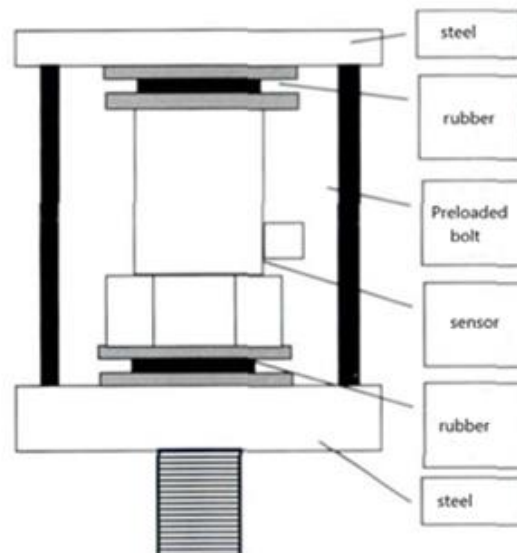


Figure 2.6.2: improvement of the mechanical filter [20]

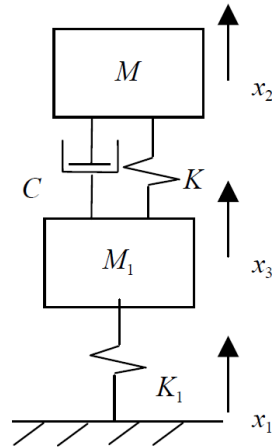


Figure 2.6.3:simplified structure [20]

2.6.2 Procedures of design

In the paper of professor E. Alberti, the procedures of designing a mechanical filter is detailed described [7]. Though several types of mechanical filters are commercially available, but some considerations about their usability must be exposed:

- 1) they are generally characterized by a non-negligible mass, thus introducing insertion error;
- 2) the cut-off frequency is constant for a specific Accelerometer-filter combination, or can be regulated with fixed steps;
- 3) they have been designed only for mono-axial accelerometers.

Despite the wide number of applications that would require a mechanical filter, there is practically no study in literature providing a complete procedure to design and realize a mechanical filter suitable to each kind of accelerometer. Professor E. Alberti describes the procedure implemented to design and realize fully tunable mechanical filters and discuss the results of an experimental campaign carried out in order to verify filters performances. The procedures contain choosing of material, modelling, analyzing, producing and testing. Finally, a mechanical filter, customizable in terms of cut-off frequency and applicable to different kind of accelerometers (with one or more measuring axes, with different shapes, etc.) is created.

In SANDIA's report, it also lists four phases [16]. The first phase was to determine if the rubber material in the isolator was the most appropriate elastic material. The second phase was to determine how the elastic material would be obtained by the commercial manufacturer. For the third phase, the shock magnitudes applied to the isolator were increased so that the upper limit of the shock magnitudes for the mechanical isolator could be determined. The last phase is the testing and evaluation of the mechanical isolator prototypes.

Generally speaking, the design of a mechanical filter needs determination of material, design of structure, producing and final test and evaluation.

2.6.3 Researches on materials

It is clear that the choose of material plays important role in the design of mechanical filters. Many kinds of rubber are used for this aim. Such high damping viscoelastic materials are employed in the design of geometrically complex, impact-absorbent components [21]. Purely passive damping treatments generally lead to reliable, low cost and robust vibration control. These can be achieved by covering part of the structure with constrained or unconstrained layers of viscoelastic materials. Several polymers exhibit the viscoelastic properties of naturally dissipating vibratory energy into heat energy. This is why they are largely used in the aerospace, aeronautical and automotive industries to provide passive vibration damping [22].

Viscoelastic materials are not the only choice. Piezoelectric materials, magnetorheological and electrorheological fluids can also be used for vibration attenuation [23]. In some advanced applications, different materials are combined. However, viscoelastic rubber is enough most of the time.

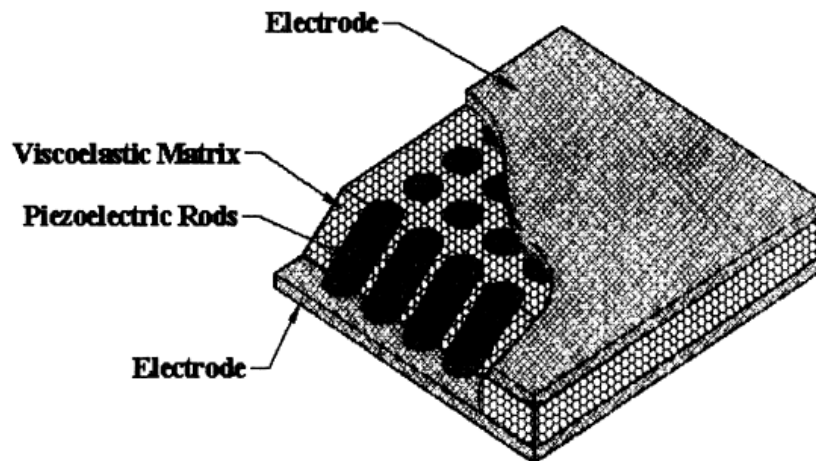


Figure 2.6.4: combine of viscoelastic and piezoelectric materials [23]

2.7 Conclusion

Although there are already mechanical filters, their working band are fixed according to different products. They are not designed with linearity in mind, and their applications are quite different.

A few international and U.S. private institutions have developed some experimental devices for their own shock measurements, but none are commercially available. These prototypes are made out of exotic materials, such as rosewood and cloth, for their unique damping and stiffness properties. Reliability and repeatability of these external filters are questionable at best. One of the accelerometer manufacturers does offer an external mechanical filter especially tuned for its own brand of transducers, but it is really intended for a general vibration environment [3].

Besides those prototypes made by institutions, there are several commercially-available versions of mechanical filters which comprise, essentially, of a metal housing and an elastomeric isolator. Because of their high stiffness and low damping, many of these commercially-available mechanical filters are not very effective in suppressing high frequency spectral component. Thus, there exists the need to re-consider the design of mechanical filters with particular emphasis on the choice of the elastomeric material, whose properties are frequency and temperature dependent, and on the optimization of the geometry of the metal housing [24].

Considering the real situation of use, designing a mechanical filter suitable for the band is better. So, simulation and experiments in the real environment will be important. However, the idea of clamped mechanical filter and the procedures to design can be useful for the work.

CHAPTER 3

TESTS AND SIMULATIONS

3.1 Basic procedure of simulation

Step 1

Build the shape of model in the “part” menu. More than one parts can be created.

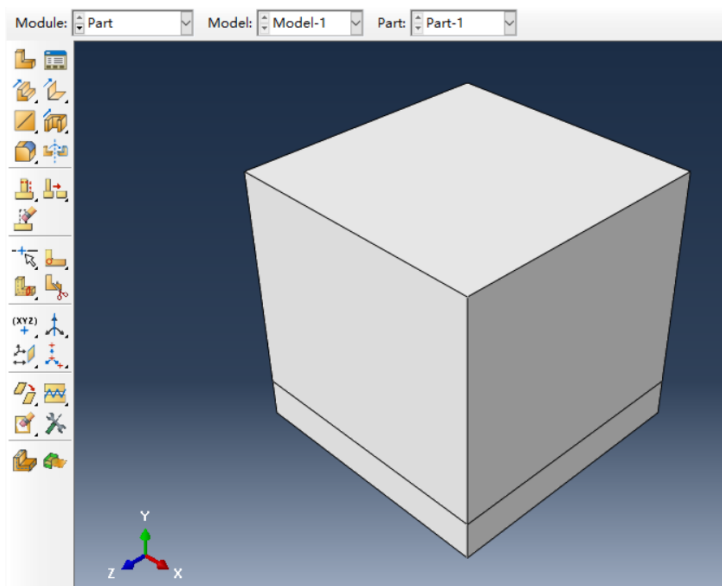


Figure 3.1.1:create parts

Step 2

Change the parts into instance in the “part” menu. If more than one parts exist, they can be merged into one.

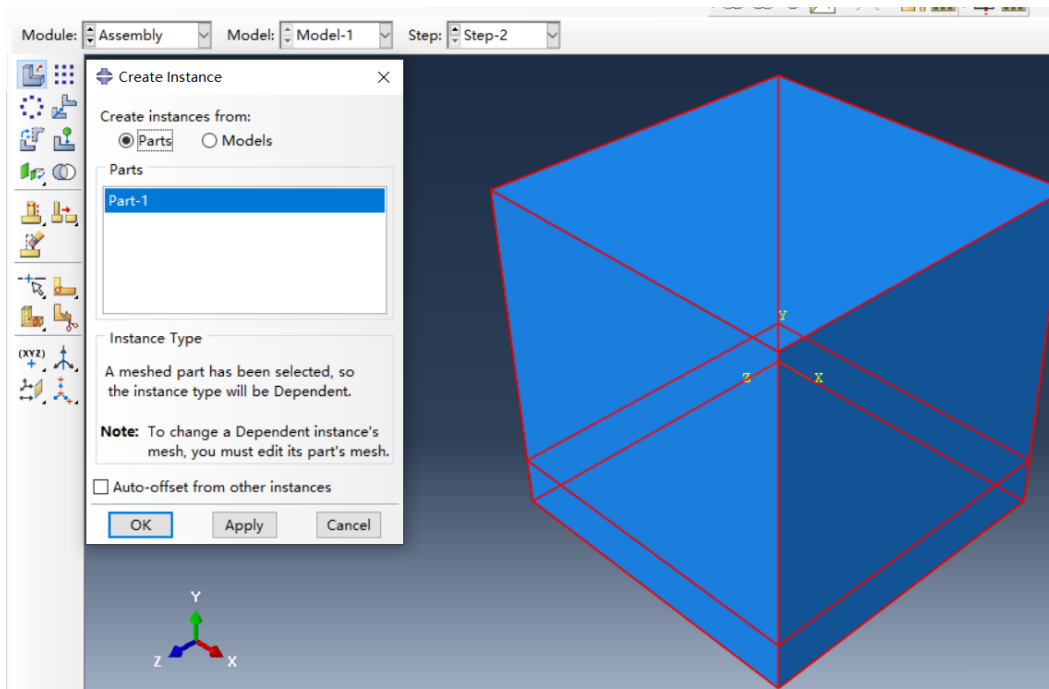


Figure 3.1.2:create instances

Step 3

Create material information in “property” menu. Density, Young’s modulus, and Poisson’s ratio are needed. Then create different sections with different materials and assign them to different regions in the model. Parameters can be saved in material library and cite freely.

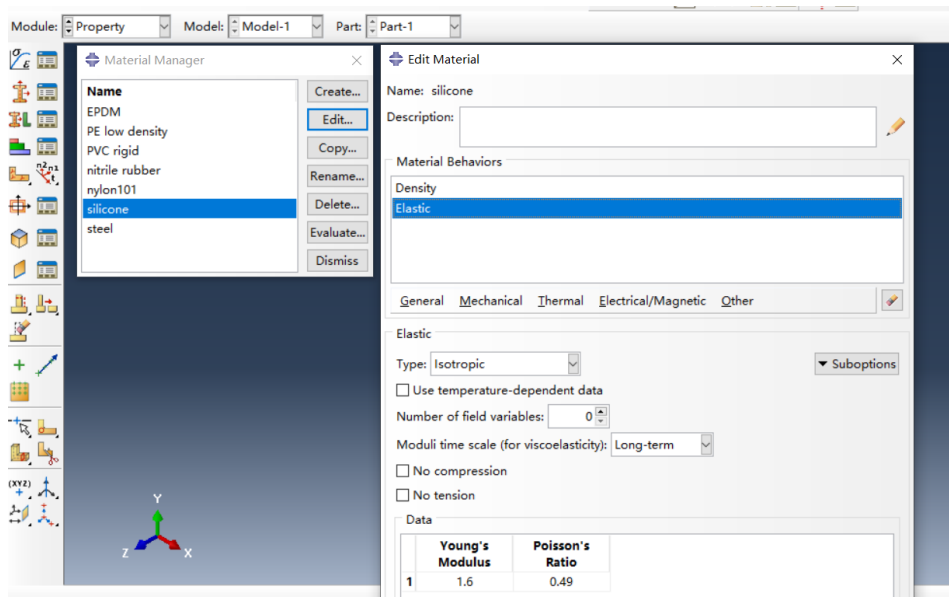


Figure 3.1.3:edit materials

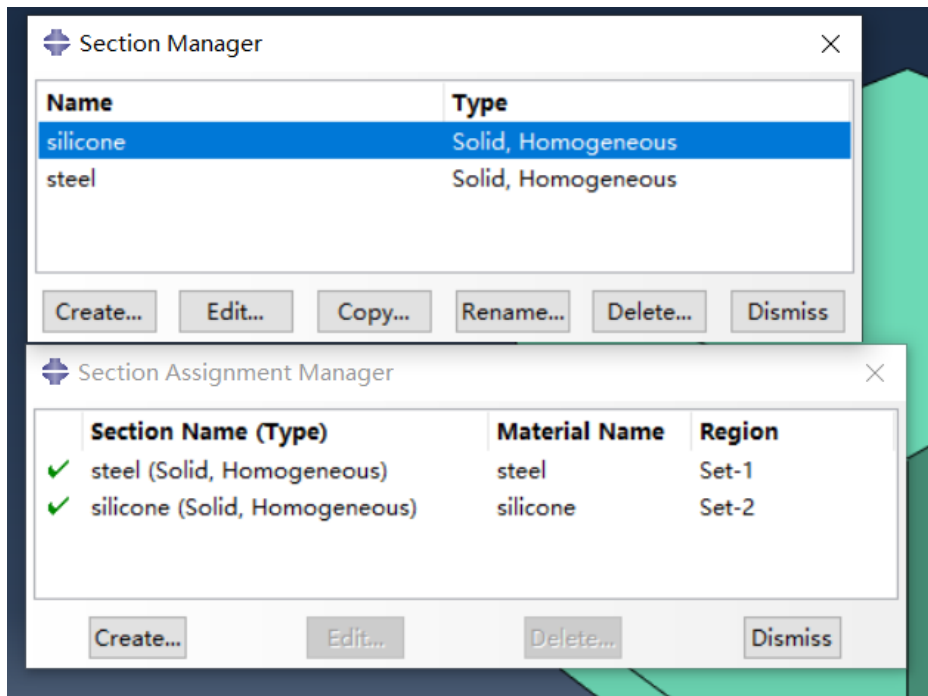


Figure 3.1.4:create sections

Step 4

In the “load” menu, boundary conditions are added. The displacement and acceleration of the base are introduced as boundary conditions too. Type the data manually or introduce the file of certain format is ok.

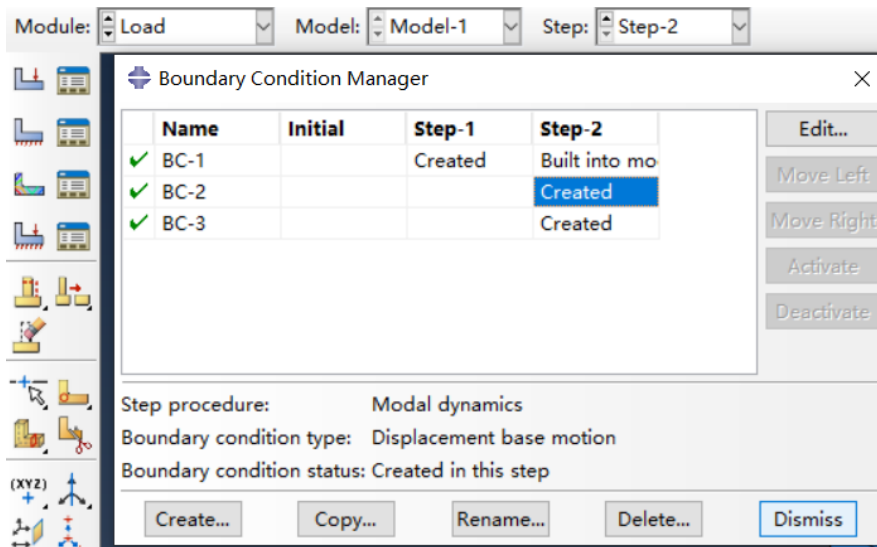
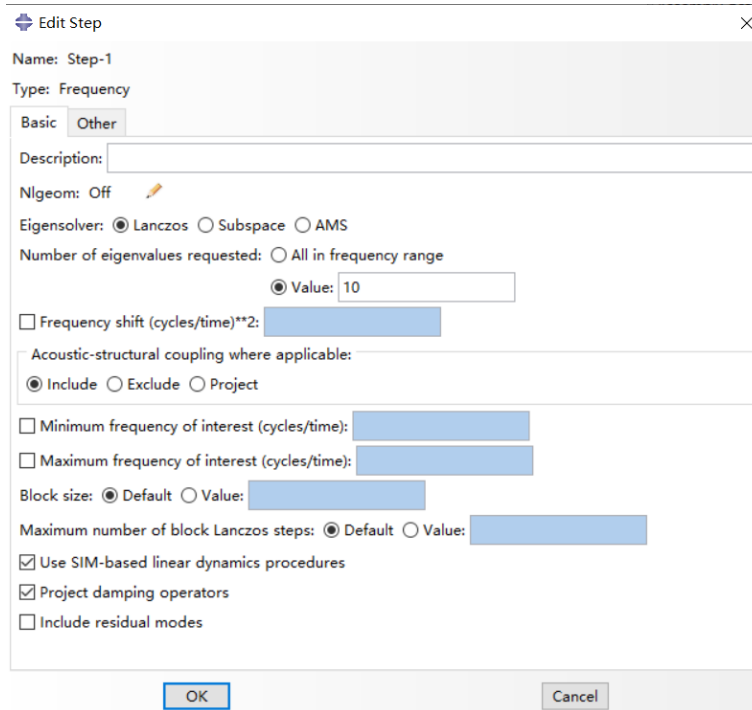


Figure 3.1.5:create boundary conditions

Step 5

Programs called “step” are created in the “step” menu. To get the natural frequency of the model, frequency step is created. The type of solver and the number of eigenvalues can be set.



The screenshot shows the 'Edit Step' dialog box for a 'Frequency' step. The 'Name' is 'Step-1' and the 'Type' is 'Frequency'. The 'Basic' tab is selected. The 'Description' field is empty. 'Nlgeom' is set to 'Off'. The 'Eigensolver' is set to 'Lanczos'. The 'Number of eigenvalues requested' is set to 'Value: 10'. There are several other options that are currently unchecked or set to 'Default'.

Edit Step [Close]

Name: Step-1
Type: Frequency

Basic Other

Description: [Text Field]

Nlgeom: Off [Edit]

Eigensolver: Lanczos Subspace AMS

Number of eigenvalues requested: All in frequency range
 Value: [Text Field: 10]

Frequency shift (cycles/time)**2: [Text Field]

Acoustic-structural coupling where applicable:
 Include Exclude Project

Minimum frequency of interest (cycles/time): [Text Field]

Maximum frequency of interest (cycles/time): [Text Field]

Block size: Default Value: [Text Field]

Maximum number of block Lanczos steps: Default Value: [Text Field]

Use SIM-based linear dynamics procedures

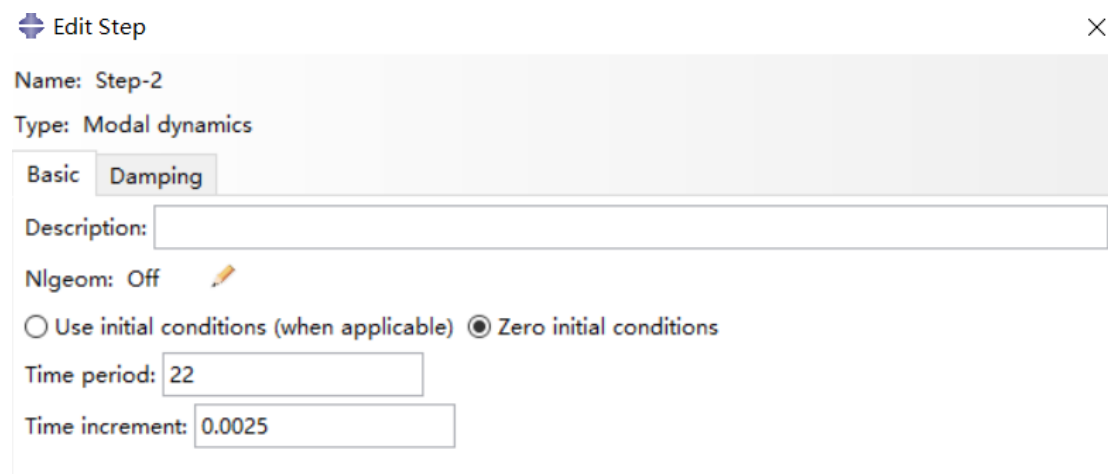
Project damping operators

Include residual modes

[OK] [Cancel]

Figure 3.1.6:create steps

By creating modal dynamics step, simulation can be done. Time period, time increment and damping information are needed.



The screenshot shows the 'Edit Step' dialog box for a 'Modal dynamics' step. The 'Name' is 'Step-2' and the 'Type' is 'Modal dynamics'. The 'Damping' tab is selected. The 'Description' field is empty. 'Nlgeom' is set to 'Off'. The 'Use initial conditions' are set to 'Zero initial conditions'. The 'Time period' is set to '22' and the 'Time increment' is set to '0.0025'.

Edit Step [Close]

Name: Step-2
Type: Modal dynamics

Basic Damping

Description: [Text Field]

Nlgeom: Off [Edit]

Use initial conditions (when applicable) Zero initial conditions

Time period: [Text Field: 22]

Time increment: [Text Field: 0.0025]

Figure 3.1.7:step configuration (1)

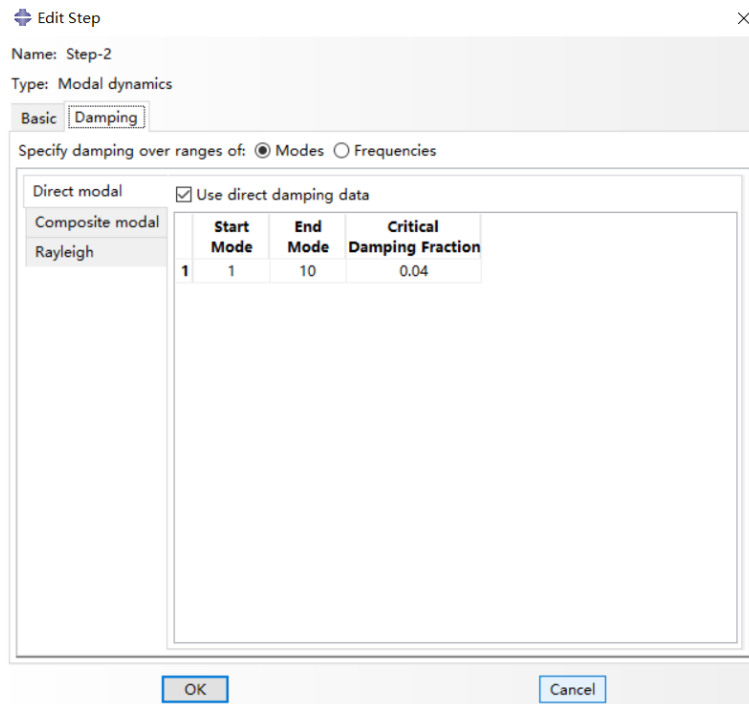


Figure 3.1.8:step configuration (2)

The field output and history output must be modified according to the result wanted.

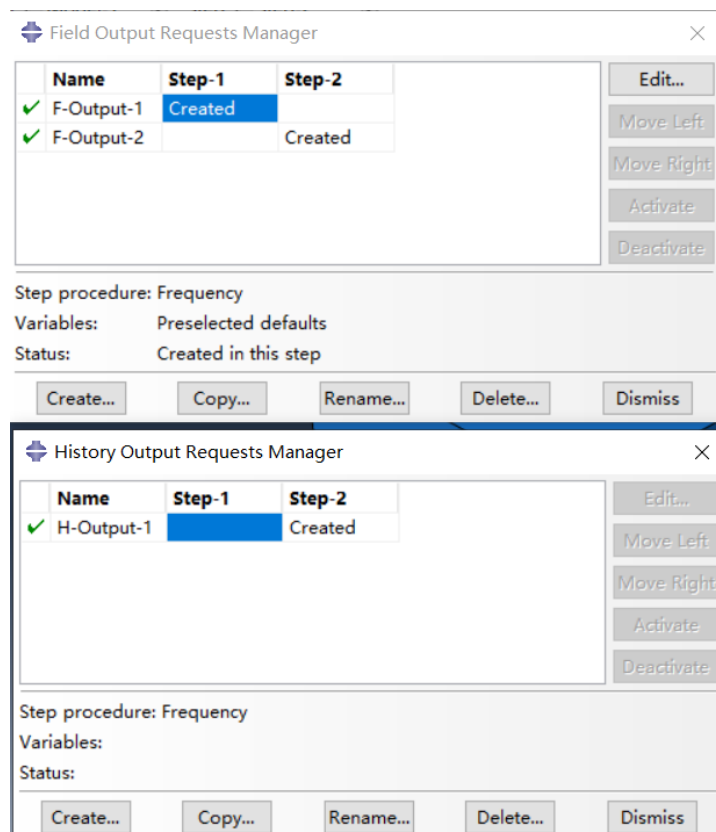


Figure 3.1.9:create outputs

Step 6

Create seeds and mesh the model. The size and shape of mesh will affect the final time needed to run.

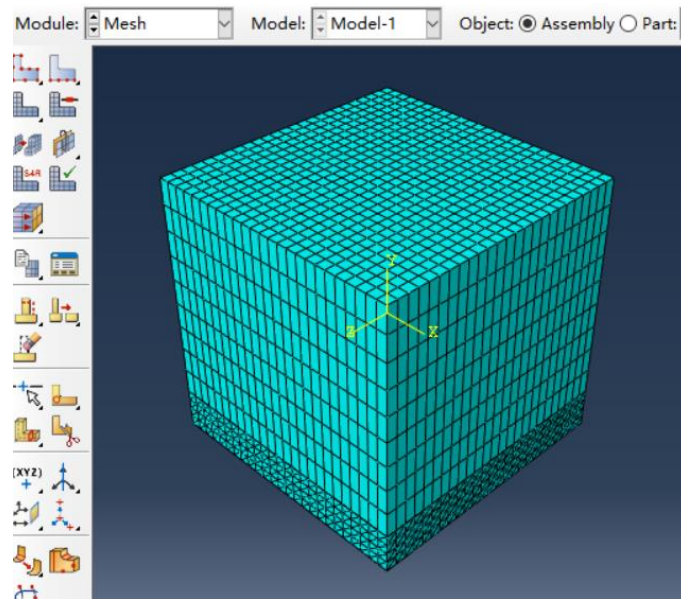


Figure 3.1.10:create seeds and mesh

Step 7

Now the job can be created and submitted. When it finishes, the result can be checked. The information of the natural frequency can be seen in the step/frame. Time history can be plot, but a series of parameters have to be set: the area of output wanted, the type of output, etc.

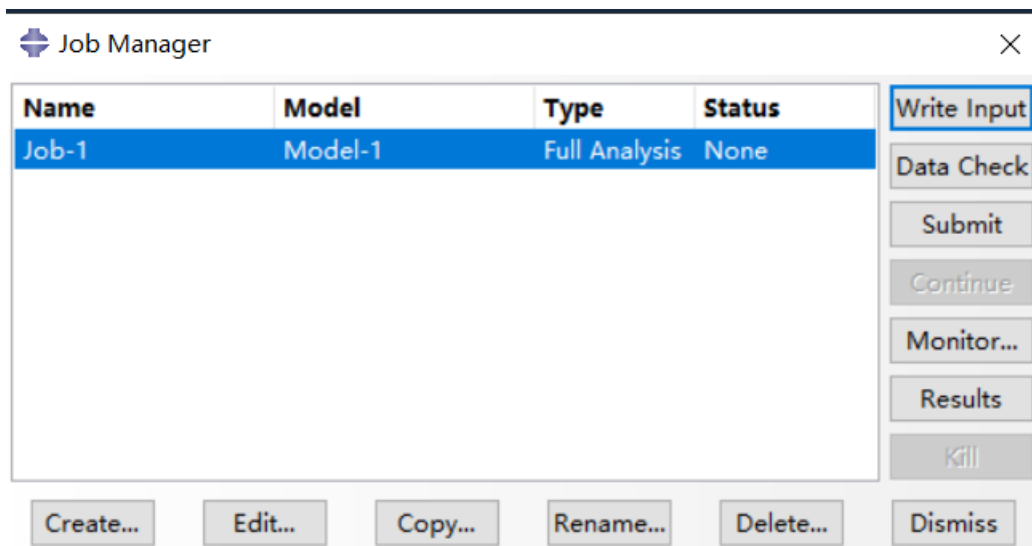


Figure 3.1.11:submit job and run

| Step Name | Description |
|-----------|-------------|
| Step-1 | |
| Step-2 | |

| Index | Description |
|-------|--|
| 0 | Increment 0: Base State |
| 1 | Mode 1: Value = 37297. Freq = 30.737 (cycles/time) |
| 2 | Mode 2: Value = 37315. Freq = 30.744 (cycles/time) |
| 3 | Mode 3: Value = 51703. Freq = 36.189 (cycles/time) |
| 4 | Mode 4: Value = 3.60849E+05 Freq = 95.606 (cycles/time) |
| 5 | Mode 5: Value = 3.61097E+05 Freq = 95.638 (cycles/time) |
| 6 | Mode 6: Value = 7.93983E+05 Freq = 141.82 (cycles/time) |
| 7 | Mode 7: Value = 1.93809E+07 Freq = 700.66 (cycles/time) |
| 8 | Mode 8: Value = 1.95334E+07 Freq = 703.41 (cycles/time) |
| 9 | Mode 9: Value = 1.95439E+07 Freq = 703.60 (cycles/time) |
| 10 | Mode 10: Value = 1.98531E+07 Freq = 709.14 (cycles/time) |

OK Apply Field Output... Cancel

Figure 3.1.12: check results

3.2 Factors affecting the natural frequency

3.2.1 Configuration

According to the basic knowledge of mechanical filters, there are many factors affecting the natural frequency, such as mass and stiffness. Increasing the size and mass of the structure is the simplest way to reduce the natural frequency, and the stiffness is related to the material. So, the type and thickness of the filter material are changed to find the relationship with the natural frequency.

The thickness is 1mm, 2mm, 3mm, 4mm, 5mm. The materials are nylon101, PE low density, nitrile rubber, silicone. The physical property of materials can be seen in figure below. Generally, lower Young's modulus means lower stiffness.

| material | nitrile rubber | silicone | EPDM | nylon101 | PE low density | PVC rigid | steel |
|-----------------|--------------------|----------------------|-----------------------|-----------------------|------------------------|----------------------|----------------------|
| density | 1g/cm ³ | 1.2g/cm ³ | 1.35g/cm ³ | 1.15g/cm ³ | 0.917g/cm ³ | 1.3g/cm ³ | 7.8g/cm ³ |
| young's modulus | 6.1Mpa | 1.6Mpa | 7.8Mpa | 1000Mpa | 172Mpa | 2410Mpa | 206000Mpa |
| poisson's ratio | 0.49 | 0.49 | 0.47 | 0.3 | 0.439 | 0.383 | 0.3 |

Figure 3.2.1: material property

First 6 modes of motion are chosen for comparison, almost all of them they are translation and single axis rotation. For different thickness, the sequence of mode maybe different, so the numbers of modes are rearranged to make them representing the same motion.

Mode 1: Y-rotation

Mode 2: Z-translation

Mode 3: X-translation

Mode 4: X-rotation

Mode 5: Z-rotation

Mode 6: Y-translation

(Mode 6 is vertical vibration, which is the most important mode.)

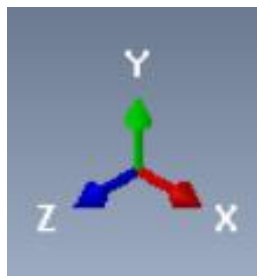


Figure 3.2.2: coordinate

3.2.2 Results

Nylon101:

| thickne ss/mm | mode1 frequency /HZ | mode2 frequency /HZ | mode3 frequency /HZ | mode4 frequency /HZ | mode5 frequency /HZ | mode6 frequency/ HZ |
|------------------|---------------------------|---------------------------|---------------------------|---------------------------|---------------------------|---------------------------|
| 1 | 4707.8 | 4807.7 | 6829.2 | 7050.5 | 7702.2 | 8277.4 |
| 2 | 4037.6 | 4749.7 | 5791.2 | 7006.1 | 7308.8 | 8210.9 |
| 3 | 3591.7 | 4704.2 | 5067 | 6970.3 | 7123 | 8153.8 |
| 4 | 3267.7 | 4665.4 | 4550.4 | 6935.9 | 7006.7 | 8095.1 |
| 5 | 3016.9 | 4630.4 | 4160.2 | 6899.6 | 6922.1 | 8024.2 |

Table 1:nylon101

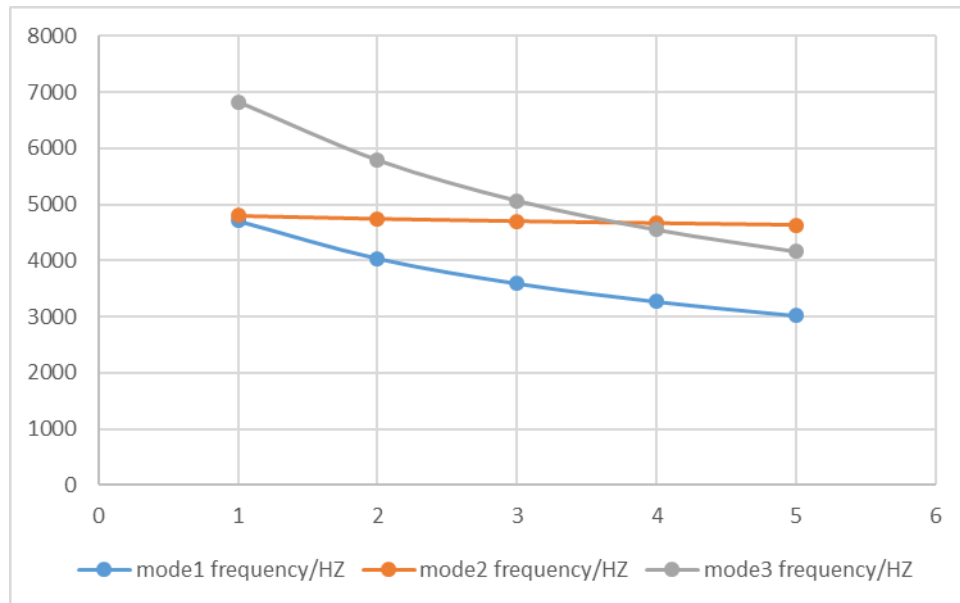


Figure 3.2.3:natural frequency(mode1,2,3)

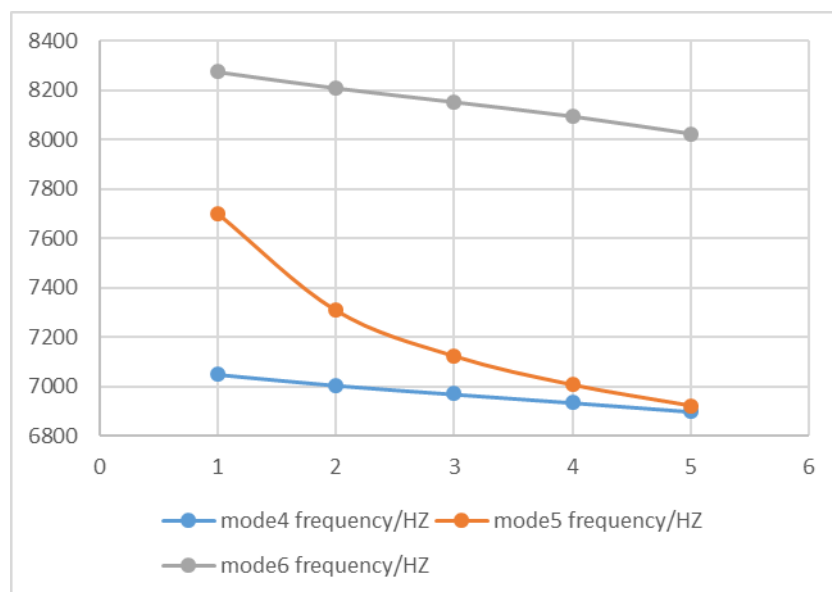


Figure 3.2.4:natural frequency(mode4,5,6)

PE low density:

| thickness/mm | mode1 frequency /HZ | mode2 frequency /HZ | mode3 frequency /HZ | mode4 frequency /HZ | mode5 frequency /HZ | mode6 frequency /HZ |
|--------------|---------------------|---------------------|---------------------|---------------------|---------------------|---------------------|
| 1 | 3415.6 | 4577.5 | 4686.8 | 4885.4 | 6975.5 | 7148.6 |
| 2 | 2610.9 | 3378.7 | 4523.7 | 3523.1 | 6833.1 | 6788.1 |
| 3 | 2170.6 | 2770.1 | 4340.2 | 2889 | 6500.8 | 5991.5 |
| 4 | 1884.4 | 2389.4 | 4137.9 | 2496.7 | 6091.4 | 5234.9 |
| 5 | 1679.2 | 2124.6 | 3937.4 | 2225.2 | 5809.3 | 4689.3 |

Table 2:PE low density

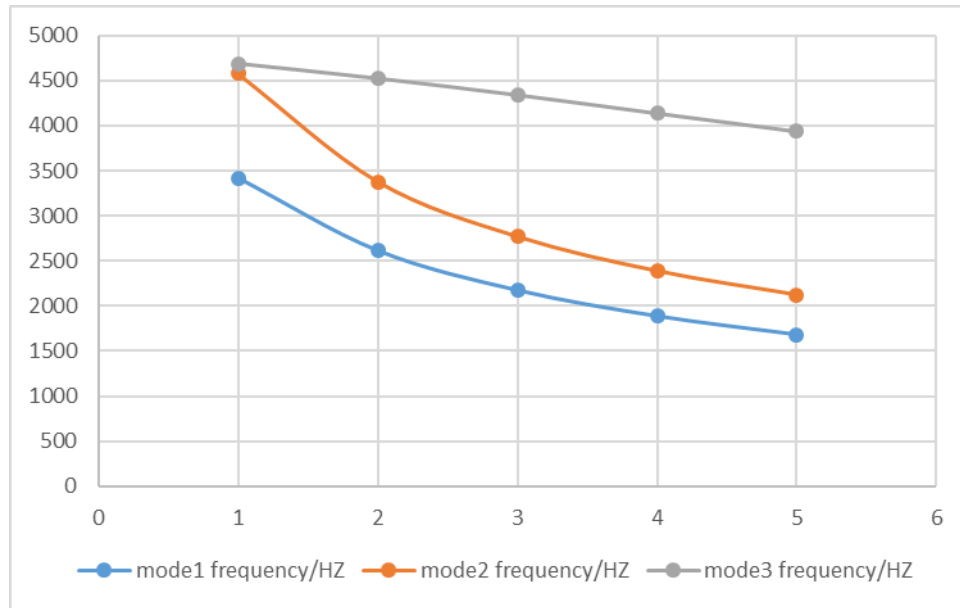


Figure 3.2.5: natural frequency(mode1,2,3)

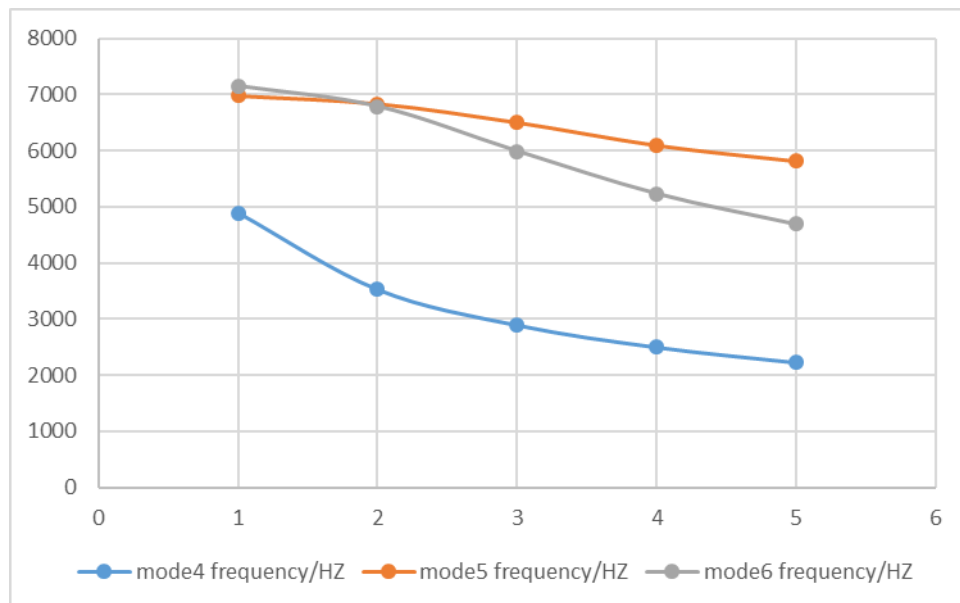


Figure 3.2.6: natural frequency(mode4,5,6)

Nitrile rubber:

| thickness/mm | mode1 frequency /HZ | mode2 frequency /HZ | mode3 frequency /HZ | mode4 frequency /HZ | mode5 frequency /HZ | mode6 frequency /HZ |
|--------------|---------------------|---------------------|---------------------|---------------------|---------------------|---------------------|
| 1 | 954.32 | 1049.2 | 1114.7 | 3189.2 | 3731.1 | 3826.3 |
| 2 | 671.81 | 724.56 | 778.77 | 2045.9 | 2420.5 | 2833.1 |
| 3 | 544.46 | 566.95 | 625.65 | 1500.9 | 1819.4 | 2293 |
| 4 | 468.45 | 465.87 | 531.76 | 1190.6 | 1448.6 | 1941.6 |
| 5 | 416.45 | 396.1 | 465.94 | 1003.8 | 1203.6 | 1676.8 |

Table 3:nitrile rubber

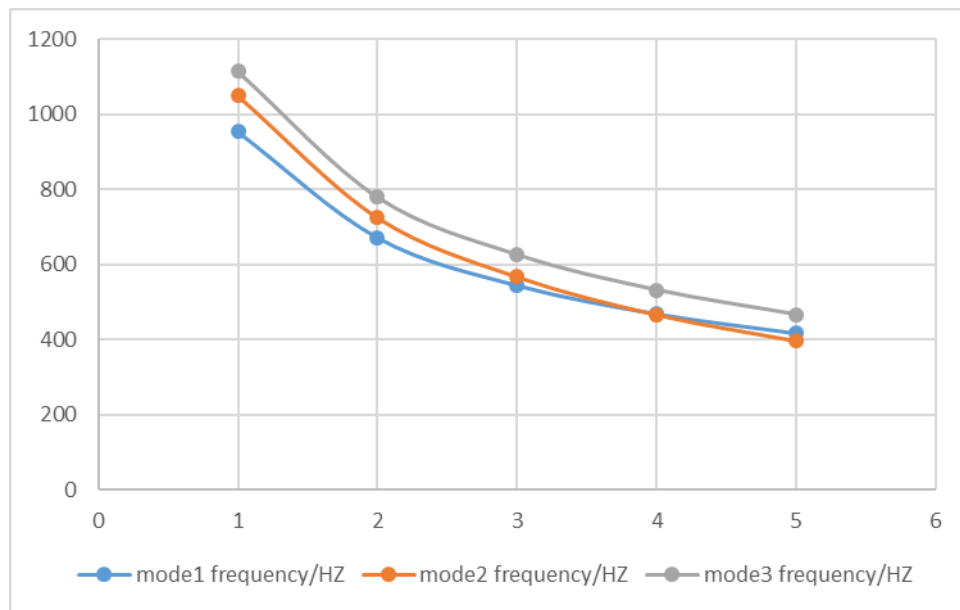


Figure 3.2.7:natural frequency(mode1,2,3)

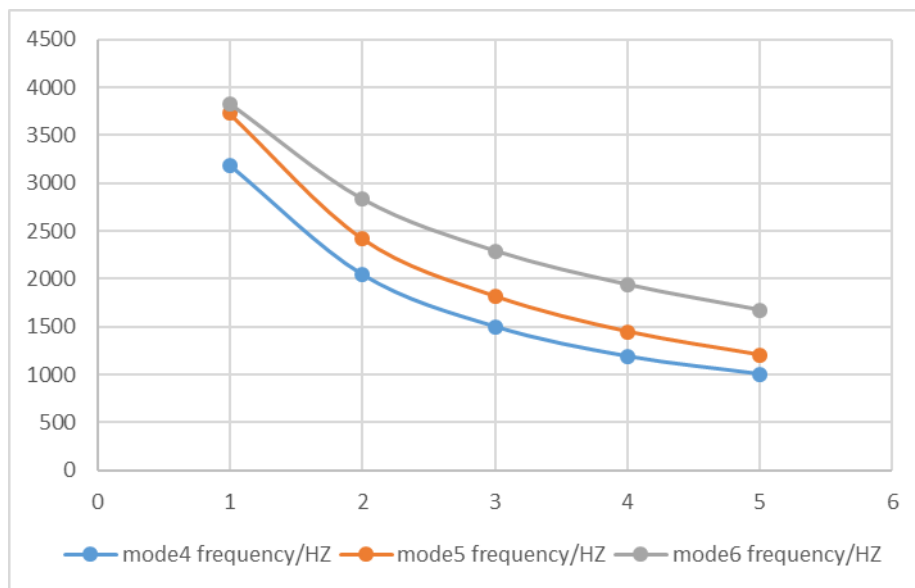


Figure 3.2.8: natural frequency(mode4,5,6)

Silicone:

| thickness/mm | mode1 frequency /HZ | mode2 frequency /HZ | mode3 frequency /HZ | mode4 frequency /HZ | mode5 frequency /HZ | mode6 frequency /HZ |
|--------------|---------------------|---------------------|---------------------|---------------------|---------------------|---------------------|
| 1 | 489.13 | 554.63 | 578.07 | 1820.9 | 2119.6 | 2683.9 |
| 2 | 343.89 | 379.1 | 403.38 | 1102.5 | 1397.2 | 1886.8 |
| 3 | 278.48 | 294.43 | 323.39 | 782.78 | 1005.3 | 1458.8 |
| 4 | 239.44 | 240.69 | 274.17 | 611.61 | 773.19 | 1162.6 |
| 5 | 212.73 | 203.97 | 239.7 | 512.17 | 629.25 | 953.59 |

Table 4:silicone

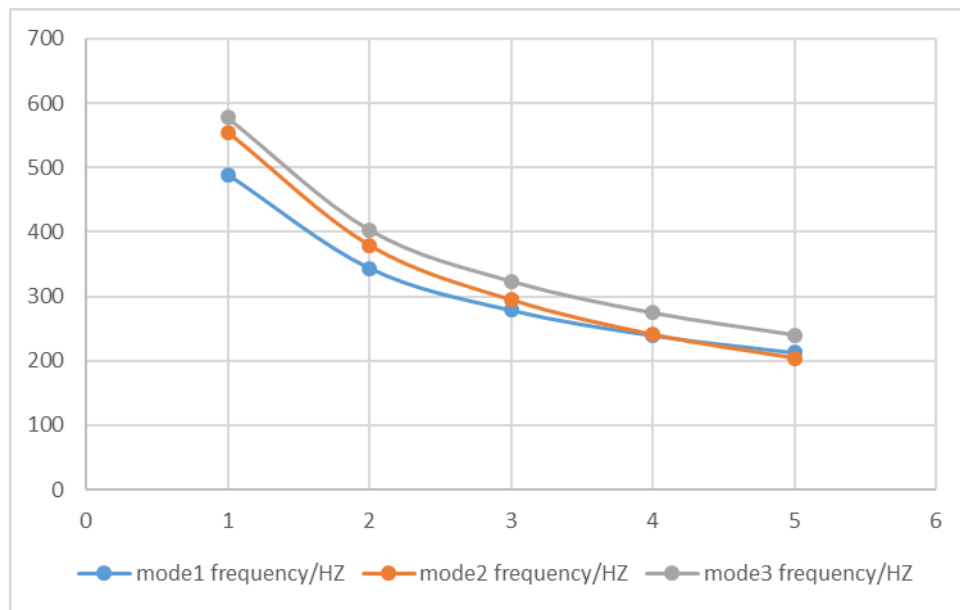


Figure 3.2.9:natural frequency(mode1,2,3)

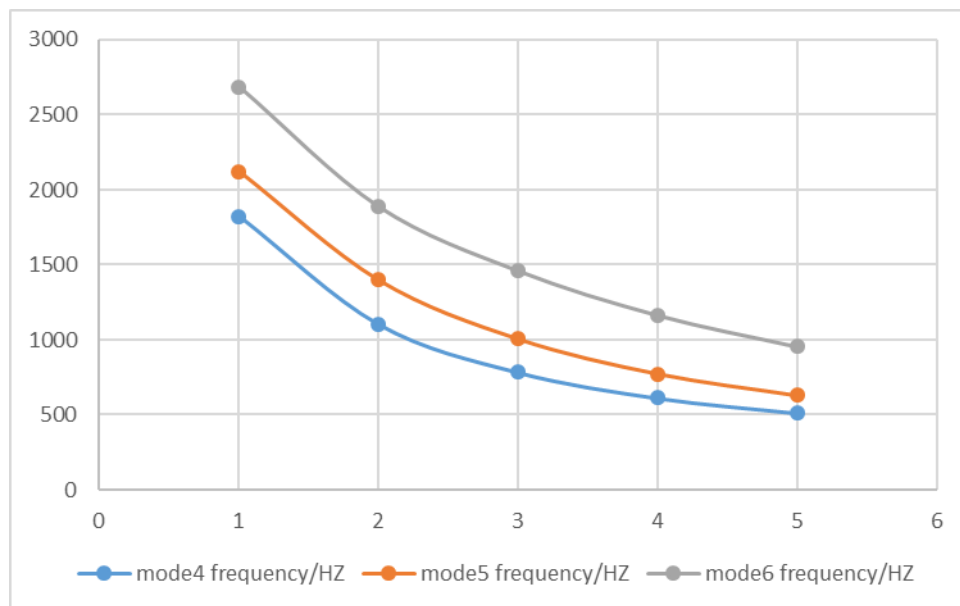


Figure 3.2.10:natural frequency(mode4,5,6)

3.2.3 Conclusion

From the results, it is clear that the increase of thickness can greatly reduce natural frequency. The stiffness (Young's modulus) is important too, in real application it cannot be changed, so at the beginning soft material should be used, such as silicone.

3.3 Polynomial reduced model

Because of the nonlinearity of rubber material, to get better simulation, Polynomial reduced model is introduced in Abaqus. The results of simulation and real tests are compared to verify if the Polynomial reduced model is reliable.

3.3.1 Configuration of real tests

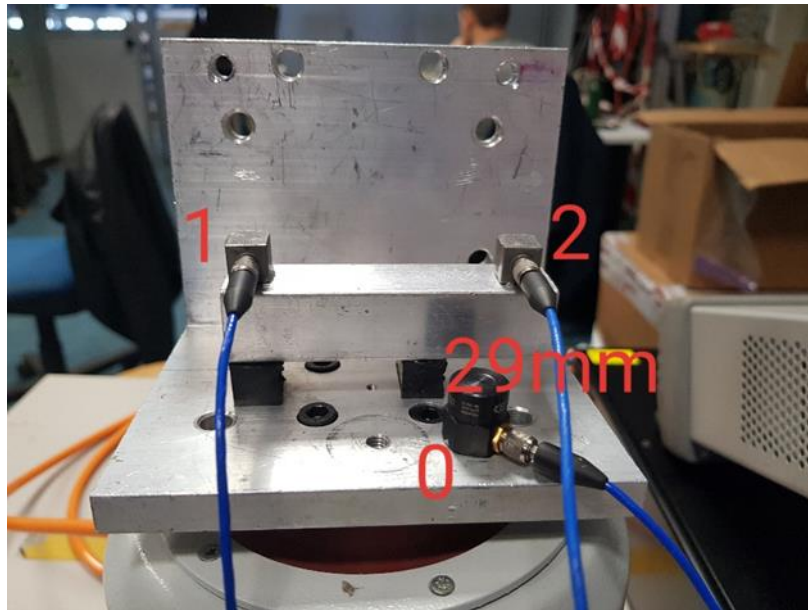


Figure 3.3.1:real test

In real tests, a beam made of aluminum is placed on the shaker. Feet made of rubber “Sorbothane 50” are glued to the surface of shaker and the bottom of the beam. Accelerometers are placed the top of beam, and one reference sensor placed on the shaker. Through the transfer function between top sensor and reference sensor, the natural frequency can be found.

3.3.2 Configuration of simulation

In the simulation, three different materials are used, so the parameters of them are needed.

Aluminum:

Density: 2.7g/cm^3

Young's modulus: 70000Mpa

Poisson's ratio: 0.3

Sorbothane 50:

Density: 1.345g/cm^3

Hyperelastic

Material type: Isotropic Anisotropic

Strain energy potential: Reduced Polynomial

Input source: Test data Coefficients

Moduli time scale (for viscoelasticity): Long-term

Strain energy potential order: 3

Use temperature-dependent data

Data

| | C10 | C20 | C30 | D1 | D2 |
|---|----------|------------|------------|----|----|
| 1 | 0.027939 | -0.0002698 | 2.6552E-05 | 0 | 0 |

Figure 3.3.2:parameters

Using Polynomial reduced model, elastic parameters such as Young's modulus and Poisson's ratio are no longer needed, coefficients of model are used instead: $N=3$, $C_{10}=2.7939e-2$, $C_{20}=-2.6980e-4$, $C_{30}=2.6552e-5$.

Sensor:

The mass of the sensors is small, but they may affect the frequency. Sensors on the top are PCB 333B30. The size is 10x10x10mm. The weight is 4g. Considering that the sensor has empty space inside and has complex structure, a material called "sensor" is simply defined: Density: 4g/cm³, Young's modulus:206000Mpa, Poisson's ratio:0.3(almost no deformation, so treated as rigid steel)

Reference sensor (on the shaker) is a Kistler accelerometer, but it is on the shaker, so its mass does not affect the response of the system. In the simulation, the reference sensor is not included.

3.3.3 Comparison of different cases

To verify Polynomial reduced model, four different cases are created. In the test the sweep is from 5Hz to 200Hz, so only frequency before 200HZ counts. In part 1,2,3, Mode 4 is vertical vibration on right foot(sensor2), mode 6 is vertical vibration on left foot(sensor1). In part 4 ,mode 5 and mode 6 are vertical vibration.

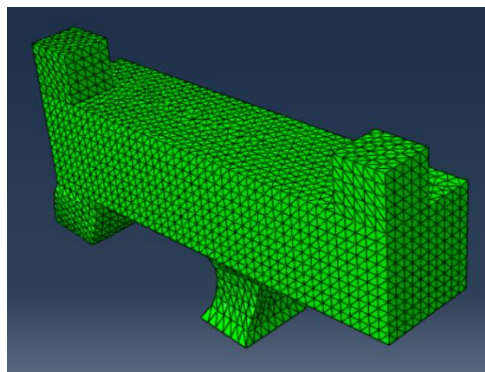


Figure 3.3.3: mode 4 of part 1 2 3

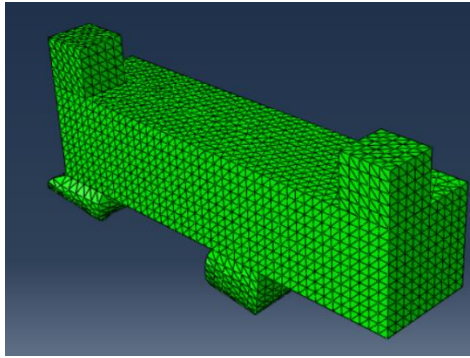


Figure 3.3.4: mode 6 of part 1 2 3

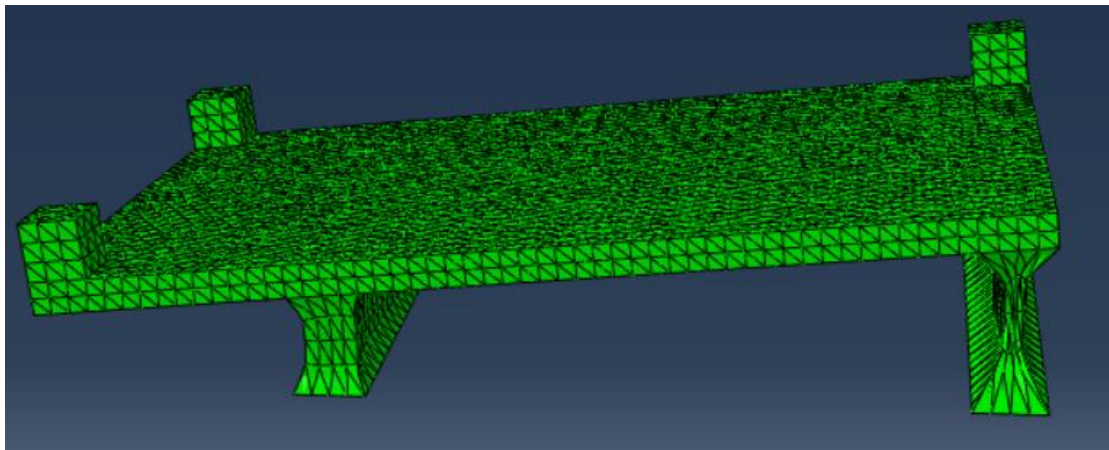


Figure 3.3.5: mode 5 of part 4

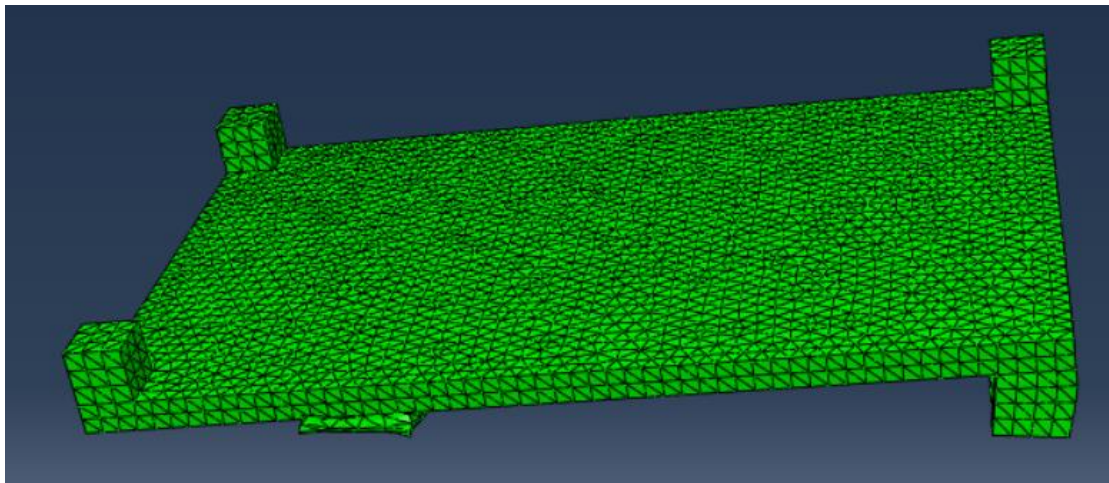


Figure 3.3.6: mode 6 of part 4

Part 1 85x20x20

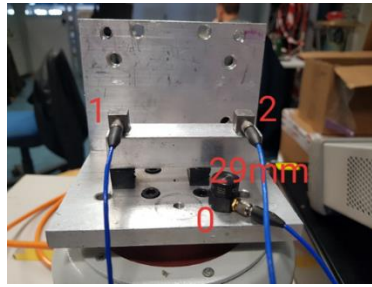


Figure 3.3.7: part 1

The distance between the right surface of the right foot and the right surface of the part is 29mm. Feet: 12x12x20mm

Natural frequency in simulation:

| Index | Description |
|-------|--|
| 0 | Increment 0: Base State |
| 1 | Mode 1: Value = 5049.6 Freq = 11.310 (cycles/time) |
| 2 | Mode 2: Value = 15225. Freq = 19.638 (cycles/time) |
| 3 | Mode 3: Value = 16434. Freq = 20.403 (cycles/time) |
| 4 | Mode 4: Value = 48646. Freq = 35.103 (cycles/time) |
| 5 | Mode 5: Value = 1.16065E+05 Freq = 54.221 (cycles/time) |
| 6 | Mode 6: Value = 1.46202E+05 Freq = 60.855 (cycles/time) |
| 7 | Mode 7: Value = 2.65684E+06 Freq = 259.42 (cycles/time) |
| 8 | Mode 8: Value = 2.70888E+06 Freq = 261.95 (cycles/time) |
| 9 | Mode 9: Value = 2.73898E+06 Freq = 263.40 (cycles/time) |
| 10 | Mode 10: Value = 2.75543E+06 Freq = 264.19 (cycles/time) |

Figure 3.3.8: natural frequency in simulation

Natural frequency in test:

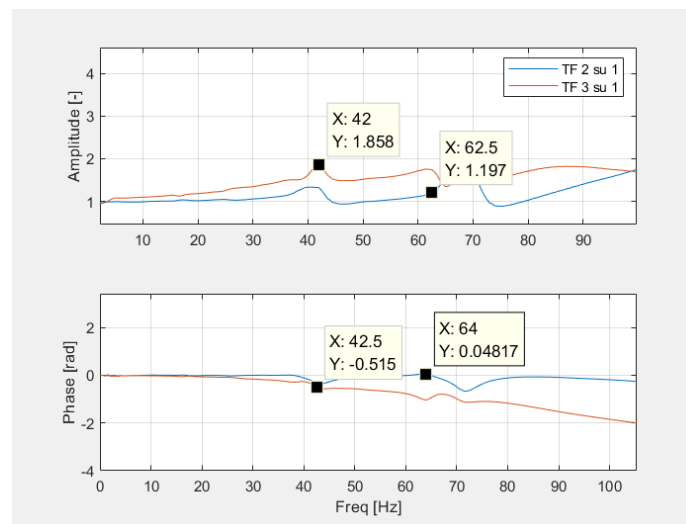


Figure 3.3.9: natural frequency in test

The frequency in simulation is 35HZ and 60HZ, while in the test they are 42HZ and 64HZ.

Part 2 123x40x15

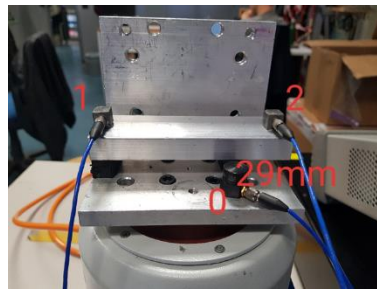


Figure 3.3.10:part 2

The distance between the right surface of the right foot and the right surface of the part is 29mm. Feet: 12x12x40mm

Natural frequency in simulation:

| Index | Description |
|-------|--|
| 0 | Increment 0: Base State |
| 1 | Mode 1: Value = 11856. Freq = 17.330 (cycles/time) |
| 2 | Mode 2: Value = 15348. Freq = 19.718 (cycles/time) |
| 3 | Mode 3: Value = 26708. Freq = 26.010 (cycles/time) |
| 4 | Mode 4: Value = 72333. Freq = 42.804 (cycles/time) |
| 5 | Mode 5: Value = 96467. Freq = 49.432 (cycles/time) |
| 6 | Mode 6: Value = 1.52771E+05 Freq = 62.207 (cycles/time) |
| 7 | Mode 7: Value = 2.46887E+06 Freq = 250.07 (cycles/time) |
| 8 | Mode 8: Value = 2.50211E+06 Freq = 251.75 (cycles/time) |
| 9 | Mode 9: Value = 2.50510E+06 Freq = 251.90 (cycles/time) |
| 10 | Mode 10: Value = 2.50783E+06 Freq = 252.04 (cycles/time) |

Figure 3.3.11: natural frequency in simulation

Natural frequency in test:

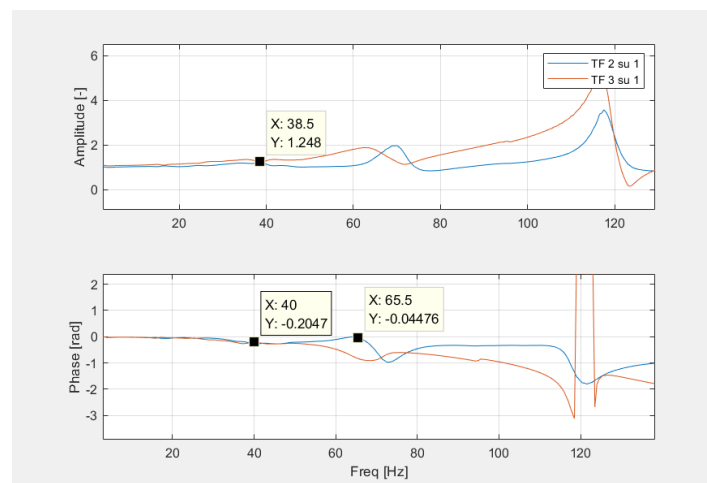


Figure 3.3.12: natural frequency in test

The frequency in simulation is 43HZ and 62HZ, while in the test they are 40HZ and 65HZ.

Part 3 161x40x4.5

The distance between the right surface of the right foot and the right surface of the part is 53mm. Feet: 12x12x40mm

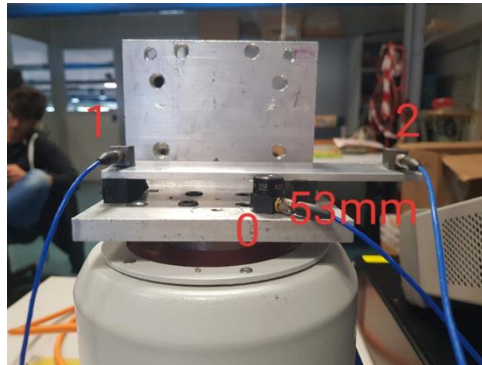


Figure 3.3.13:part 3

Natural frequency in simulation:

| Index | Description |
|-------|--|
| 0 | Increment 0: Base State |
| 1 | Mode 1: Value = 24819. Freq = 25.074 (cycles/time) |
| 2 | Mode 2: Value = 36154. Freq = 30.262 (cycles/time) |
| 3 | Mode 3: Value = 62668. Freq = 39.842 (cycles/time) |
| 4 | Mode 4: Value = 1.24444E+05 Freq = 56.144 (cycles/time) |
| 5 | Mode 5: Value = 2.01244E+05 Freq = 71.397 (cycles/time) |
| 6 | Mode 6: Value = 3.40536E+05 Freq = 92.876 (cycles/time) |
| 7 | Mode 7: Value = 2.47021E+06 Freq = 250.14 (cycles/time) |
| 8 | Mode 8: Value = 2.50376E+06 Freq = 251.84 (cycles/time) |
| 9 | Mode 9: Value = 2.50690E+06 Freq = 251.99 (cycles/time) |
| 10 | Mode 10: Value = 2.55680E+06 Freq = 254.49 (cycles/time) |

Figure 3.3.14: natural frequency in simulation

Natural frequency in test:

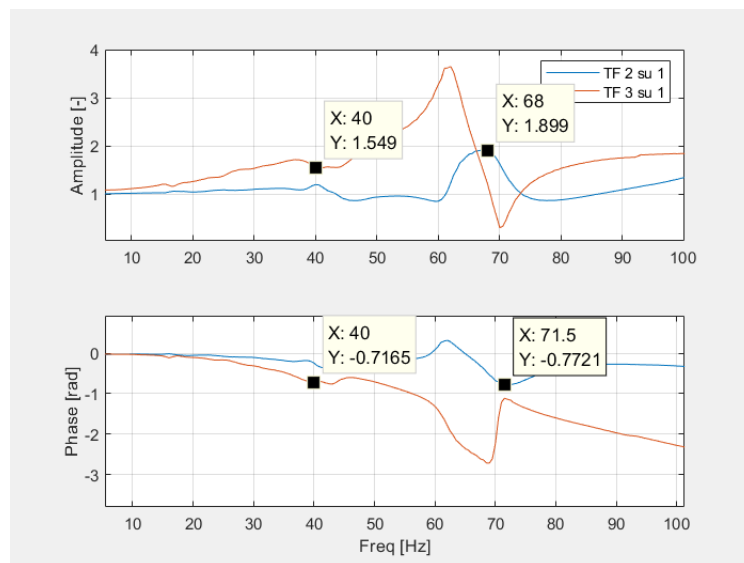


Figure 3.3.15: natural frequency in test

Part 4 165x100x5.5

The distance between the right surface of the right foot and the right surface of the part is 43mm. Feet: 12x12x64mm

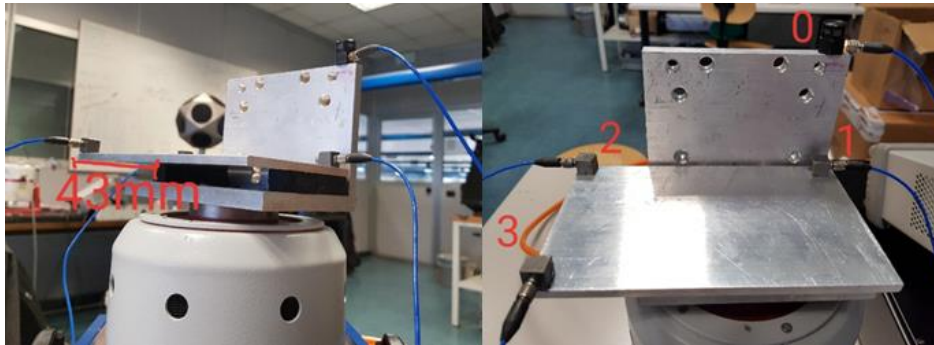


Figure 3.3.16: part 4

Natural frequency in simulation:

| Index | Description |
|-------|--|
| 0 | Increment 0: Base State |
| 1 | Mode 1: Value = 14524. Freq = 19.181 (cycles/time) |
| 2 | Mode 2: Value = 20687. Freq = 22.891 (cycles/time) |
| 3 | Mode 3: Value = 29834. Freq = 27.490 (cycles/time) |
| 4 | Mode 4: Value = 41517. Freq = 32.429 (cycles/time) |
| 5 | Mode 5: Value = 1.18105E+05 Freq = 54.696 (cycles/time) |
| 6 | Mode 6: Value = 2.50754E+05 Freq = 79.697 (cycles/time) |
| 7 | Mode 7: Value = 2.47253E+06 Freq = 250.26 (cycles/time) |
| 8 | Mode 8: Value = 2.48533E+06 Freq = 250.91 (cycles/time) |
| 9 | Mode 9: Value = 2.48970E+06 Freq = 251.13 (cycles/time) |
| 10 | Mode 10: Value = 2.52064E+06 Freq = 252.68 (cycles/time) |

Figure 3.3.17: natural frequency in simulation

Natural frequency in test:

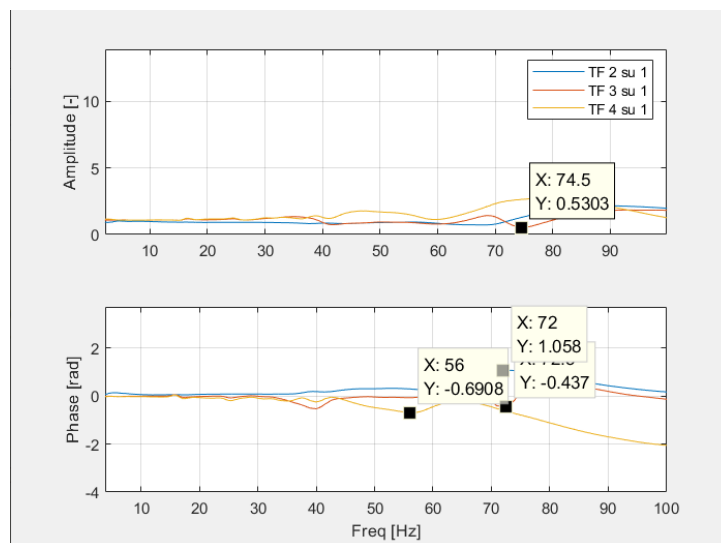


Figure 3.3.18: natural frequency in test

Conclusion:

In part 1 and part 2, because of beam shape, almost only vertical vibration is triggered, so the frequencies of mode 4 and mode 6 are close to the result of test, though error about 5 HZ occurs.

Part 3 and part 4 are more like a plate, so maybe other modes are triggered too. In part 3, the frequencies of mode 3 and mode 5 can be found in the test (both have vertical components), but the frequency of pure vertical motion is lost.

In the real test, the frequency may be the result of different modes, so it is difficult to find same frequency of a single mode; meanwhile, the test uses many sensors, each sensor will have different results, it is difficult to relate the mode frequency with the right sensor result. So, it is acceptable to have some error.

3.4 Creating of suitable model

To make the sensor work properly, the natural frequency of the whole structure should be low. The ideal value is less than 50HZ, so a suitable geometry needs to be created. The thesis creates several different models and compare them to find a best solution.

3.4.1 Common settings

The materials used to build models are steel and rubber “Sorbothane 50”.The parameters of two materials are same as those in previous chapters. Because of the symmetry, cylinder models are used. The size should be limited considering the installation:the maximum volume is from 60x60x60mm to 70x70x70mm .The aim is to reach first natural frequency lower than 50HZ on the vertical direction,with a size not so large.

3.4.2 Basic model

The simplest model is to add a layer of rubber on the bottom of the steel cylinder. The diameter is 60mm, the height of the steel part is 60mm, and the height of the rubber is 5mm.



Figure 3.4.1:basic model

With this model, the first vibration mode is not vertical. Mode 1 and mode 2 are translation in horizontal plane, mode 3 is axial torsion, mode 4 and 5 are bending, and mode 6 is vertical vibration. The natural frequency of mode 6 is 173.91 HZ.

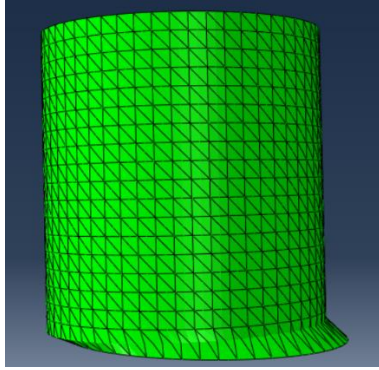


Figure 3.4.2:translation(basic model)

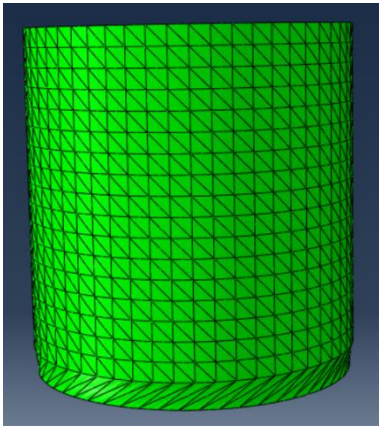


Figure 3.4.3:torsion(basic model)

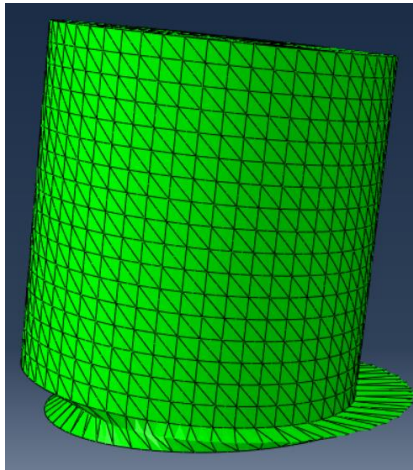


Figure 3.4.4:bending(basic model)

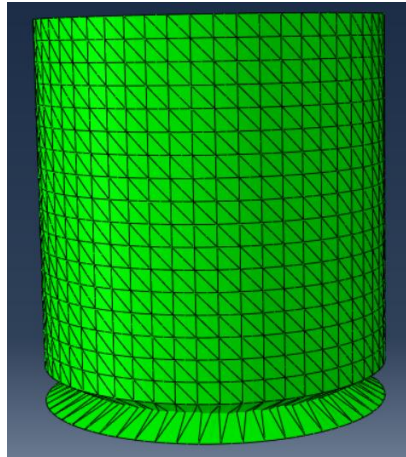


Figure 3.4.5: vertical vibration (basic model)

| Index | Description |
|-------|--|
| 0 | Increment 0: Base State |
| 1 | Mode 1: Value = 18690. Freq = 21.759 (cycles/time) |
| 2 | Mode 2: Value = 18705. Freq = 21.767 (cycles/time) |
| 3 | Mode 3: Value = 23765. Freq = 24.535 (cycles/time) |
| 4 | Mode 4: Value = 2.58194E+05 Freq = 80.871 (cycles/time) |
| 5 | Mode 5: Value = 2.59038E+05 Freq = 81.003 (cycles/time) |
| 6 | Mode 6: Value = 1.19398E+06 Freq = 173.91 (cycles/time) |
| 7 | Mode 7: Value = 1.65801E+07 Freq = 648.06 (cycles/time) |
| 8 | Mode 8: Value = 1.66664E+07 Freq = 649.74 (cycles/time) |
| 9 | Mode 9: Value = 1.66665E+07 Freq = 649.74 (cycles/time) |
| 10 | Mode 10: Value = 1.68012E+07 Freq = 652.36 (cycles/time) |

Figure 3.4.6: natural frequency (basic model)

Generally, other motions should be limited, because the focus point is vertical vibration.

3.4.3 Model with steel shell

To reduce the influences of unwanted vibration modes, the motions in other directions need to be constrained. A steel shell is added outside the steel cylinder, and rubber is used not only under the steel cylinder, but also around the side face. So, the rubber covers the steel except the top.

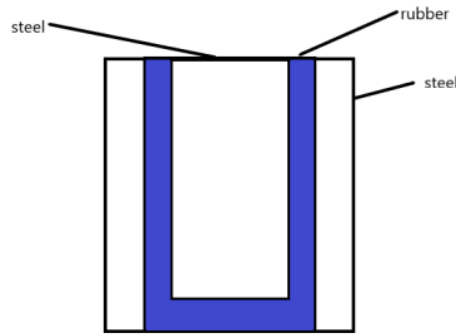


Figure 3.4.7: sketch of the model (model with steel shell)

The outer diameter of the shell is 60mm, and the inner diameter of the shell is 56mm, the height is 65mm.

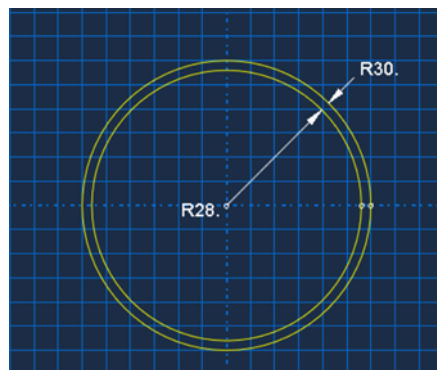


Figure 3.4.8: dimension of the shell (model with steel shell)

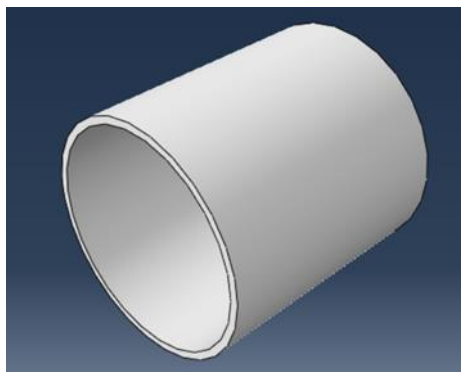


Figure 3.4.9: steel shell (model with steel shell)

The shape of the rubber part is like a cup. The thickness is 5mm both on the side face and the bottom. So, the outer diameter is 56mm and the inner diameter is 46mm. The rubber is as high as the shell, 65mm.

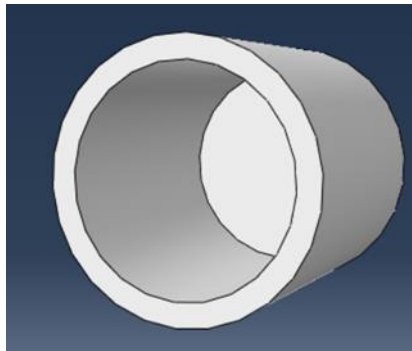


Figure 3.4.10:rubber (model with steel shell)

The diameter of the steel mass is 46mm and the height is 60mm.

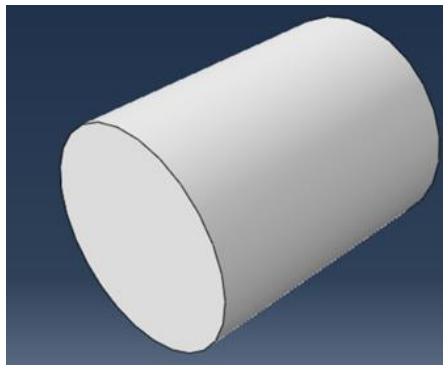


Figure 3.4.11:steel mass (model with steel shell)

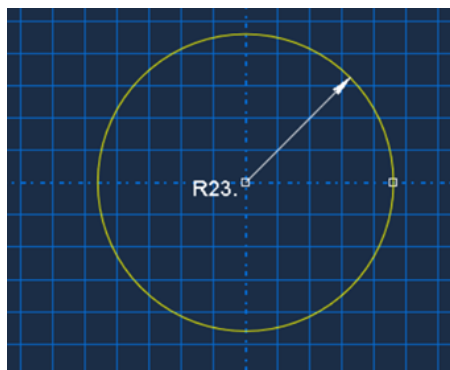


Figure 3.4.12: diameter of the steel mass (model with steel shell)

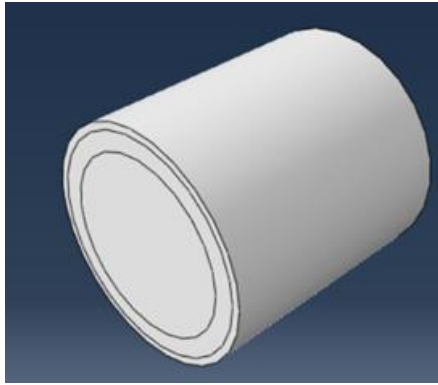


Figure 3.4.13:total model (model with steel shell)

The first vibration mode is vertical, mode 2 is torsion, and modes 3,4,5,6 are all bending. The natural frequency of mode 1 is 59.361 HZ. It is clear that the influence of unwanted vibration modes is smaller, the idea of adding a shell works; and the natural frequency of vertical vibration reduces, however, still larger than expectation. So, the model needs to be changed.

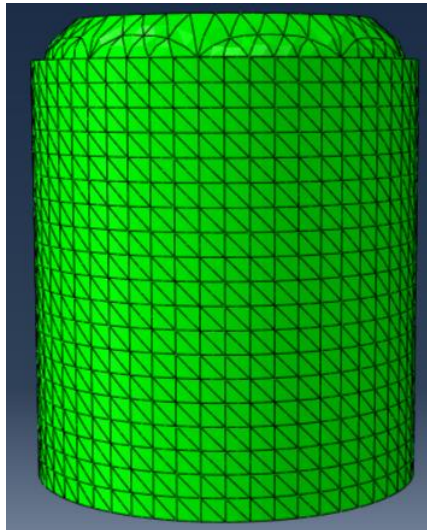


Figure 3.4.14:mode 1 (model with steel shell)

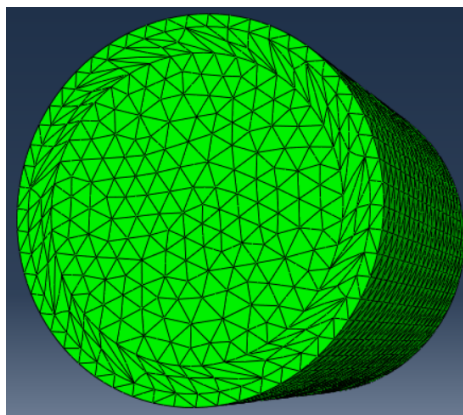


Figure 3.4.15:mode 2 (model with steel shell)

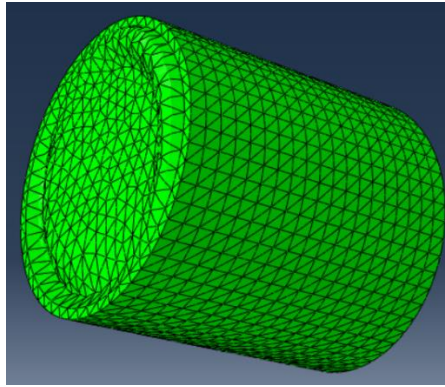


Figure 3.4.16: mode 3 (model with steel shell)

| Index | Description | | |
|-------|-------------|-------------------------|-----------------------------|
| 0 | Increment | 0: Base State | |
| 1 | Mode | 1: Value = 1.39111E+05 | Freq = 59.361 (cycles/time) |
| 2 | Mode | 2: Value = 3.30136E+05 | Freq = 91.446 (cycles/time) |
| 3 | Mode | 3: Value = 1.50460E+06 | Freq = 195.22 (cycles/time) |
| 4 | Mode | 4: Value = 1.50654E+06 | Freq = 195.35 (cycles/time) |
| 5 | Mode | 5: Value = 4.67298E+06 | Freq = 344.05 (cycles/time) |
| 6 | Mode | 6: Value = 4.67344E+06 | Freq = 344.06 (cycles/time) |
| 7 | Mode | 7: Value = 4.86895E+06 | Freq = 351.19 (cycles/time) |
| 8 | Mode | 8: Value = 5.21767E+06 | Freq = 363.55 (cycles/time) |
| 9 | Mode | 9: Value = 5.21786E+06 | Freq = 363.55 (cycles/time) |
| 10 | Mode | 10: Value = 5.61599E+06 | Freq = 377.17 (cycles/time) |

Figure 3.4.17: natural frequency (model with steel shell)

3.4.4 Model without base interaction

Obviously, the vertical vibration mainly conducts from the base to the steel mass. The first two designs use flexible material to absorb the vibration, and the effect is not so huge; so, this thesis goes further: prevent the bottom from interaction with the base. Because the rubber is tightly adhered to the steel mass, remove the rubber on the bottom, then the steel mass is hung in the air. In this way, vertical vibration can only conduct through the side face.

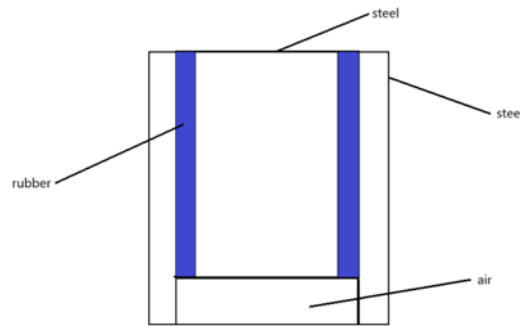


Figure 3.4.18: sketch of the model (model without base interaction)

The shape and dimension of the steel shell and the steel mass are the same as in the last model. The outer diameter of the shell is 60mm, and the inner diameter of the shell is 56mm, the height is 65mm. The diameter of the steel mass is 46mm and the height is 60mm.

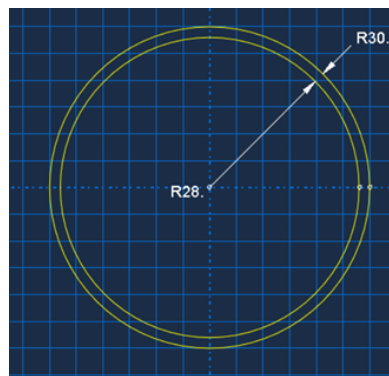


Figure 3.4.19: dimension of the shell (model without base interaction)

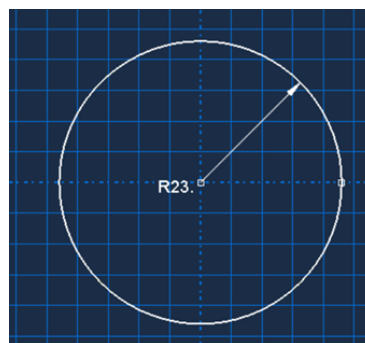


Figure 3.4.20: diameter of steel mass (model without base interaction)

The difference is the rubber: the outer diameter of the rubber is 56mm, and the inner diameter of the rubber is 46mm, the height is 60mm. Then, the distance between the bottom and the base is 5mm.

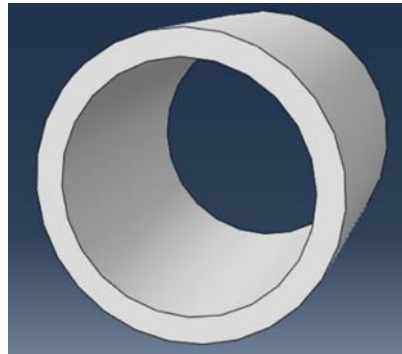


Figure 3.4.21:rubber (model without base interaction)

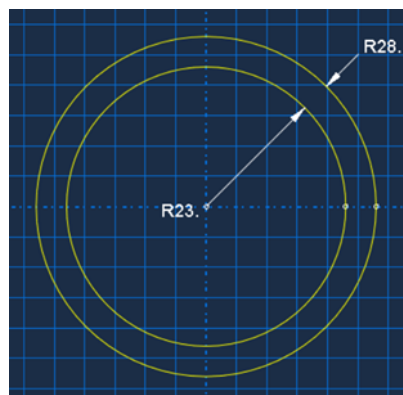


Figure 3.4.22: dimension of rubber (model without base interaction)

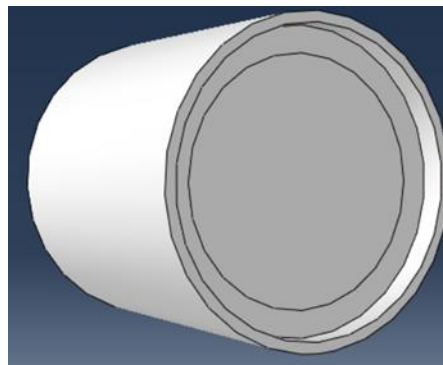


Figure 3.4.23:total model (model without base interaction)

The first vibration mode is vertical, mode 2 is torsion, and modes 3,4,5,6 are all bending. The natural frequency of mode 1 is 57.789HZ. Compared with last model, in vertical direction, the natural frequency is reduced a bit. And in some modes, the natural frequencies increase, that's because those modes are in other unwanted directions and they are affected by the rubber on the bottom.

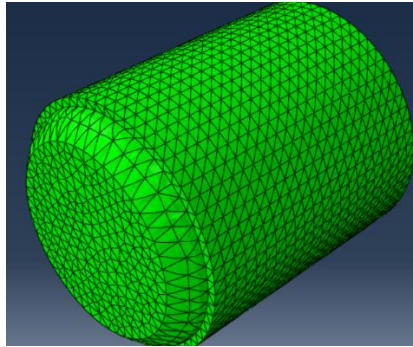


Figure 3.4.24: mode 1 (model without base interaction)

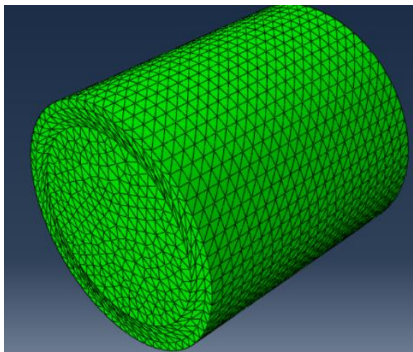


Figure 3.4.25: mode 2 (model without base interaction)

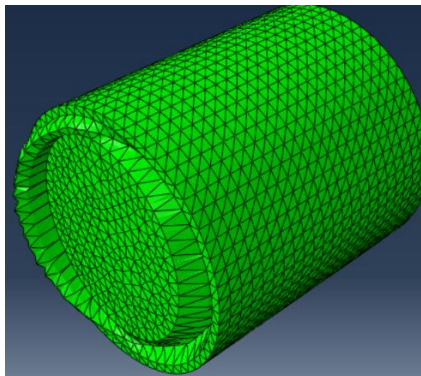


Figure 3.4.26: mode 3 (model without base interaction)

| Index | Description | |
|-------|-------------|---|
| 0 | Increment | 0: Base State |
| 1 | Mode | 1: Value = 1.31842E+05 Freq = 57.789 (cycles/time) |
| 2 | Mode | 2: Value = 3.17083E+05 Freq = 89.620 (cycles/time) |
| 3 | Mode | 3: Value = 1.34993E+06 Freq = 184.92 (cycles/time) |
| 4 | Mode | 4: Value = 1.35503E+06 Freq = 185.27 (cycles/time) |
| 5 | Mode | 5: Value = 4.69015E+06 Freq = 344.68 (cycles/time) |
| 6 | Mode | 6: Value = 4.70420E+06 Freq = 345.19 (cycles/time) |
| 7 | Mode | 7: Value = 1.65452E+07 Freq = 647.38 (cycles/time) |
| 8 | Mode | 8: Value = 1.65477E+07 Freq = 647.42 (cycles/time) |
| 9 | Mode | 9: Value = 1.65997E+07 Freq = 648.44 (cycles/time) |
| 10 | Mode | 10: Value = 1.66011E+07 Freq = 648.47 (cycles/time) |

Figure 3.4.27: natural frequency (model without base interaction)

3.4.5 Improved model

The way of hanging the mass in the air works, but the result needs to be smaller. Generally, the natural frequency can be expressed as $\omega = \sqrt{\frac{k}{m}}$, while k is stiffness, m is the mass. It's difficult to change the stiffness because the material is already determined, so, the mass should be increased to get lower natural frequency. The density of material is constant, and the only way is to increase the size. The density of mass is much higher than rubber, so, the aim is to make the steel mass as big as possible. The idea is that: instead of using a large rubber, using just two short rubber rings, and more space can be used for the steel mass.

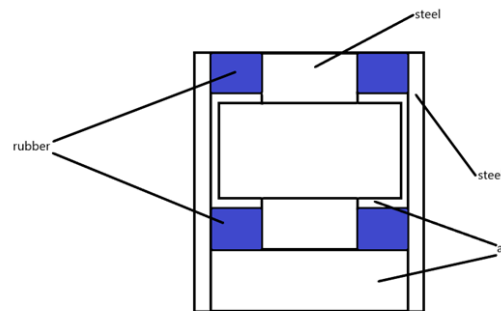


Figure 3.4.28: sketch of the model (improved model)

The outer diameter of steel shell is 60mm and the inner diameter is 56mm; the height is 60mm, shorter than previous models, because a much better performance of this model is needed, which needs smaller space.

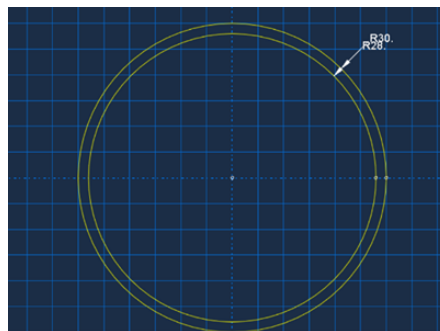


Figure 3.4.29: dimension of the shell (improved model)

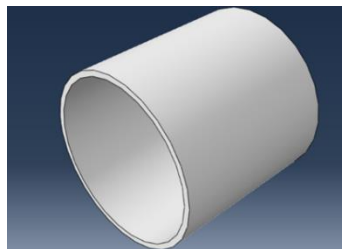


Figure 3.4.30: steel shell (improved model)

The outer diameter of two rubber rings is 56mm and the inner diameter is 28mm; the height is 10mm.

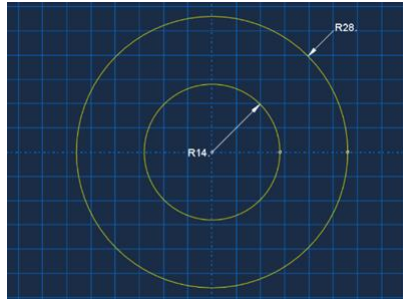


Figure 3.4.31: dimension of rubber ring (improved model)

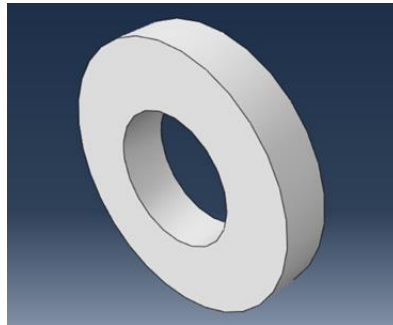


Figure 3.4.32:rubber ring (improved model)

The steel mass can be seen as one big cylinder with one small cylinder inside. The diameter of the big cylinder is 50mm, the diameter of the small cylinder is 28mm. The height of the big cylinder is 32mm, and the height of each smaller part is 12mm, so the total height is 56mm. Rubber rings are fixed on two sides, so the free space between rubber ring and steel mass is 2mm.

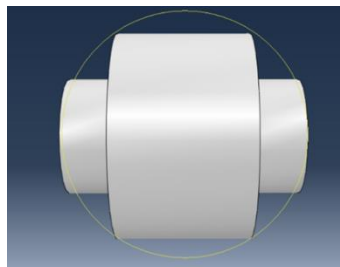


Figure 3.4.33:steel mass (improved model)

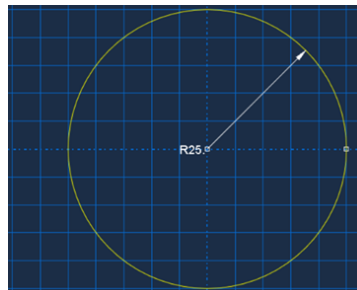


Figure 3.4.34: diameter of big cylinder (improved model)

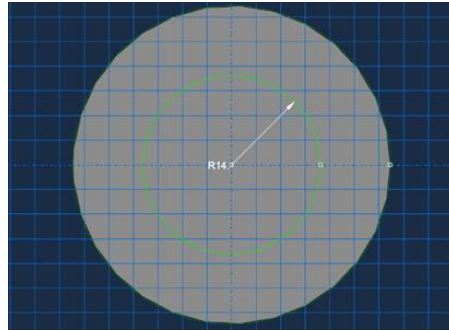


Figure 3.4.35: diameter of small cylinder (improved model)

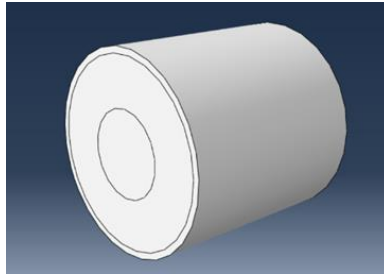


Figure 3.4.36: total model (improved model)

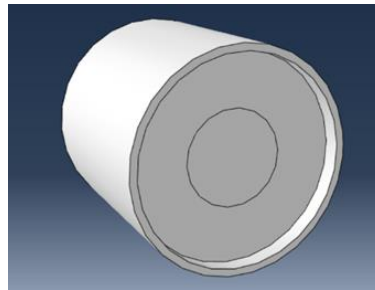


Figure 3.4.37: bottom view (improved model)

The first vibration mode is vertical, and the natural frequency reduces to 16.484 HZ; mode 2 is torsion; mode 3 and 4 are translation, but the motion of steel mass is out of boundary, which means the mass may collide with the shell in real case; mode 5 and 6 are bending. Whatever, in this model, the natural frequency in vertical direction is reduced greatly.

| Index | Description |
|-------|--|
| 0 | Increment 0: Base State |
| 1 | Mode 1: Value = 10728. Freq = 16.484 (cycles/time) |
| 2 | Mode 2: Value = 22048. Freq = 23.632 (cycles/time) |
| 3 | Mode 3: Value = 43593. Freq = 33.230 (cycles/time) |
| 4 | Mode 4: Value = 43595. Freq = 33.231 (cycles/time) |
| 5 | Mode 5: Value = 83944. Freq = 46.112 (cycles/time) |
| 6 | Mode 6: Value = 84033. Freq = 46.136 (cycles/time) |
| 7 | Mode 7: Value = 1.71935E+06 Freq = 208.69 (cycles/time) |
| 8 | Mode 8: Value = 1.73921E+06 Freq = 209.89 (cycles/time) |
| 9 | Mode 9: Value = 1.74697E+06 Freq = 210.36 (cycles/time) |
| 10 | Mode 10: Value = 1.75378E+06 Freq = 210.77 (cycles/time) |

Figure 3.4.38: natural frequency (improved model)

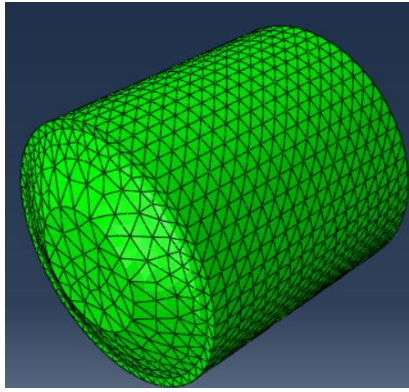


Figure 3.4.39: mode 1 (improved model)

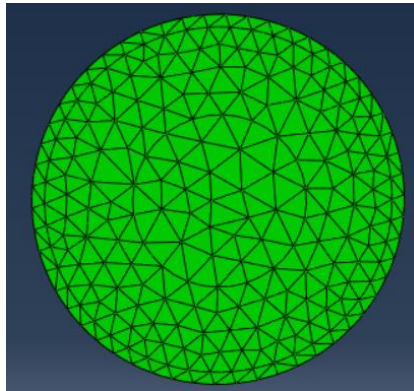


Figure 3.4.40: mode 2 (improved model)

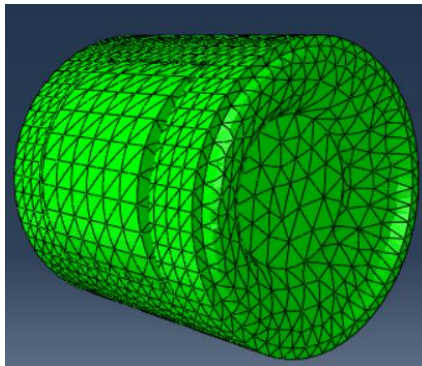


Figure 3.4.41: mode 3 (improved model)

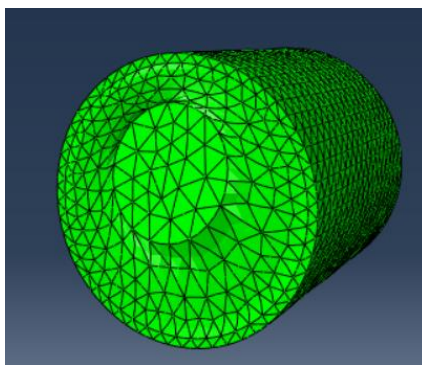


Figure 3.4.42: mode 5 (improved model)

3.4.6 Improved model with larger size

To avoid the possible collision, the total size is increased a bit, to get more space between the shell and the mass. The shape of different parts and the whole structure is the same, so those figures (sketch of model, shell, rubber ring, steel mass, total model and bottom view) are omitted.

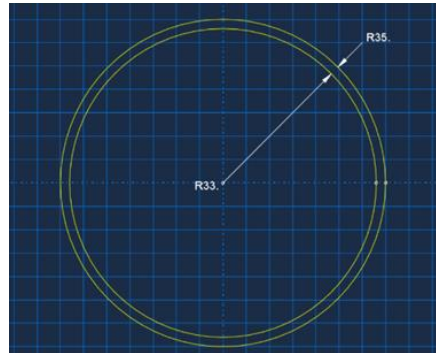


Figure 3.4.43: dimension of shell (improved model with larger size)

The outer diameter of steel shell is 70mm and the inner diameter is 66mm; the height is 60mm.

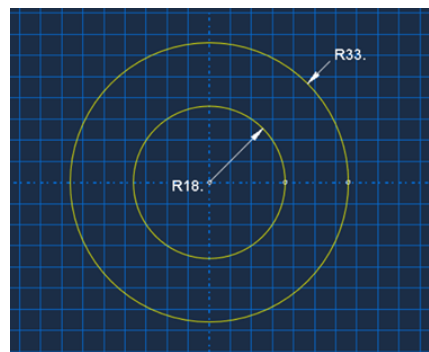


Figure 3.4.44: dimension of rubber ring (improved model with larger size)

The outer diameter of two rubber rings is 66mm and the inner diameter is 36mm, each height is 10mm.

The steel mass can be seen as one big cylinder with one small cylinder inside. The diameter of the big cylinder is 50mm, the diameter of the small cylinder is 36mm. The height of the big cylinder is 32mm, and the height of each smaller part is 12mm, so the total height is 56mm. Rubber rings are fixed on two sides, so the free space between rubber ring and steel mass is 2mm.

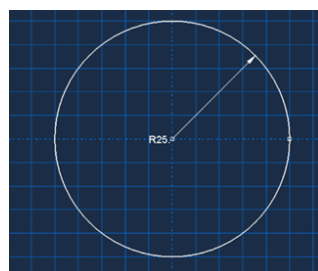


Figure 3.4.45: diameter of bigger cylinder (improved model with larger size)

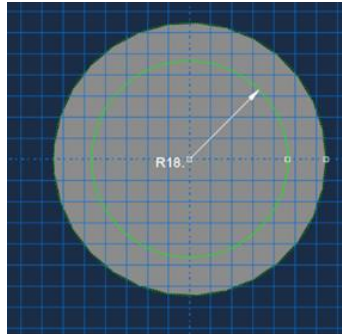


Figure 3.4.46: diameter of smaller cylinder (improved model with larger size)

The first vibration mode is vertical, and the natural frequency reduces to 16.337 HZ; mode 2 is torsion; mode 3 and 4 are translation, with little possibility of collision; mode 5 and 6 are bending. With this model, the low natural frequency with little collision can be reached, but it needs more space.

| Index | Description |
|-------|--|
| 0 | Increment 0: Base State |
| 1 | Mode 1: Value = 10536. Freq = 16.337 (cycles/time) |
| 2 | Mode 2: Value = 34308. Freq = 29.479 (cycles/time) |
| 3 | Mode 3: Value = 44546. Freq = 33.591 (cycles/time) |
| 4 | Mode 4: Value = 44558. Freq = 33.596 (cycles/time) |
| 5 | Mode 5: Value = 79170. Freq = 44.782 (cycles/time) |
| 6 | Mode 6: Value = 79177. Freq = 44.784 (cycles/time) |
| 7 | Mode 7: Value = 1.48618E+06 Freq = 194.02 (cycles/time) |
| 8 | Mode 8: Value = 1.50423E+06 Freq = 195.20 (cycles/time) |
| 9 | Mode 9: Value = 1.50551E+06 Freq = 195.28 (cycles/time) |
| 10 | Mode 10: Value = 1.50755E+06 Freq = 195.41 (cycles/time) |

Figure 3.4.47: natural frequency (improved model with larger size)

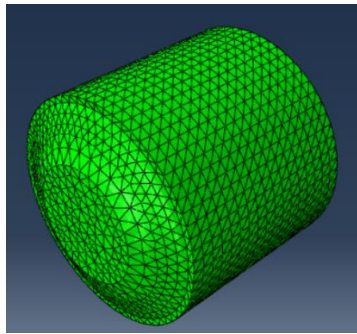


Figure 3.4.48: mode 1 (improved model with larger size)

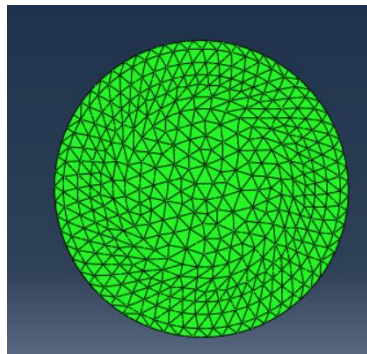


Figure 3.4.49: mode 2 (improved model with larger size)

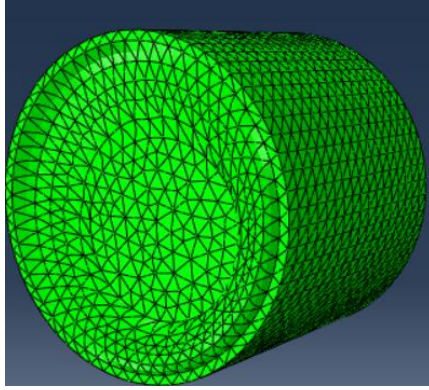


Figure 3.4.50: mode 3 (improved model with larger size)

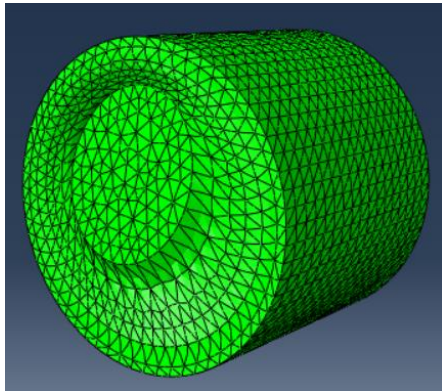


Figure 3.4.51: Figure 3.4.50: mode 5 (improved model with larger size)

3.5 Dynamic analysis

Except for the natural frequency, using the simulation, some dynamic analysis can be carried.

3.5.1 Collision risk assessment

In the improved model, there is the risk of collision in the natural frequency analysis. However, it is not necessarily that the collision must happen in the real case. The real situation will be affected by the input signal, those dangerous modes may not be triggered.

The random gaussian noise is used as the input signal. In the real case, the vibration is mainly in vertical direction, so the input is assumed as vertical acceleration only.

The highest natural frequency of first 10 modes are around 200 HZ. To catch those modes, the frequency range should be higher than 200 HZ. Choosing the sampling frequency of 800 HZ, the frequency range is up to 400 HZ. To save time, low pass filter can be used to cut the signal in the frequency range higher than 200 HZ. However, higher frequency range is helpful during the analysis, so it is a balance between speed and precision. In this case, a low pass filter of 300 HZ is used, so the range of signal is reduced to 300 HZ. Finally, the signal is a gaussian noise, the length is 1 second, the range is up to 300 HZ while the sampling frequency is 800 HZ.

The time history and the spectrum of the input gaussian signal (both unfiltered and filtered) are shown in figures below:

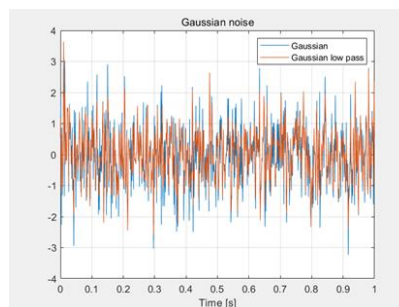


Figure 3.5.1: time history of the noise

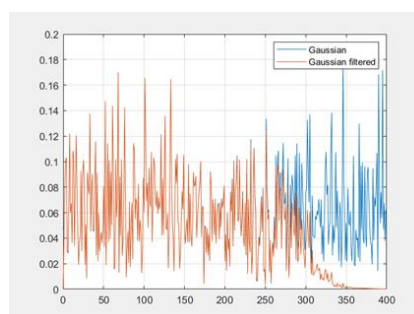


Figure 3.5.2: spectrum of the noise

Using the gaussian noise as input signal, the risk of collision is simply assessed by checking dynamic response.

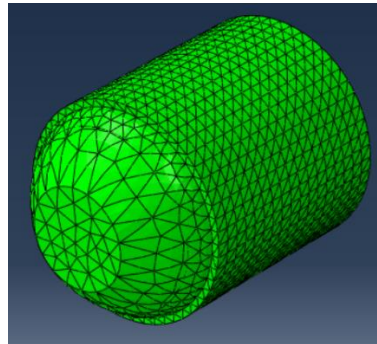


Figure 3.5.3: motion of improved model

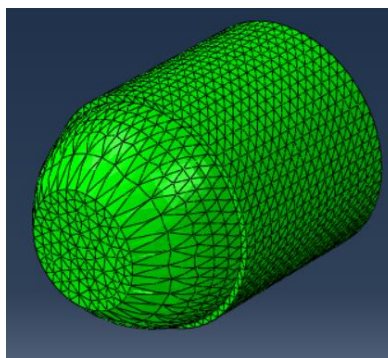


Figure 3.5.4: motion of improved model with larger size

The result of dynamic simulation shows that: for these two models, when having only vertical acceleration as input, the motion is mainly vertical. Those translation modes are not triggered. Since both models are safe, only the improved model is chosen for further analysis.

3.5.2 Rough FRF estimation

The transfer function is the characteristic of a system, different excitations should lead to the same result theoretically. In real case, the precision will be different according to the choice of excitation, however, the previous gaussian noise can still be used for a rough FRF estimation. From ABAQUS, the signals of the acceleration on the bottom and the top are collected, then introduced into the MATLAB to calculate the transfer function.

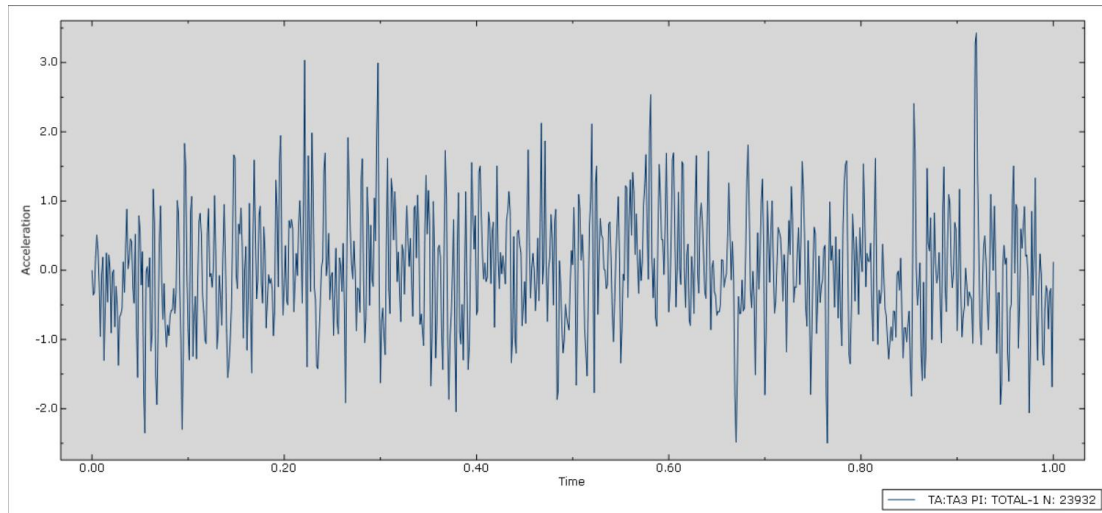


Figure 3.5.5: acceleration on the bottom (input: noise)

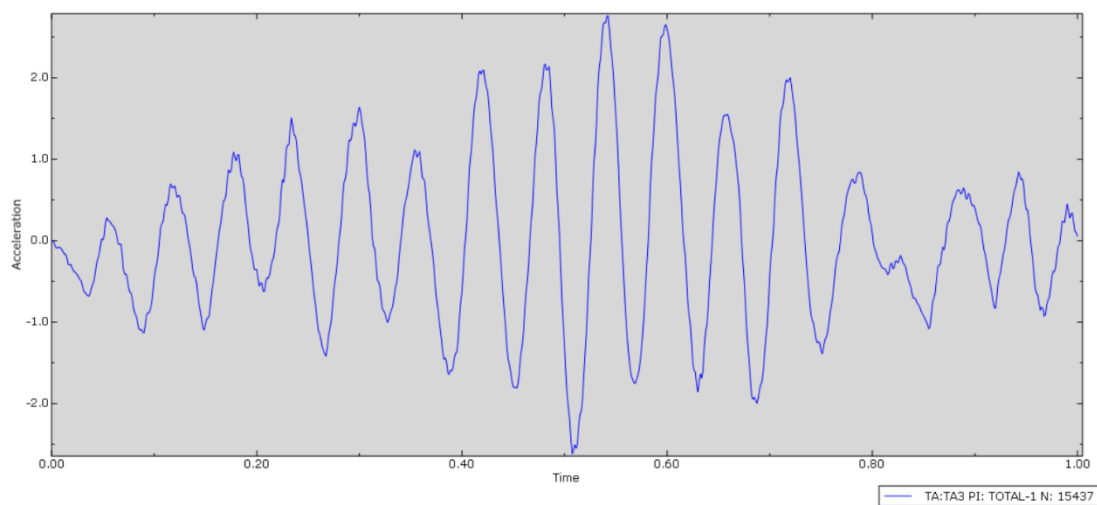


Figure 3.5.6: acceleration on the top (input: noise)

From the time history, it's clear that the input is noise, and the output is more regular. There are about 16 peaks in 1 second, so the frequency is around 16 HZ, very close to the natural frequency. And the maximum amplitude reduces a bit, which is good.

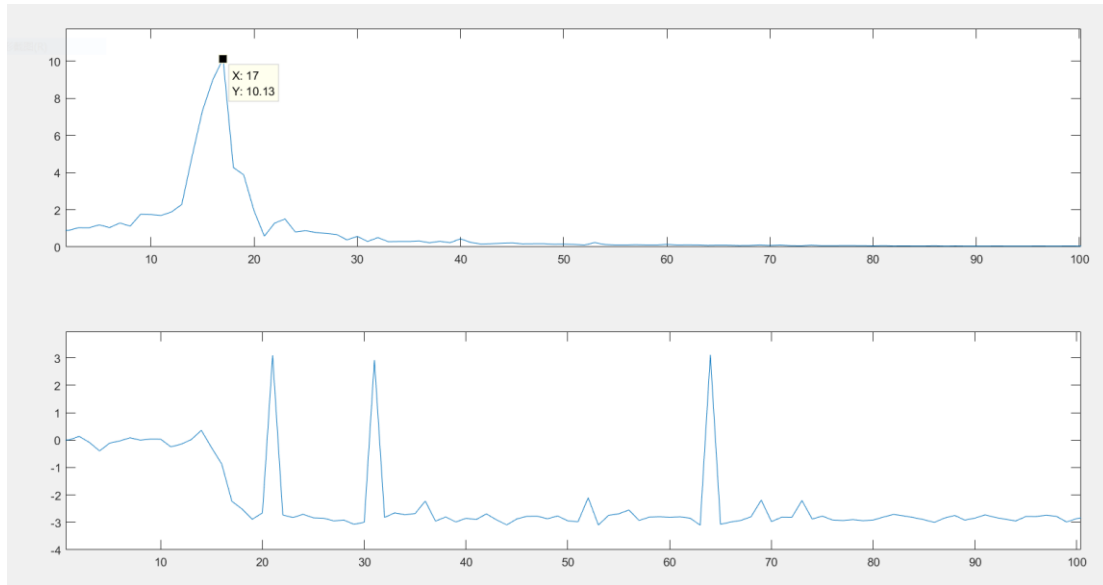


Figure 3.5.7:FRF (input: noise)

| Index | Description |
|-------|--|
| 0 | Increment 0: Base State |
| 1 | Mode 1: Value = 10728. Freq = 16.484 (cycles/time) |
| 2 | Mode 2: Value = 22048. Freq = 23.632 (cycles/time) |
| 3 | Mode 3: Value = 43593. Freq = 33.230 (cycles/time) |
| 4 | Mode 4: Value = 43595. Freq = 33.231 (cycles/time) |
| 5 | Mode 5: Value = 83944. Freq = 46.112 (cycles/time) |
| 6 | Mode 6: Value = 84033. Freq = 46.136 (cycles/time) |
| 7 | Mode 7: Value = 1.71935E+06 Freq = 208.69 (cycles/time) |
| 8 | Mode 8: Value = 1.73921E+06 Freq = 209.89 (cycles/time) |
| 9 | Mode 9: Value = 1.74697E+06 Freq = 210.36 (cycles/time) |
| 10 | Mode 10: Value = 1.75378E+06 Freq = 210.77 (cycles/time) |

Figure 3.5.8: natural frequency (improved model)

From the amplitude of the FRF, the most obvious peak is 17 HZ, which is close to the frequency of mode 1, which is vertical vibration.

The ratio of the peak and the static point is about 11. This ratio should be equal to $1/2h$, h is damping ratio. The modal damping is set as 0.04, the ratio should be 12.5, but because of the Polynomial reduced model, the value of h may change.

3.5.3 Dynamic analysis using real data

Though by using gaussian noise as excitation, some information can be gathered, to make the simulation more reasonable, the best way is to use the real data of the rail.

From the work of professor Marzio Falco, a series of data of the real railway are available. Generally, those data are about displacement and acceleration. The acceleration data has two parts, the absolute acceleration of sleeper(A5B), and the relative acceleration of the rail compared with the sleeper(A2B). By adding them, the absolute acceleration of the rail can be got. In the same way, the absolute displacement is S2B(relative) plus S3B(sleeper). In the dynamic analysis, only the acceleration data are used.

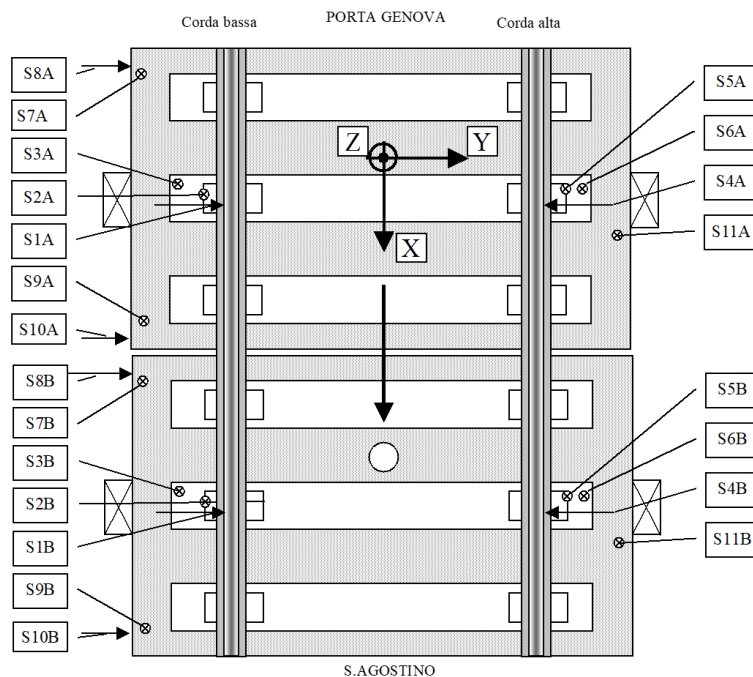


Figure 3.5.9: displacement

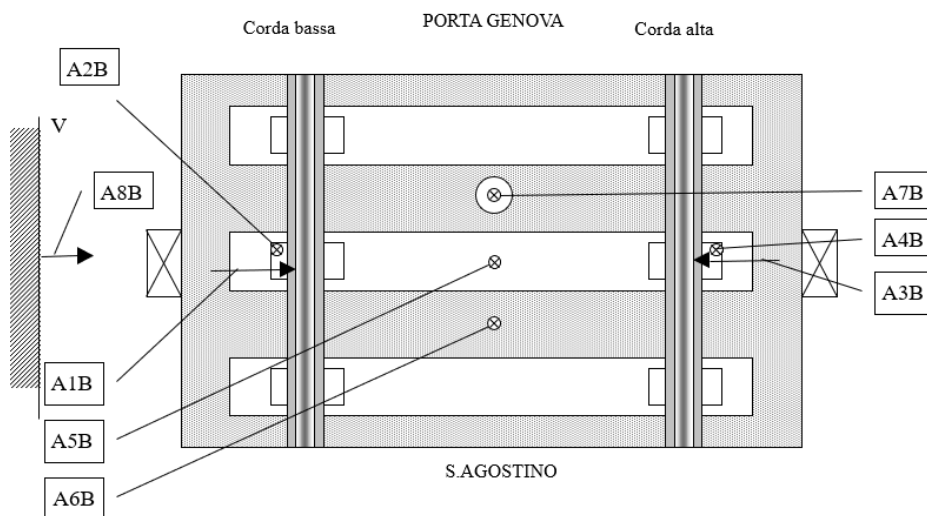


Figure 3.5.10: acceleration

The original signal is shown in figures below. The sampling frequency is 3000 HZ, so the frequency range is up to 1500 HZ. The signal is 22 seconds long.

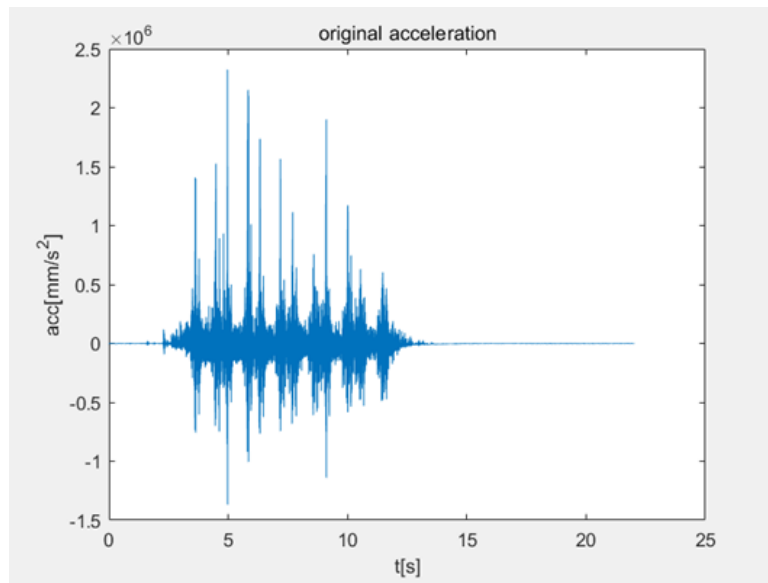


Figure 3.5.11: original acceleration

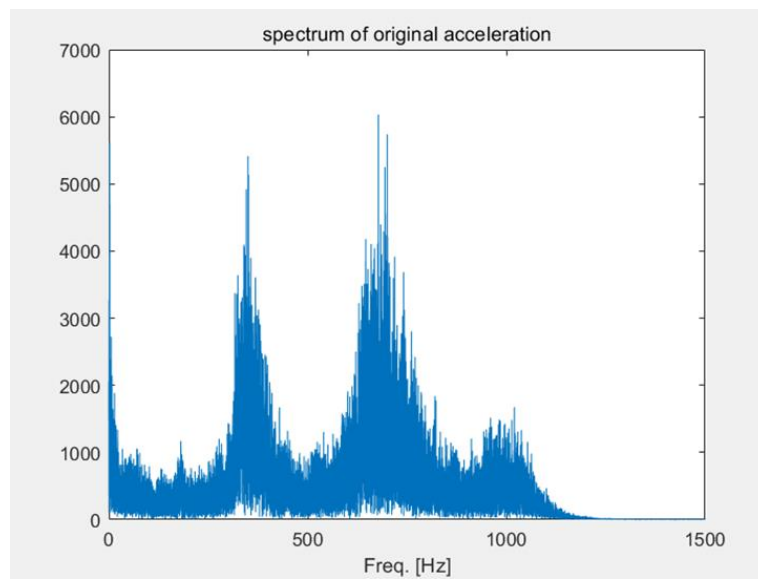


Figure 3.5.12: spectrum of original acceleration

This signal is so huge that it is too difficult for ABAQUS to process, due to hardware limits.

However, some data processing techniques can be used to simplify the signal. Firstly, from the spectrum, the main frequency components are between 0 HZ and 1000 HZ. So, the signal can be resampled. The resampling frequency is 2000 HZ, and the new spectrum is up to 1000 HZ.

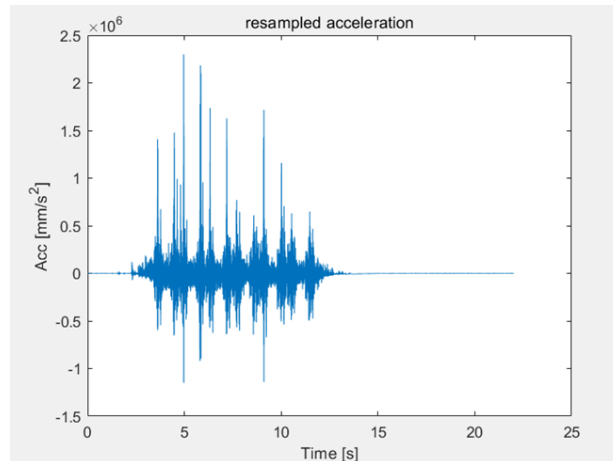


Figure 3.5.13: resampled acceleration

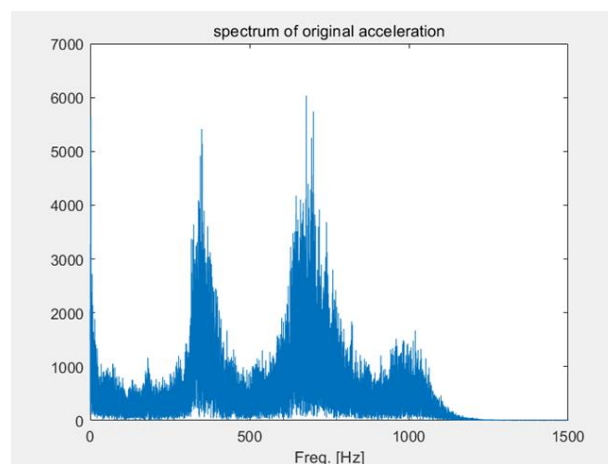


Figure 3.5.14: spectrum of resampled signal

Secondly, to shown characteristics in frequency domain, the whole signal is not necessarily needed, just part of time history may contain all frequencies of interest. The time history from 3s to 5s is cut and taken as the input signal. The spectrum shows that it contains frequency from 0 HZ to 1000 HZ. Now the signal can be introduced into ABAQUS as input signal.

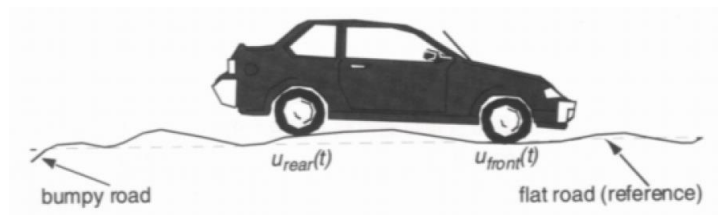


Figure 3.5.15: base motion

The input acceleration can be seen as base motion, for example an earthquake. The output is base motion plus a forced motion due to the base motion. The eigenmodes must be acquired with the DOFs of the base all fixed, so, in Frequency step, the DOFs contained in base motion should be all fixed and in modal dynamic step the DOFs are added.

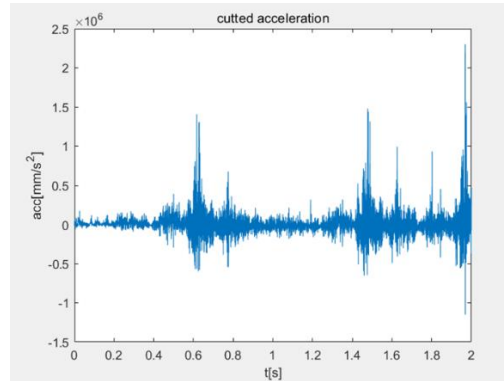


Figure 3.5.16: short signal after cut

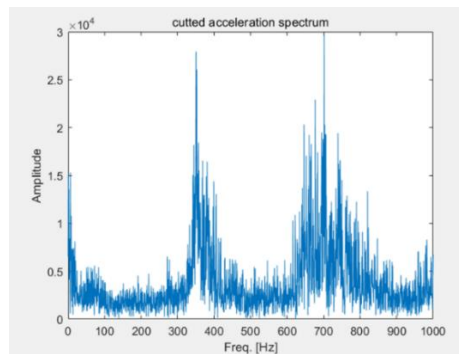


Figure 3.5.17: spectrum of short signal

The acceleration on the bottom and the top are collected from ABAQUS. It can be seen that the acceleration on the bottom is very noisy, while the acceleration on the top shows some periodicity. The number of the peaks in 1 second is around 17(not so regular due to the short signal), means the natural frequency is close to 17 HZ as expected. And the peak acceleration on the top is lower than the bottom in spite of the amplification effect, which means the system reduces the vibration, so accelerometers with lower range can be used.

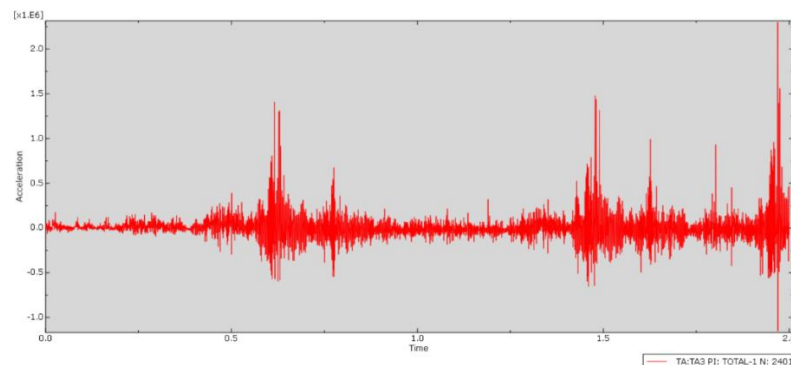


Figure 3.5.18: acceleration on the bottom (input: real data)

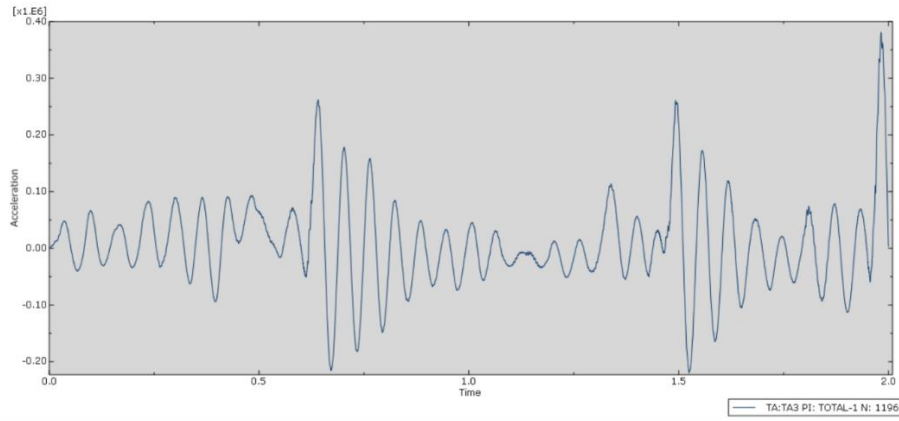


Figure 3.5.19: acceleration on the top (input: real data)

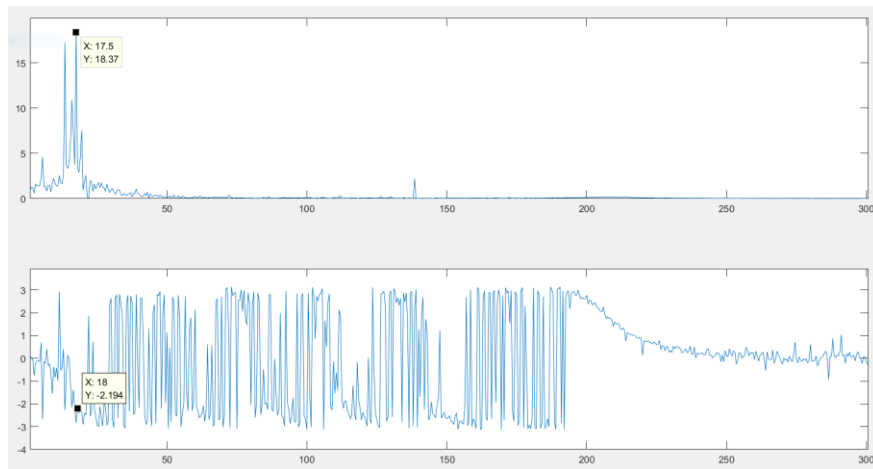


Figure 3.5.20:FRF (input: real data)

From the FRF, the natural frequency is about 18 HZ according to the phase and the amplitude, which is very close to 16.484 HZ. Using real data as input, the model has a natural frequency close to the theoretical value, and can effectively eliminate those high frequency components.

The ratio of the peak and the static point is about 14.5. This ratio should be equal to $1/2h$, h is damping ratio. The modal damping is set as 0.04, the ratio should be 12.5, but because of the Polynomial reduced model, the value of h may change, so generally this result is right.

CHAPTER 4

REAL MODEL SIMULATION AND TEST

4.1 Real model

In all the models before, rubber rings are connected to the shell directly. It may be possible to use glue to bind them, but it is not so reliable.

To make the model applicable in real tests, it is necessary to consider the way of connection and fixation. One common solution is to use fasteners. So, the model is redesigned using bolt and nut while maintaining the basic structure (two rubber rings, one steel mass like a flange plate). Size requirement is the same, but because of material limit (steel rod to produce steel shell), the diameter is much smaller.

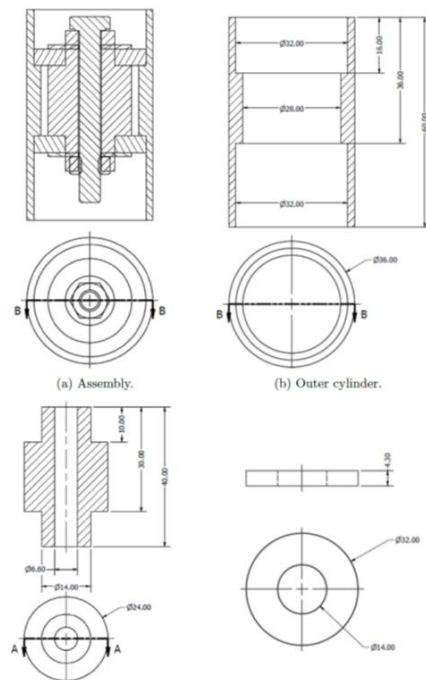


Figure 4.1.1: real model shape

4.2 Geometry parameter

The steel shell can be seen as three parts: top, mid and bottom. The outer diameter of top is 36mm, the inner diameter is 32mm, the height is 16mm. The outer diameter of mid is 36mm, the inner diameter is 28mm, the height is 20mm. The outer diameter of bottom is 36mm, the inner diameter is 32mm, the height is 24mm.

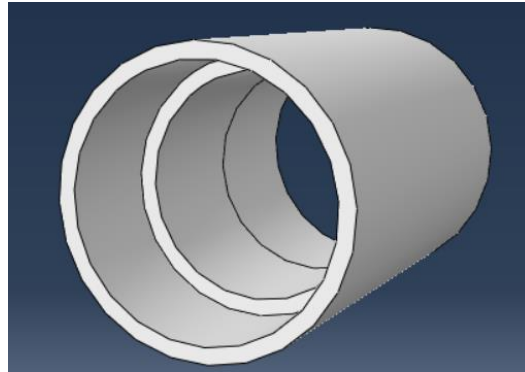


Figure 4.2.1:shell

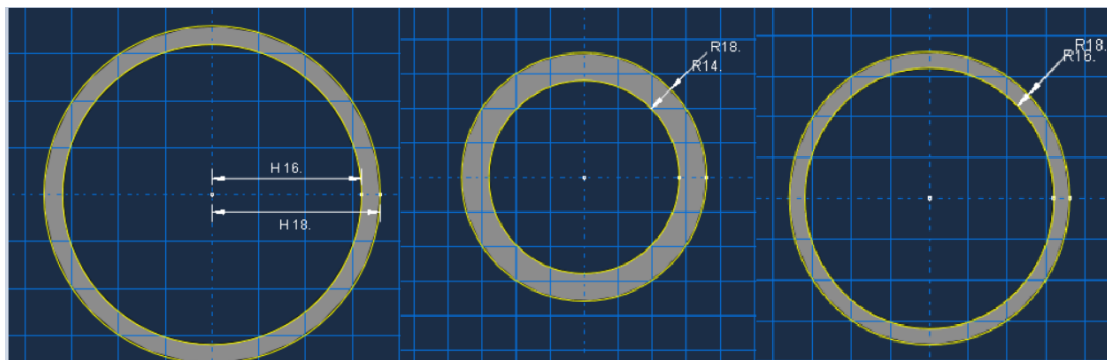


Figure 4.2.2:diameter (top, mid, bottom)

Two rubber rings are the same. The outer diameter is 32mm, the inner diameter is 14mm, the height is 4.3mm.

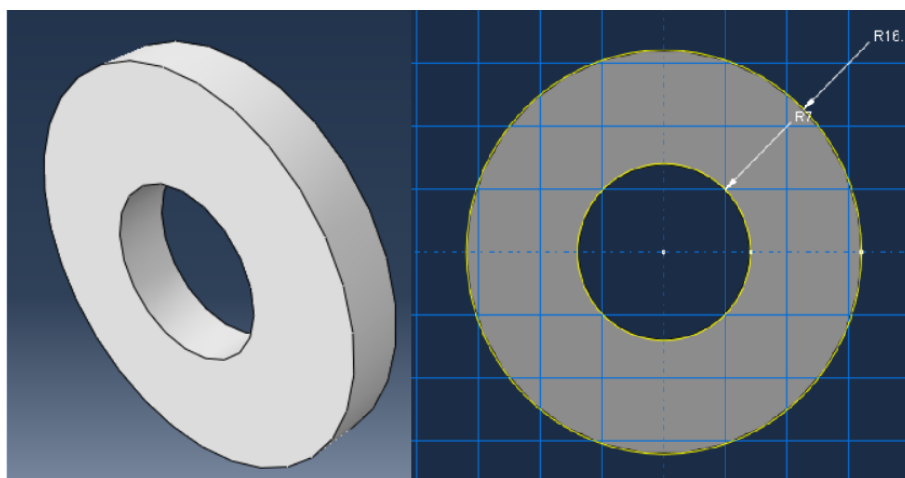


Figure 4.2.3:rubber dimension

The steel mass can be seen as a big cylinder with three steps of cut extrude. The diameter of the original cylinder is 24mm, the height is 40mm. Cut 1 and cut 2 are two rings cut from two side. The outer diameter is 24mm, the inner diameter is 14mm, the height is 10mm. Cut 3 is a through hole. The diameter is 6.6mm and the height is 40mm.

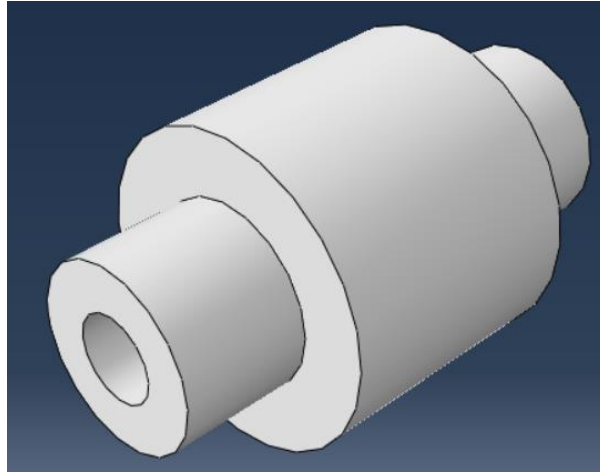


Figure 4.2.4:steel mass

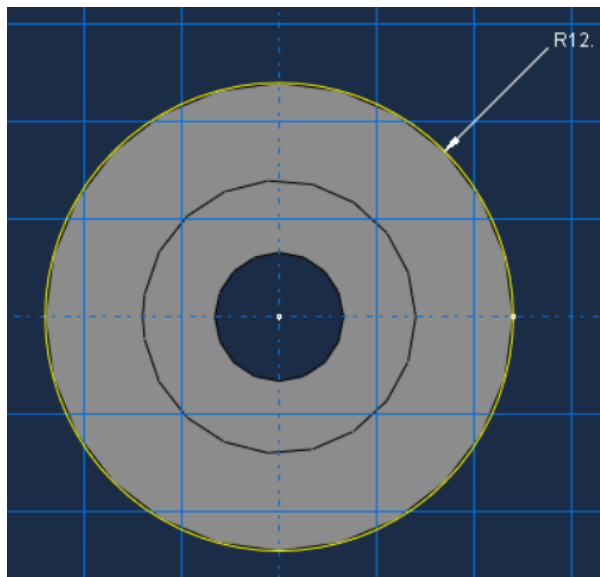


Figure 4.2.5:original cylinder

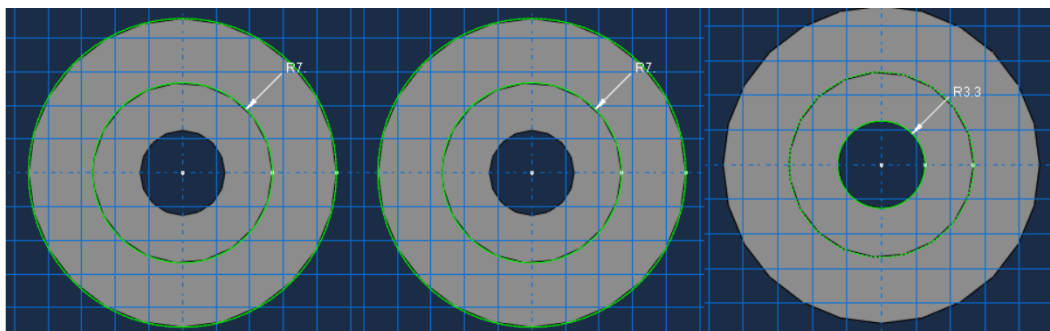


Figure 4.2.6:cut 1 2 3

The bolt screw is standard M6 screw. The dimension of the head is shown in the figure below. The thickness of head is 4mm. The diameter of the cylinder part is 6mm, the length is 50mm.



Figure 4.2.7: bolt screw

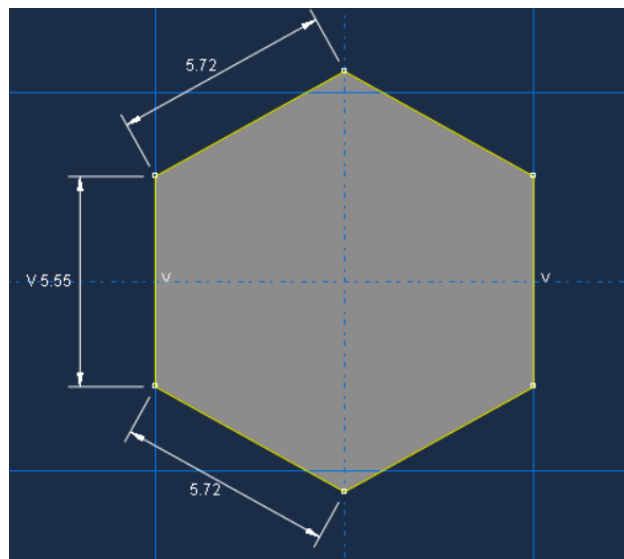


Figure 4.2.8: dimension of head

The nut has the same shape of the head of bolt screw. The thickness is 5.2mm. A through hole with 6mm diameter is inside it.

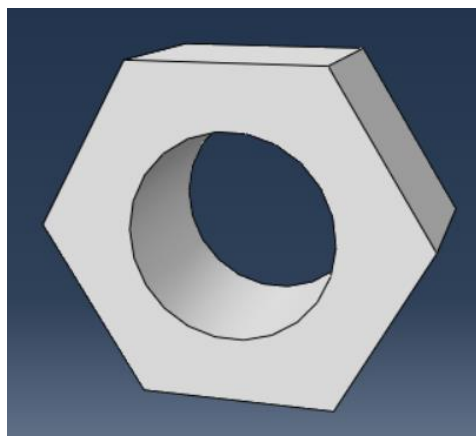


Figure 4.2.9: nut

Two gaskets need to be used between the interaction plane of bolt screw, nut and the steel mass. The outer diameter is 12mm, the inner diameter is 6.6mm, and the thickness is 1.6mm.

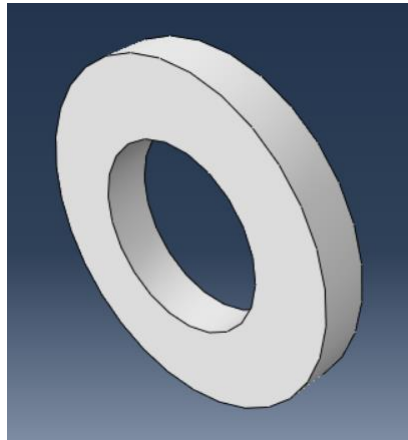


Figure 4.2.10:gasket

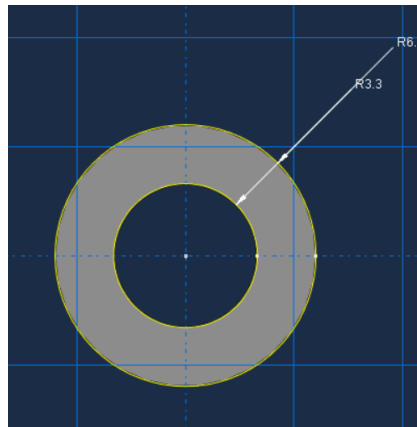


Figure 4.2.11:gasket dimension

As introduced in Polynomial reduced model, a sensor is considered, though the weight can be neglected. The size is 10x10x10mm. The weight is 4g. Considering that the sensor has empty space inside and has complex structure, a material called “sensor” is simply defined: Density: 4g/cm³, Young's modulus:206000Mpa, Poisson's ratio:0.3(almost no deformation, so treated as rigid steel).

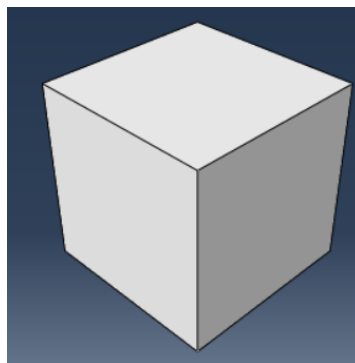


Figure 4.2.12:sensor

Finally, all these components are assembled together to form an entity.

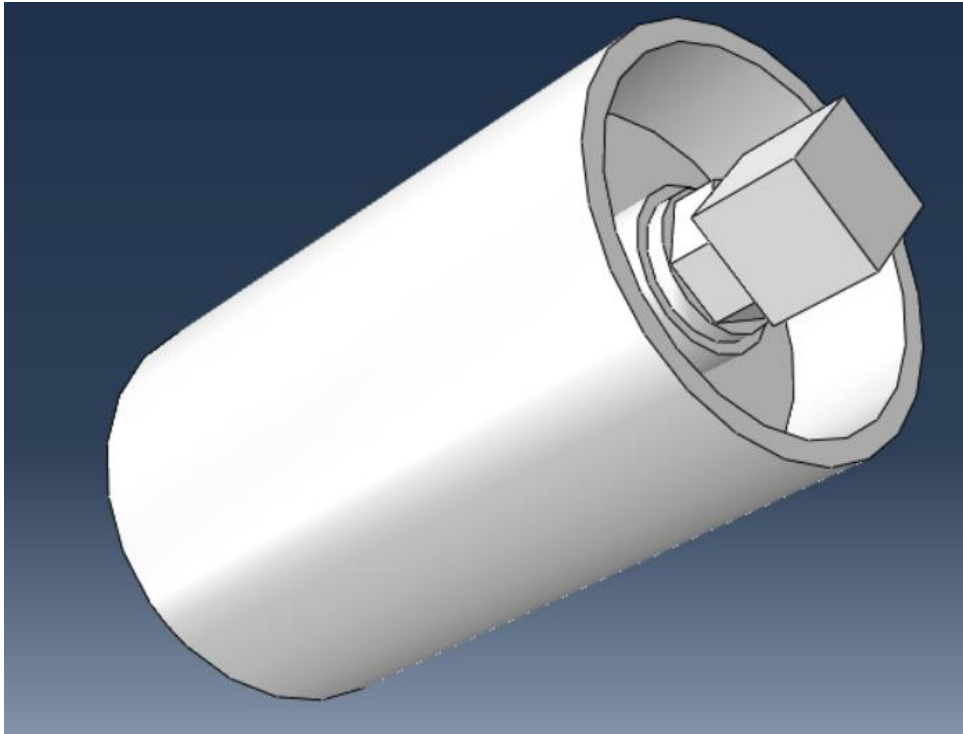


Figure 4.2.13:final model

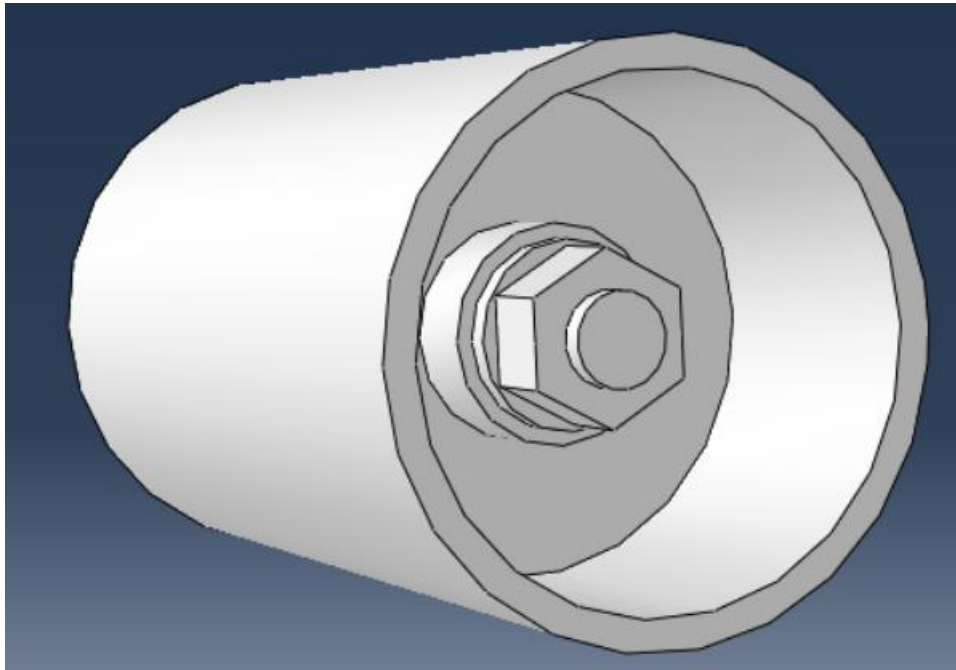


Figure 4.2.14:bottom view

4.3 Simulation of real model

After the build of real model, series of simulation are run as before.

4.3.1 Natural frequency

| Index | Description |
|-------|--|
| 0 | Increment 0: Base State |
| 1 | Mode 1: Value = 74448. Freq = 43.426 (cycles/time) |
| 2 | Mode 2: Value = 1.36354E+05 Freq = 58.770 (cycles/time) |
| 3 | Mode 3: Value = 1.36545E+05 Freq = 58.811 (cycles/time) |
| 4 | Mode 4: Value = 1.69096E+05 Freq = 65.446 (cycles/time) |
| 5 | Mode 5: Value = 1.69665E+05 Freq = 65.557 (cycles/time) |
| 6 | Mode 6: Value = 2.07389E+05 Freq = 72.479 (cycles/time) |
| 7 | Mode 7: Value = 1.04718E+07 Freq = 515.03 (cycles/time) |
| 8 | Mode 8: Value = 1.07009E+07 Freq = 520.63 (cycles/time) |
| 9 | Mode 9: Value = 1.15799E+07 Freq = 541.59 (cycles/time) |
| 10 | Mode 10: Value = 1.15892E+07 Freq = 541.81 (cycles/time) |

Figure 4.3.1:natural frequency

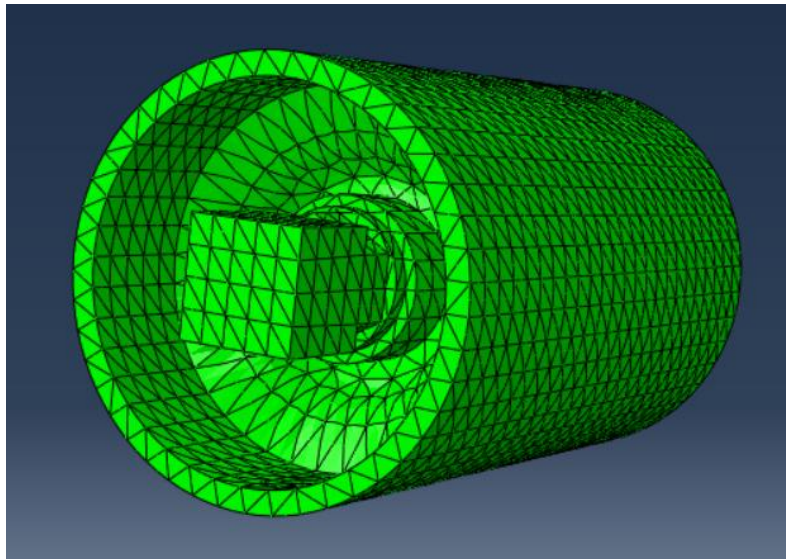


Figure 4.3.2:mode 1

The natural frequency of mode 1, which means vertical vibration, is 43.426 Hz. Because the size of model reduces a lot, the natural frequency increases, but still less than 50 Hz, so the model is acceptable.

4.3.2 FRF simulation using real data

The real acceleration data of railway is introduced into Abaqus as input, then collecting the output data and using MATLAB to calculate frequency response function.

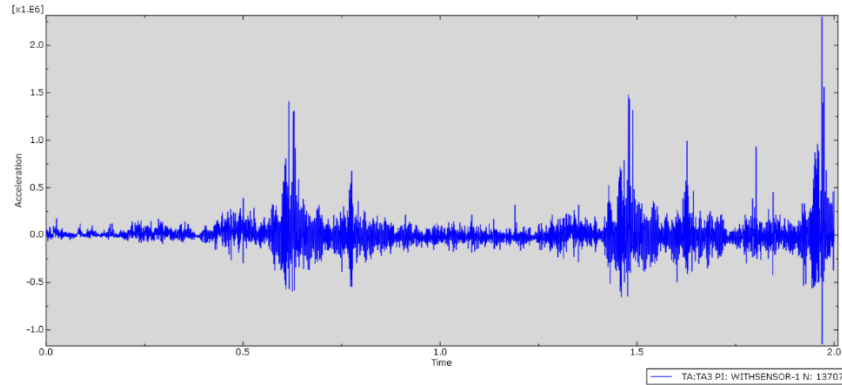


Figure 4.3.3: acceleration on the bottom

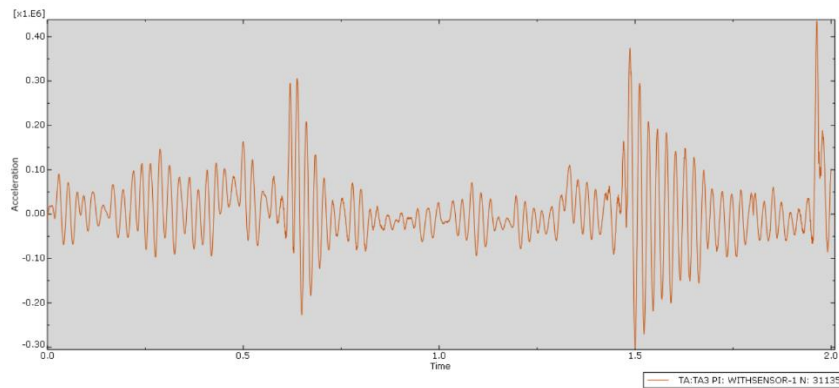


Figure 4.3.4: acceleration on the top

Comparing the acceleration on the bottom and top, the amplitude is reduced, and the signal is much more regular. There are about 43 peaks in one second on the figure of acceleration on the top, which means the natural frequency is close to 43 Hz, while the result of frequency step is 43.426 Hz. The result of FRF calculation is 44 Hz, the error is little, so the results match well.

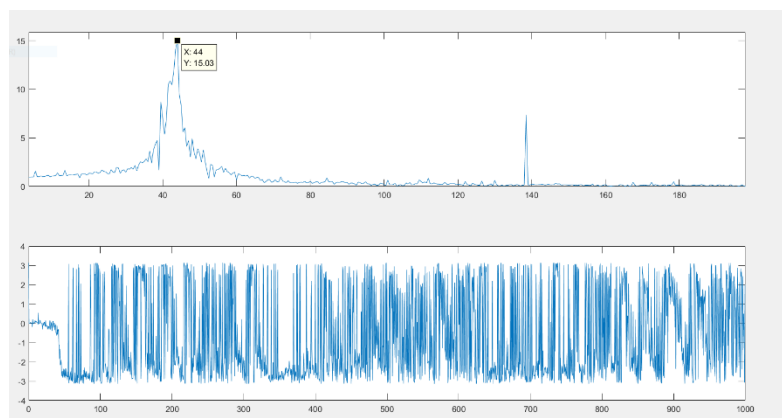


Figure 4.3.5: FRF simulation

4.4 Test of real model and comparison

After the build of real model, it is produced and a vibration test is carried out. Data are collected from the test and generate a FRF figure.

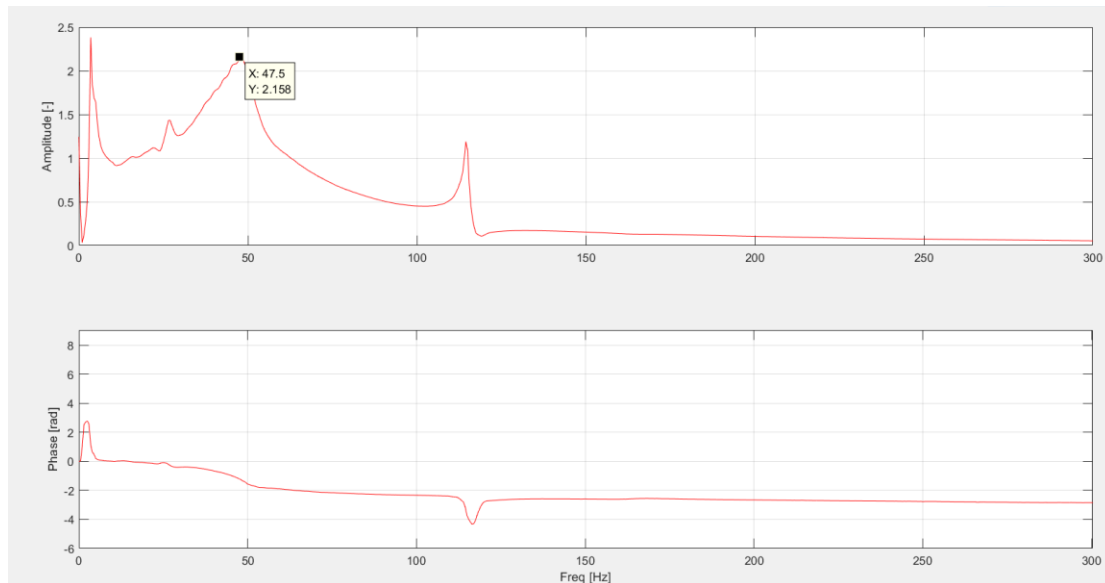


Figure 4.4.1: FRF from test

Compared with the figure of FRF getting from simulation of real model, there are two main problems.

First, the natural frequency is a little bit different, in the simulation it is 44 Hz and the real value is 47.5 Hz.

Second, the ratio between maximum amplitude and basic amplitude, which is called dynamic amplification factor, varies a lot. In the simulation, it is 12.7 while the real value is about two.

Parameters identification of mechanical systems

Damping ratio r/r_c :

Half power points method

One d.o.f. system
Dynamic amplification factor (FRF)
 $a = \Omega/\omega_0$, $h = r/r_c$

$$\left| \frac{X}{\delta_{st}} \right| = \frac{1}{\sqrt{(1-a^2)^2 + 4a^2h^2}}$$

Quick estimation $\left| \frac{X}{\delta_{st}} \right|_{MAX} \cong \frac{1}{2h}$

$\left| \frac{X}{\delta_{st}} \right| = \frac{1}{2h\sqrt{2}}$ at the "half power" frequencies (points) Ω_1 and Ω_2

As it can be proved $\frac{\Omega_2^2 - \Omega_1^2}{\omega_0^2} = 4h$ assuming that $\Omega_1 + \Omega_2 \cong 2\omega_0 \rightarrow \frac{\Omega_2^2 - \Omega_1^2}{\omega_0^2} = 4h = 2 \frac{\Omega_2 - \Omega_1}{\omega_0} \rightarrow h$

Ω_1 and Ω_2 can be found by intersecting the plot of the experimental curve at $0.5\sqrt{2}$ of the peak value

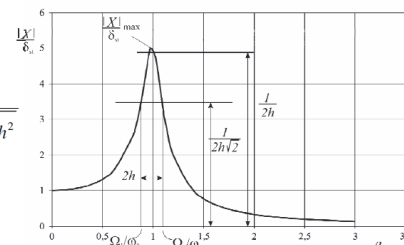


Figure 4.4.2: relationship between dynamic amplification factor and damping ratio

The dynamic amplification factor equals to $1/2h$ theoretically, while h is damping ratio. During simulation, because of lack of damping information, h is generally set as 0.04, which is a commonly used setting. According to the formula $1/2h$, the dynamic amplification factor should be 12.5. Because the effect of material, the damping ratio changes, so dynamic amplification factor changes to 12.7.

The second problem lies in the wrong value of damping ratio used, so dynamic amplification factor cannot be correct. In real application, it is usually a big problem because it is difficult to know the exact damping ratio of material. The solution is to get damping ratio from experiment first and then run the simulation.

Even if the damping ratio is correct, problem still exists. The first problem is related to material parameter setting. Though the Polynomial reduced model has been used to describe hyperelastic property of rubber, the real property is much more complex. For example, some soft rubber may have viscoelasticity, which is related to damping property. In theory, the natural frequency means the frequency without the influence of damping, but actually it may change the result of simulation a bit.

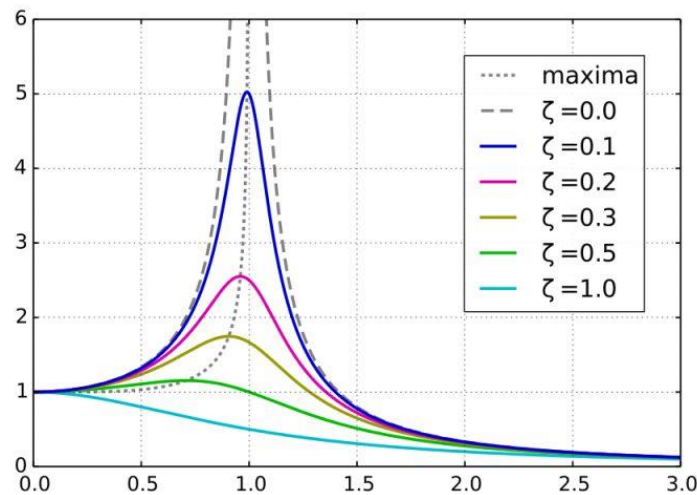


Figure 4.4.3: relationship between maximum amplitude and damping ratio

Actually, the frequency where the maximum amplitude occurs is not the natural frequency exactly, it should be smaller. When the damping ratio is very small, for example, 0.04 as usually set, it can be considered the same as the natural frequency. When the damping ratio is high, the difference cannot be neglected. The value $1/2h$ is not the maximum value too, it locates at the position of the natural frequency. This is another reason for the difference between the dynamic amplification factor.

In the initial aim a natural frequency less than 50 Hz is wanted, it is not so accurate because the natural frequency is considered as dangerous frequency where the maximum amplitude appears. Since in the real test the maximum amplitude appears at 47.5 Hz, it is still workable.

4.5 Simulation using different parameters

From the result of the test, a rough estimation of damping can be made. It is about 0.25. And some more detailed properties about Sorbothane 50 are provided. Instead of using the Polynomial reduced model, the hyperelastic property is described by Neo-Hooke model, which is simpler. The viscoelastic property is taken into account too.

| <i>Material</i> | <i>Model</i> | <i>C₁₀</i> |
|----------------------|--------------|-----------------------|
| Sorbothane 50 (2016) | Neo-Hooke | 4.3824e-2 |

Table 5: Neo-Hooke model

| | | | | |
|-------------------------|-------|-----------|----------|-----------|
| Sorbothane 50 (2016) | e_1 | 6.3442e-1 | τ_1 | 1.0011e-4 |
| | e_2 | 1.5196e-1 | τ_3 | 1.0802e-3 |
| | e_3 | 8.1414e-2 | τ_3 | 4.6761e-3 |
| | e_4 | 5.6374e-2 | τ_4 | 2.3452e-2 |
| | e_5 | 3.2583e-2 | τ_5 | 2.7065e-1 |

Table 6: viscoelastic property definition

Then these parameters are used to simulate the real model again.

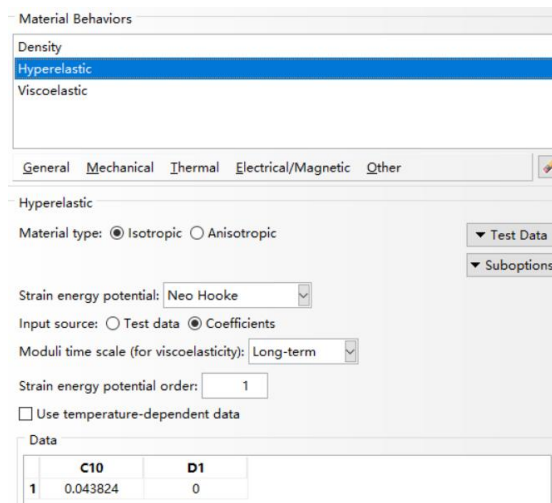


Figure 4.5.1: Neo-Hooke model

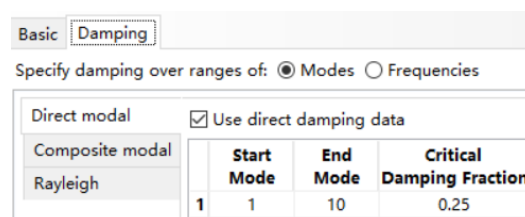


Figure 4.5.2: damping

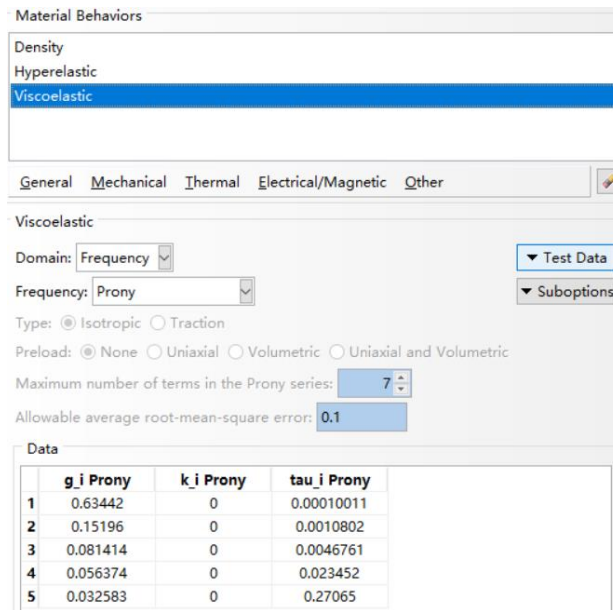


Figure 4.5.3: viscoelasticity

The new natural frequency of mode 1 (vertical vibration) is 54.387 Hz. According to the damping ratio 0.25, the dangerous frequency is about 49 Hz.

| Index | Description |
|-------|--|
| 0 | Increment 0: Base State |
| 1 | Mode 1: Value = 1.16775E+05 Freq = 54.387 (cycles/time) |
| 2 | Mode 2: Value = 2.13874E+05 Freq = 73.604 (cycles/time) |
| 3 | Mode 3: Value = 2.14173E+05 Freq = 73.655 (cycles/time) |
| 4 | Mode 4: Value = 2.65224E+05 Freq = 81.965 (cycles/time) |
| 5 | Mode 5: Value = 2.66117E+05 Freq = 82.103 (cycles/time) |
| 6 | Mode 6: Value = 3.25301E+05 Freq = 90.774 (cycles/time) |
| 7 | Mode 7: Value = 1.64257E+07 Freq = 645.03 (cycles/time) |
| 8 | Mode 8: Value = 1.67849E+07 Freq = 652.05 (cycles/time) |
| 9 | Mode 9: Value = 1.81637E+07 Freq = 678.30 (cycles/time) |
| 10 | Mode 10: Value = 1.81783E+07 Freq = 678.57 (cycles/time) |

Figure 4.5.4: natural frequency

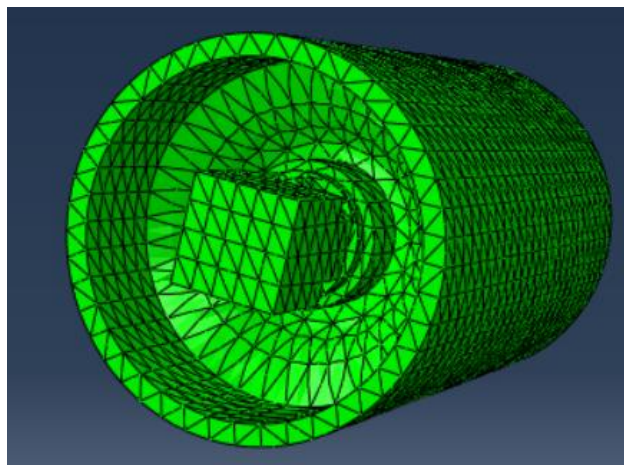


Figure 4.5.5: mode 1

Again, the acceleration of the top and bottom are collected to calculate the FRF.

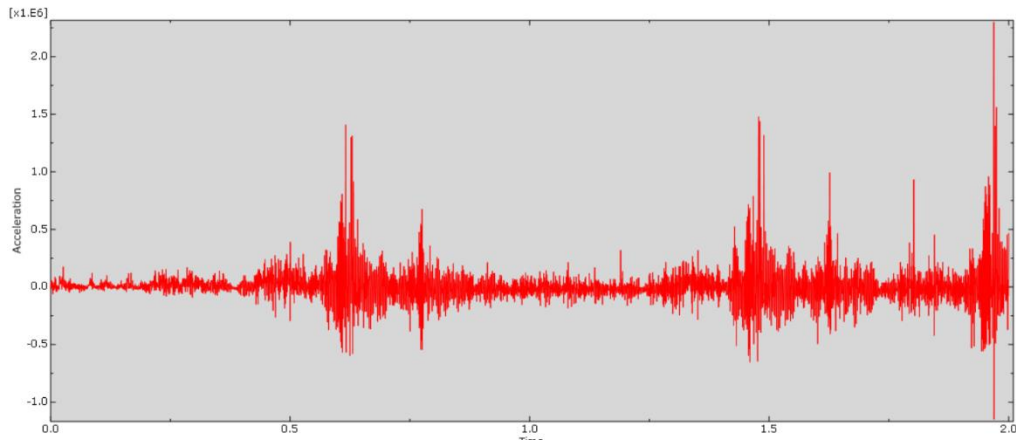


Figure 4.5.6: acceleration on the bottom

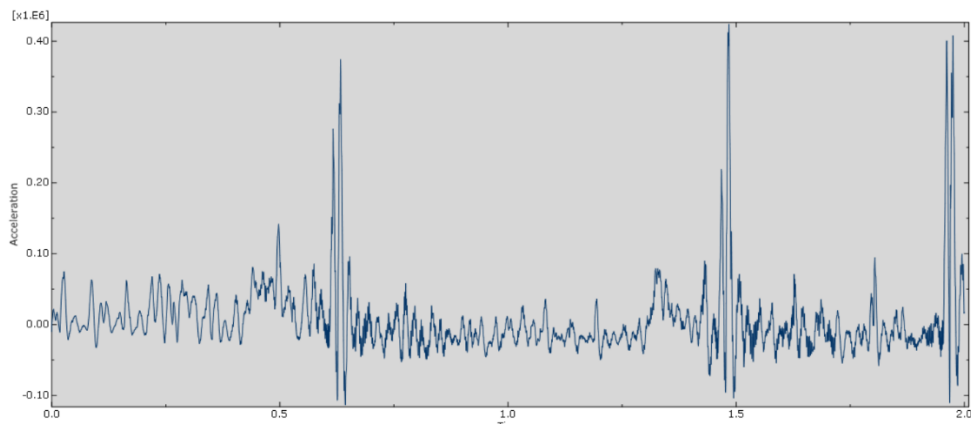


Figure 4.5.7: acceleration on the top

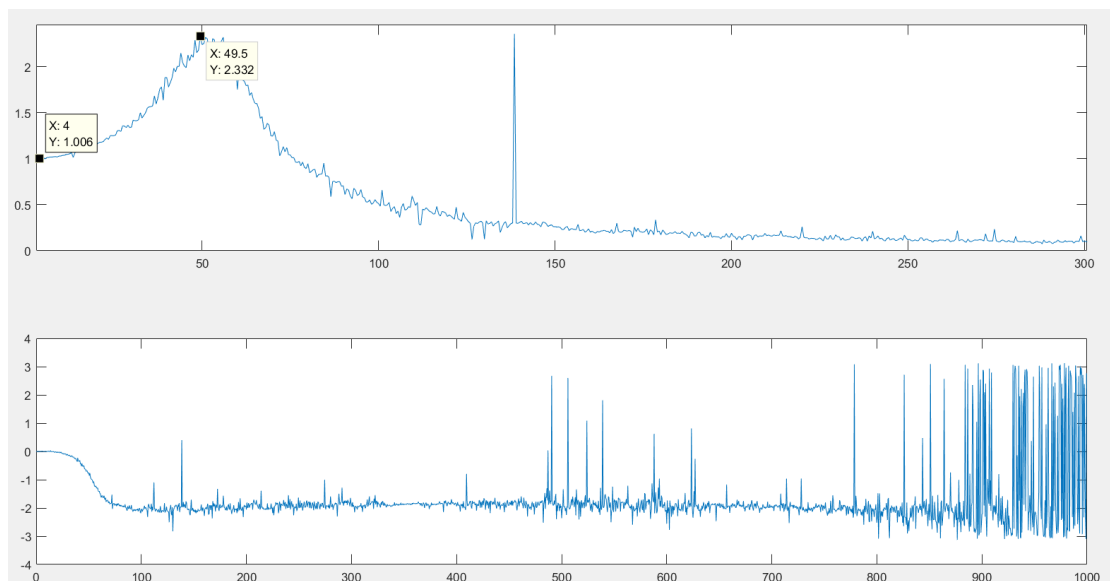


Figure 4.5.8:FRF

From the FRF, the dangerous frequency is 49.5 Hz, which is similar as prediction. The dynamic amplification factor is close to 2(theoretical value) too.

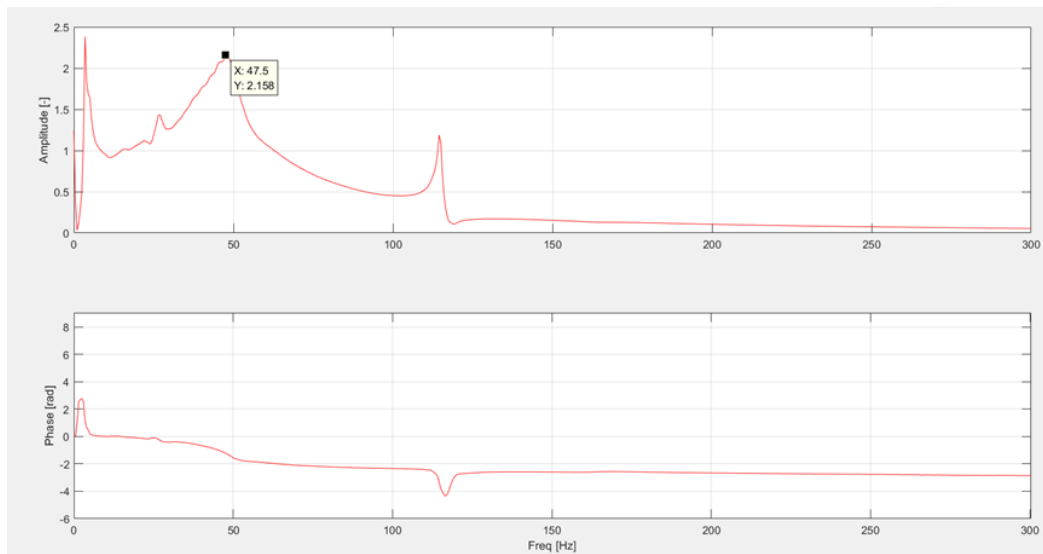


Figure 4.5.9:FRF from test

Compared with the result of the test, this time the simulation matches better. The error of dangerous frequency is only 4%, which is reliable.

4.6 Conclusions

From the test, it proves that the real model has an ideal low dangerous frequency, which means need of sensors of low frequency range. And the simulation has a reliable result similar to the test. However, there are still some shortcomings.

Though the result of test proves that the dangerous frequency getting from frequency step and modal dynamic step is almost correct, with just a little error, it is not so accurate. The frequency step does not consider the parameter related to damping perfectly. Modal dynamic is based on frequency step, so it is not so accurate too.

Actually, the step “Steady-state dynamics, Direct” is better for simulation of some rubber very soft. This step can take viscoelastic property into account better, which is related to damping. The drawback of this step is that it uses sweep sine to get a steady state response, not able to use the real data as an excitation. Though the natural frequency will not be affected by excitation type except for accuracy, the real excitation is different from that stable simple harmonic signal, so as the resulted motion.

Another drawback of the step “Steady-state dynamics, Direct” is that the output is response according to changing frequency, not time history. The dangerous frequency can be easily got because no need of FRF transformation, but the dynamic amplification factor and damping ratio cannot be found. Generally, it can only be used to find dangerous frequencies, and it is time consuming.

Modal dynamic has the advantage of fast speed and the ability of using base motion as excitation, which is ideal to make use of the real railway acceleration data.

The step “Dynamic, explicit” is another direct approach, which has some advantages of both “Steady-state dynamics, Direct” and Modal dynamic at same time. However, it takes more time even than the step “Steady-state dynamics, Direct”.

Taking into account of the advantages of these steps, Modal dynamic is finally chosen to get a balanced performance.

References

- [1] Chua D K H, Koh C G, Lo K W, Performance of urban rail transit system: vibration and noise study[J]. Journal of performance of constructed facilities, 1997, 11(2): 67-75.
- [2] Esveld.C, Modern Railway Track. TU-Delft, 2001.
- [3] Anthony Chu,Endevco Company, “Problems in high-shock measurement”.
- [4] Lakušić S, Ahac M, Rail traffic noise and vibration mitigation measures in urban areas[J]. Technical Gazette, 2012, 19(2): 427-435.
- [5] E. O. Doebelin, “Measurements Instruments and Methods”, McGraw-Hill, 2004, ISBN 883866148-0.
- [6] Professor Jens Trampe Broch, "Mechanical Vibration and Shock Measurements".
- [7] Alberti E, Moschioni G, Saggin B, et al, Mechanical Filters for Accelerometers: Design and Metrological Characterization[C]//2006 IEEE Instrumentation and Measurement Technology Conference Proceedings. IEEE, 2006: 2254-2259.
- [8] ISO 5348 “Mechanical Vibration and Shock, Mechanical Mounting of Accelerometers”.
- [9] PCB product catalog.
- [10] Endevco product catalog.
- [11] Bruel & Kjaer product catalog.
- [12] JIANG Rui Xing, Development and Application of Mechanical Filter(MF)[J].Electronics Machinery Engineering, 1999(2):3-9.
- [13] Bruce Lent,Endevco Company, “Steps to selecting the right accelerometer”.
- [14] Patrick L. Walter, Ph. D, PCB technical note 29: Guidance for the Filtering of Dynamic Force, Pressure, Acceleration (and Other) Signals.

- [15] WINFREE N A, JOSEPH H K, Predicted transfer function of the sandia accelerometer mount[C]//Proceedings of 72nd Shock and Vibration Symposium, 2001.
- [16] Vesta I. Bateman, Fred A. Brown, and Michael A. Nusser, “High Shock,High Frequency Characteristics of a Mechanical Isolator for a Piezoresistive Accelerometer,the ENDEVCO 7270AM6*,” SANDIA REPORT,Sandia National Laboratories, 2000.
- [17] Endevco Company, “INSTRUCTION MANUAL For Model 7255A, Pyrotron Accelerometer IM7255A, Revision A”.
- [18] PCB Company, “Field Evaluations of a Damped MEMS Shock Sensor”.
- [19] Sill.R, Development of a damped piezoresistive MEMS high shock sensor[C]//78th Shock and Vibration Symposium. 2007.
- [20] CHEN Hui, JIANG Nan, Design of mechanical filter for shock acceleration measuring [J]. China Measurement & Test, 2018, 44(10):115-122.
- [21] Rusovici R, Lesieutre G A, Inman D J, Modeling of shock propagation and attenuation in viscoelastic components[J]. Shock and Vibration, 2001, 8(5): 287-301.
- [22] Trindade M A, Benjeddou A, Hybrid active-passive damping treatments using viscoelastic and piezoelectric materials: review and assessment[J]. Journal of Vibration and Control, 2002, 8(6): 699-745.
- [23] Garg D P, Anderson G L, Structural damping and vibration control via smart sensors and actuators[J]. Journal of Vibration and Control, 2003, 9(12): 1421-1452.
- [24] S.O. Oyadij, K.T. Feroz and G.R. Tomlinson, “Design of Polymer-Based Mechanical Filters for Shock Measurement Accelerometers”, Proceedings of SPIE - The International Society for Optical Engineering, 1996, v 2720 pag. 305-316.